FlightDeck

Thomas M. Sailer
February 4, 2021

draft

Contents

1 Introduction

This manual describes the VFRNav package. VFRNav consists of the following main programs:

- VFRNav
- FlightDeck

VFRNav is optimized for small resolution displays, such as the Nokia N810 tablet having a resolution of 800x600 pixels.

FlightDeck on the other hand requires at least 1024x768 screen resolution. The remainder of this document describes the FlightDeck application. Despite the package name, it is also suitable for IFR flights.

1.1 User Interface

FlightDeck features a user interface similar to state of the art glass cockpit avionics. Its user interface is organized into a set of pages. At the bottom of the screen, there are 12 "soft keys", which map to the function keys F1 to F12 (but can of course also be clicked). The first five soft keys activate a page in a page group. Subsequent presses of the same soft key advances to the next page in the same page group. The page groups are:

- NAV – Main Navigation Pages
  - NAV:M – Map Page
  - NAV:AD – Airport Map Page
- WPT – Waypoint Information
  - WPT:ARPT – Airport Information Page
  - WPT:NAV – Navaid Information Page
  - WPT:INT – Intersection Information Page
  - WPT:AWY – Airway Segment Information Page
  - WPT:ASPC – Airspace Information Page
  - WPT:MAP – Map Element Information Page
  - WPT:FPL – Flight Plan Waypoint Information Page
- FPL – Flight Plans
  - FPL – Current Flight Plan Page
  - FPLS – Stored Flight Plan Directory Page
  - FPL – Avionics GPS Flight Plan Import Page
- AUX – Auxilliary
  - AUX – Document Directory Page
  - AUX – Document Page
  - AUX – Performance Calculator Page
  - AUX – Current Flight Plan Sunrise Sunset Page
- SENS – Sensor Configuration
  - SENS:LOG – System Log Page
  - SENS:X – Sensor Configuration Pages

Built-in keyboard widgets allow FlightDeck to be operated without keyboard solely with a pen, a mouse or by tapping on touchscreen enabled devices.

1.2 Sensors

FlightDeck supports the connection of various sensors:

- Position Sensors (GPS devices) supported by gpsd
- Avionics GPS devices outputting King format
- liblocation supported position sensors
- PlayStation Move controller as attitude and heading sensor
- MS5534 barometric sensor

Multiple sensors of the same kind, for example multiple GPS devices, are supported. User selectable priorities specify which sensor is used for what type of information under what circumstances.

1.3 Databases and Configuration Files

FlightDeck requires map and aviation information databases. Global databases are stored under `/usr/share/vfrnav`. Per user modifications to the global databases (record deletes and additions) are stored under `$(HOME)/.vfrnav`.

Databases may be created from various sources and file formats; conversion utilities are included. Alternatively, worldwide coverage database files may be downloaded from `http://www.baycom.org/~tom/vfrnav/data/repoview/`. Unfortunately, there is no accurate, up-to-date, official publication; the accuracy and actuality of the information contained in the databases cannot be guaranteed – the user is required to check that the information meets his requirements.

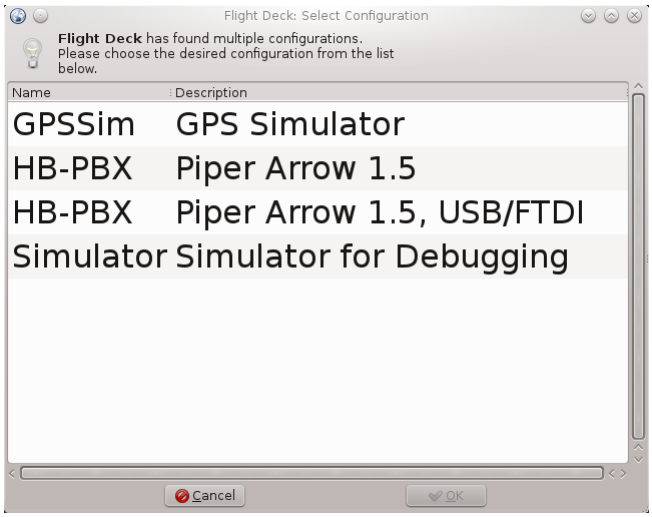

Figure 1: Splash Screen

FlightDeck supports multiple configurations; on start-up, FlightDeck searches for available configurations and presents the user with a list of the configurations found. The user can then select one that will be used. Figure 1 shows the configuration selection dialog.

Global configurations are stored under `/usr/share/vfrnav/flightdeck`, per user configurations are stored under `$(HOME)/.vfrnav/flightdeck`. Per user configurations take precedence over global configurations. Configuration files use a simple name=value ascii format, with section names in square brackets. They should use a file name of the form *xx*`.cfg`.

Configurations store the sensor setup, as well as user settings so that the next run with the same configuration continues with the same settings as the last run ended.

Each configuration should reference an aircraft definition file. Aircraft definition files are stored under `$(HOME)/.vfrnav/aircraft`. They describe the aircraft and contain Weight & Balance and Performance tables.

2 Navigation Page Group

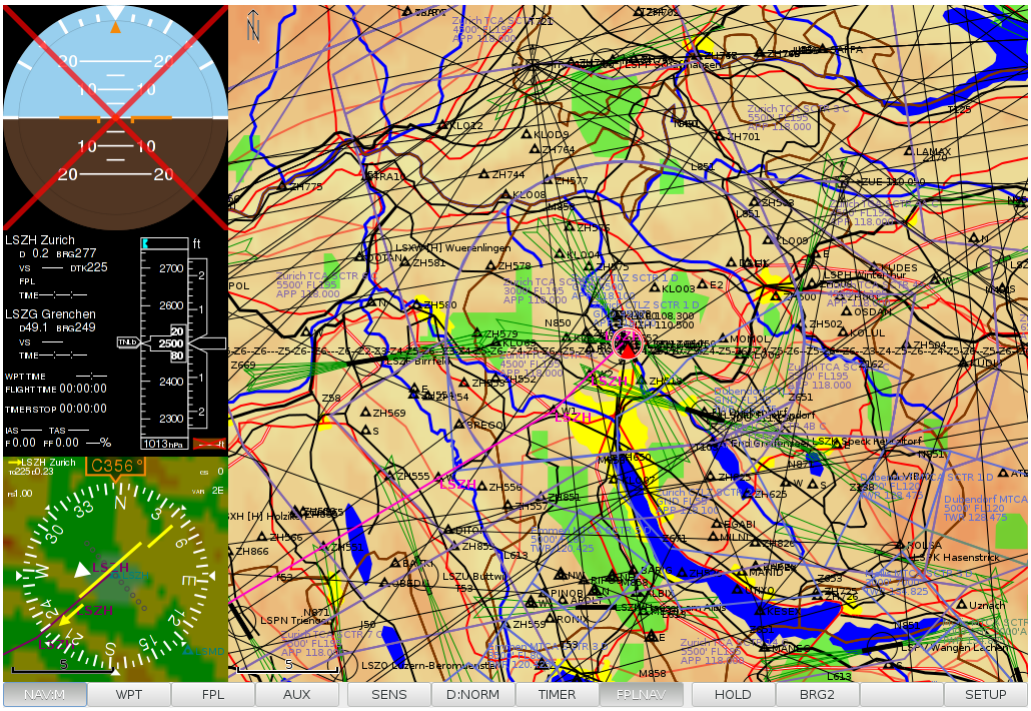

Figure 2: Nav Page: Map

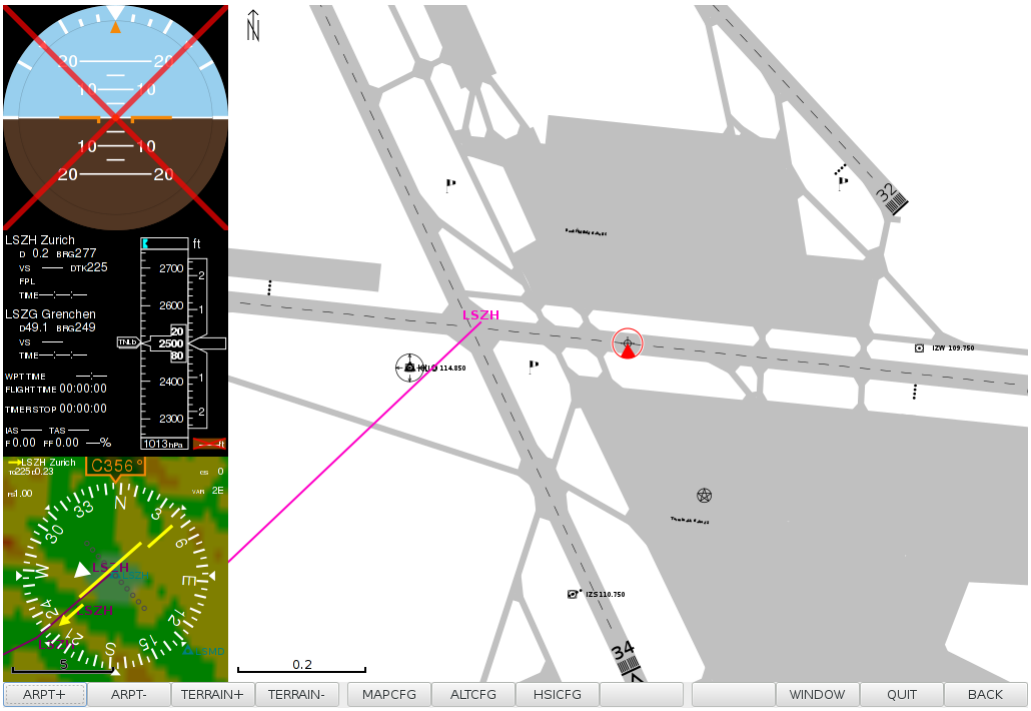

Figure 3: Nav Page: Airport Map

The main navigation page (Figure 2) consists of five parts: the soft keys at the bottom, the vector map with an aircraft symbol occupying the largest space on the left, an attitude indicator on the top left, an altitude indicator and flight plan informations in the middle on the left side, and a horizontal situation indicator on the bottom left.

Clicking on the NAV soft key again switches to the airport map page. This page looks the same, except that the vector map is replaced by an airport map (if airport map data is available).

2.1 Attitude Indicator

The Attitude Indicator in the top left edge works like a standard Attitude Indicator, displaying roll and pitch angles. It only works if an attitude sensor is connected, such as the PlayStation Move.

A trapezoid below the orange sky pointer indicates slip.

2.2 Flight Plan Information

Flight Plan information is displayed on the center left edge. Distance (in nmi), magnetic track, vertical speed, desired track and time to the next flight plan or direct-to waypoint are displayed first, followed by distance, magnetic track, vertical speed and time to the destination.

WPT TIME counts the time since passing the last waypoint, flight time counts the time since departure. TIMER is a generic up-counting timer that can be started and stopped using a soft key.

IAS and TAS display entered or calculated air speeds, and F, FF and % display fuel consumed since start, calculated fuel flow (from the aircraft model), and calculated engine power relative to maximum rated engine power.

2.3 Altitude Indicator

The central element of the Altitude Indicator is the altitude tape. The vertical speed indicator is located on the right side of the altitude tape. A magenta diamond indicates the vertical speed required to meet the next waypoint altitude target.

The altitude bug altitude is displayed above the tape. The current altimeter setting (or STD, for standard) is displayed below the tape. The white number on brown background in the bottom right edge indicates terrain altitude at the current position. Brown background inside the altitude tape also indicates terrain altitude (and below).

A yellow chevron at the left edge of the tape indicates the desired altitude to reach the next waypoint altitude target (similar to a “glide slope”). A red chevron indicates the configured minimum.

Since altitude is an important parameter (especially for IFR traffic), and most aircraft have many different altitude sensors, white labels may be displayed at the left edge of the tape for each altitude source, even if it was not selected to provide the system altitude. This allows the pilot to monitor the accuracy of all altitude sources.

Clicking into the altitude indicator opens the Altitude Configuration Dialog (Figure 5).

2.4 Horizontal Situation Indicator

The HSI displays compass and horizontal navigation information. The current heading is displayed in orange at the top if magnetic heading information is available (eg. from a connected PlayStation Move sensor). If no heading sensor is available, the heading may be entered manually, in which case it will be displayed prefixed with an M. In the absence of any heading information, the current course is displayed, prefixed with a C. If heading information is available, the course is displayed as a magenta diamond on the periphery of the compass rose.

A magenta arc at the top periphery of the compass rose indicates turn rate. An arrow head indicates that the turn rate is larger than approximately one and a half of a standard rate turn, otherwise the end of the arc indicates the heading 6 seconds into the future.

The yellow pointer indicates the desired track to the next waypoint, as well as the deviation from it.

An optional second cyan pointer may be set to point to any waypoint.

The top left corner displays where the pointer(s) point to.

The top right corner displays air data, and the magnetic variation at the present position.

The bottom right corner displays wind information, if heading information and air data is available.

Terrain information may be optionally displayed in the background of the HSI. Terrain graphics is normally black. Terrain that is less than 2000ft below the current altitude is displayed in green, terrain less than 1000ft below is displayed in yellow, terrain less than 500ft below is displayed in light orange, terrain less than 200ft below is displayed in dark orange, and terrain above the current altitude is displayed in red. The current position is the center of the compass rose.

Optionally, the terrain graphics may also display the current flight plan, airports, navaids and intersections.

Furthermore, the locations reachable from the current position and altitude in unpowered glide may be displayed in gray. The glide area graphics considers aircraft performance (glide ratio), wind (the wind manually entered in the flight plan page, *not* the automatically calculated wind), and topography, giving the pilot a good idea which emergency landing locations may be feasible.

There are some inaccuracies in the computation the pilot needs to consider:

- Best glide speed is taken as TAS, while for most aircraft it is IAS – only relevant for wind corrections
- The available terrain information is relatively coarse
- The algorithm does not enforce any minimum height for crossing mountain ridges

Clicking into the HSI opens the HSI Configuration Dialog (Figure 6).

2.5 Soft Keys

The following functions are available on the soft keys:

D:NORM Map Declutter; reduces the information displayed on the vector map

D:NORM Display user selected information

D:ASPC Display User selected information minus Topography, Terrain and Airways

D:AWY Display User selected information minus Topography, Terrain and Airspaces

D:TERR Display User selected information minus Airways and Airspaces

TIMER Starts and Stops an utility up-counting timer (for timed IFR approach segments, or holdings)

FPLNAV Enable or Disable Flight Plan Navigation. When enabling, it selects Direct To the nearest waypoint of the actual flight plan

HOLD Enables or Disables Hold mode. In Hold mode, waypoint sequencing is stopped, and guidance is provided inbound the next waypoint on a selected radial. Enabling Hold pops up the hold dialog (Figure 4), allowing the user to select the holding inbound track.

BRG2 Enables or Disables the second (cyan) bearing pointer in the HSI. Note that before enabling the bearing pointer, it should be set to point to a waypoint either in one of the waypoint pages or the flight plan page.

SETUP Activates the Setup soft keys.

2.6 Setup Soft Keys

The Setup soft keys provide the following functions:

MAP+ Zoom the vector map in

MAP− Zoom the vector map out

ARPT+ Zoom the airport map in

ARPT− Zoom the airport map out

TERRAIN+ Zoom the terrain map underlying the HSI in

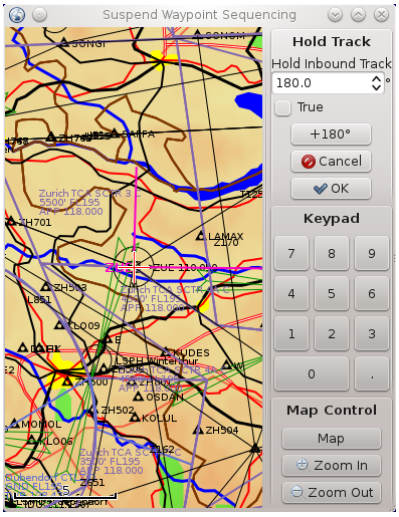

Figure 4: Hold Dialog

TERRAIN– Zoom the terrain map underlying the HSI out

MAPCFG Open the Map Configuration Dialog (Figure 7)

ALTCFG Open the Altitude Configuration Dialog (Figure 5)

HSICFG Open the HSI Configuration Dialog (Figure 6)

WINDOW/FULLSCREEN Toggles between Windowed and Fullscreen (borderless) Mode

QUIT Terminates the FlightDeck Application

BACK Return to the Main Soft Keys

2.7 Altitude Configuration Dialog

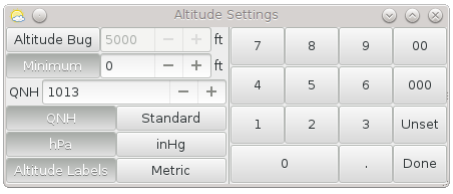

Figure 5: Altitude Configuration Dialog

Figure 5 shows the altitude configuration dialog.

Altitude Bug Enable/Disable the altitude bug, and enter its altitude

Minimum Enable/Disable the minimum indicator, and enter its altitude

QNH Current Altimeter Setting

QNH/Standard Switch between the current Altimeter Setting (“Altitudes”) and Standard (“Flight Level”)

hPa/inHg Switch between Hectopascals and Inches of Mercury as Altimeter Setting Unit

Altitude Labels Enable/Disable Altitude Labels, i.e. display of Altitudes of non-selected Altitude Sources

Metric Switch between Metric ("m") and Imperial ("ft") units

Important: Do *not* just enter 1013 or 29.92 into the QNH field when switching to standard, but use the Standard switch, because the current QNH is needed by FlightDeck even in standard mode to compute barometric altitudes from true altitude sources, such as GPS.

2.8 HSI Configuration Dialog

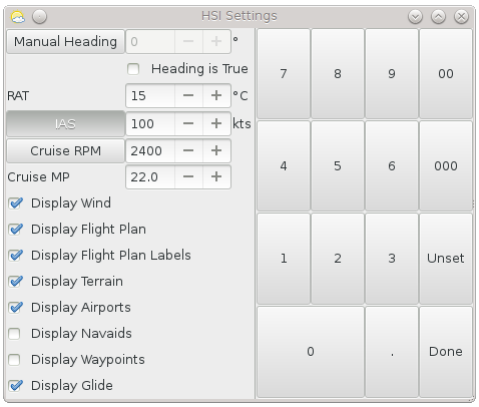

Figure 6: HSI Configuration Dialog

Figure 6 shows the HSI configuration dialog.

Manual Heading Enable/Disable the manual heading, and enter the current heading; manual heading may be magnetic or true

RAT Enter the Ram Air Temperature (i.e. what the thermometer reads); using TAS and current altitude, FlightDeck computes the current outside air temperature (OAT). When altitude changes, FlightDeck uses the ISA lapse rate to adjust the outside air temperature.

IAS Select and Enter Indicated Airspeed. What needs to be entered is actually Calibrated Airspeed, FlightDeck currently cannot correct for Instrument Errors. If selected, TAS is computed from the given IAS value, and altitude.

Cruise RPM/MP Enter cruise RPM and Manifold Pressure (MP) Settings. If selected, the TAS is computed from Aircraft performance data, given the current Density Altitude, and the selected RPM/MP values. If the current vertical speed is at least 150ft/min climbing, v_Y is used instead.

Display Wind whether the calculated wind (given TAS and Heading) should be displayed

Display Flight Plan whether the current flight plan should be displayed below the compass rose

Display Flight Plan Labels whether flight plan waypoints should have labels

Display Terrain whether terrain map should be displayed below the compass rose

Display Airports whether airports should be displayed

Display Navaids whether navaids should be displayed

Display Waypoints whether intersections should be displayed

Display Glide whether places reachable by unpowered glide shoudl be displayed

2.9 Map Configuration Dialog

Figure 7 shows the map configuration dialog.

This dialog configures what information should be displayed on the vector map.

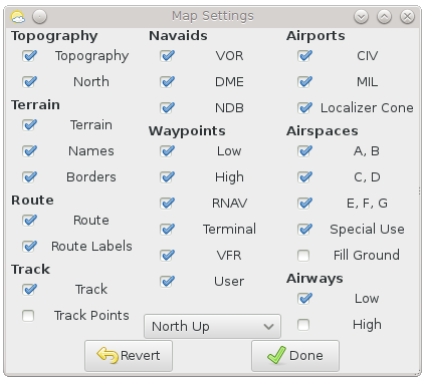

Figure 7: Map Configuration Dialog

3 Waypoint Page Group

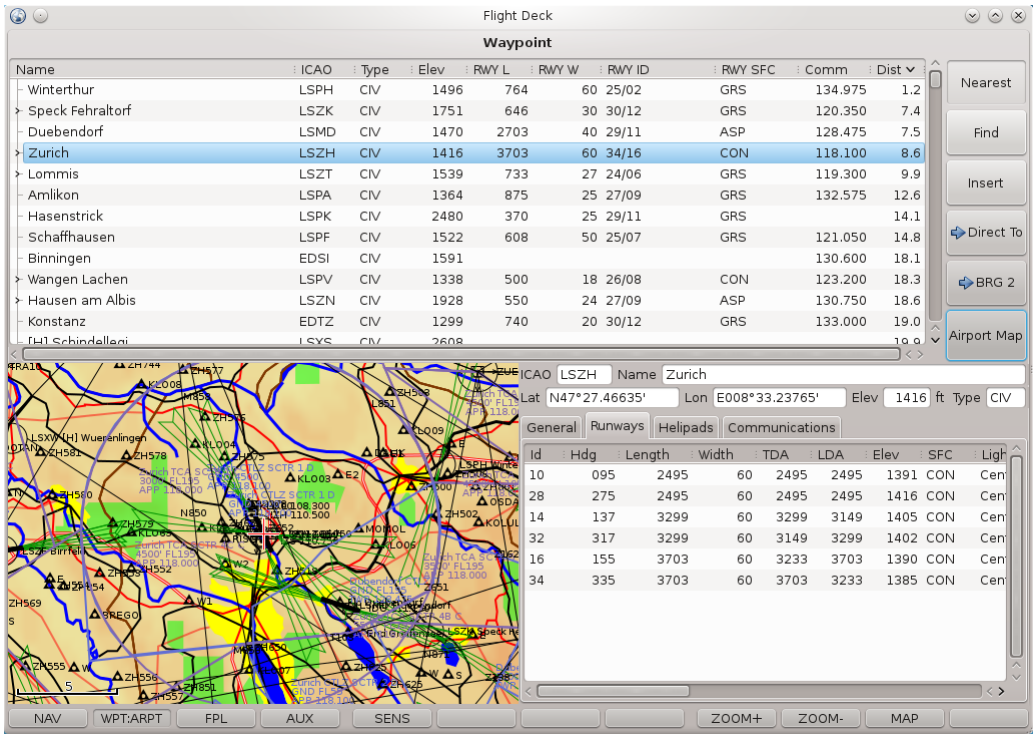

Figure 8: Waypoint Page: Airport

The waypoint page group displays information about database elements. Database elements may be searched by entering text, nearest to the current position (when entered using the WPT soft key) or nearest to the currently selected flight plan waypoint (when entered by clicking on insert in the flight plan page). Distance values are updated if the current position changes.

Selected database elements may be used as direct-to target, or as target for the second HSI pointer (BRG2).

The waypoint pages consist of 3 major parts: the top half of the screen is used by the element list, the bottom left half displays the element on the vector map, and the bottom right half displays textual information about the selected element.

Figure 8 shows the waypoint airport information page with the vector map displayed, while Figure 10 shows the same page with the airport map.

If the airport database contains approach or departure procedures, they may be displayed by clicking on the expander next to the airport name.

Airports that are within glide distance (*without considering terrain*, but considering wind entered on the flight plan page) are displayed in italics.

Airports that have no suitable runway (considering entered mass from the Weight & Balance page, and wind entered on the flight plan page) are coloured red. Airports whose “best” runway only allows either landing or takeoff, but not both, are coloured orange. The same colour scheme is applied to the runway list as well.

Figure 10 shows the waypoint navaid information page.

Figure 11 shows the waypoint intersection information page.

Figure 12 shows the waypoint map elment information page. Map elements include cities and lakes.

Soft Keys

D:NORM Declutter Mode, same as in the main menu

ZOOM+ Zoom Map In

ZOOM− Zoom Map Out

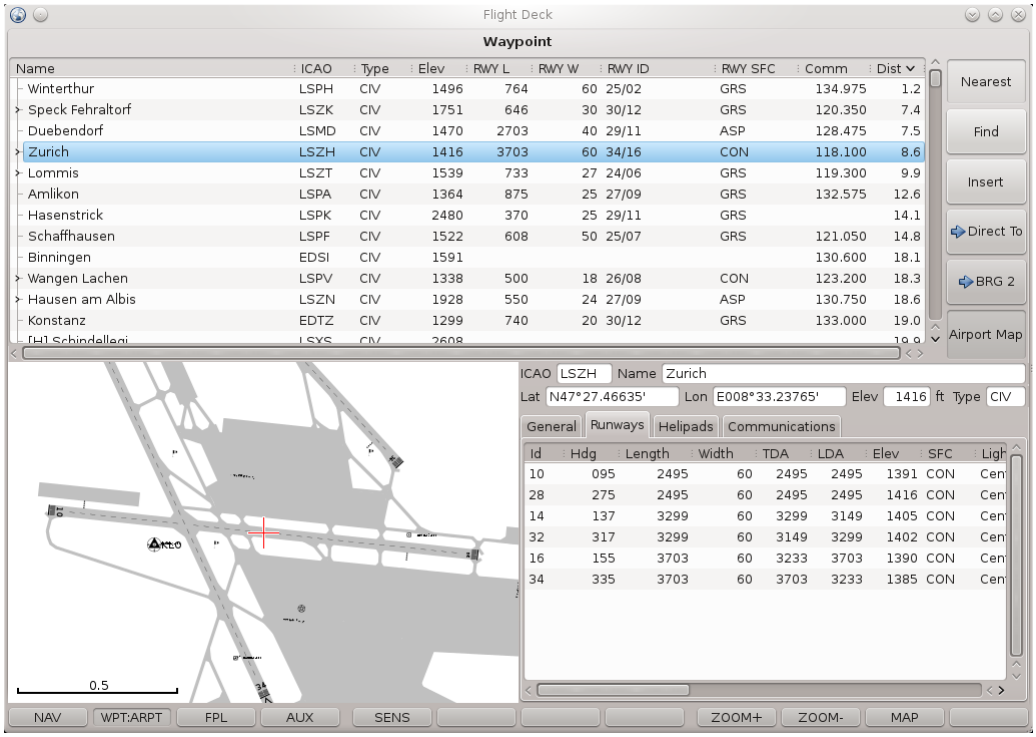

Figure 9: Waypoint Page: Airport with Airport Map

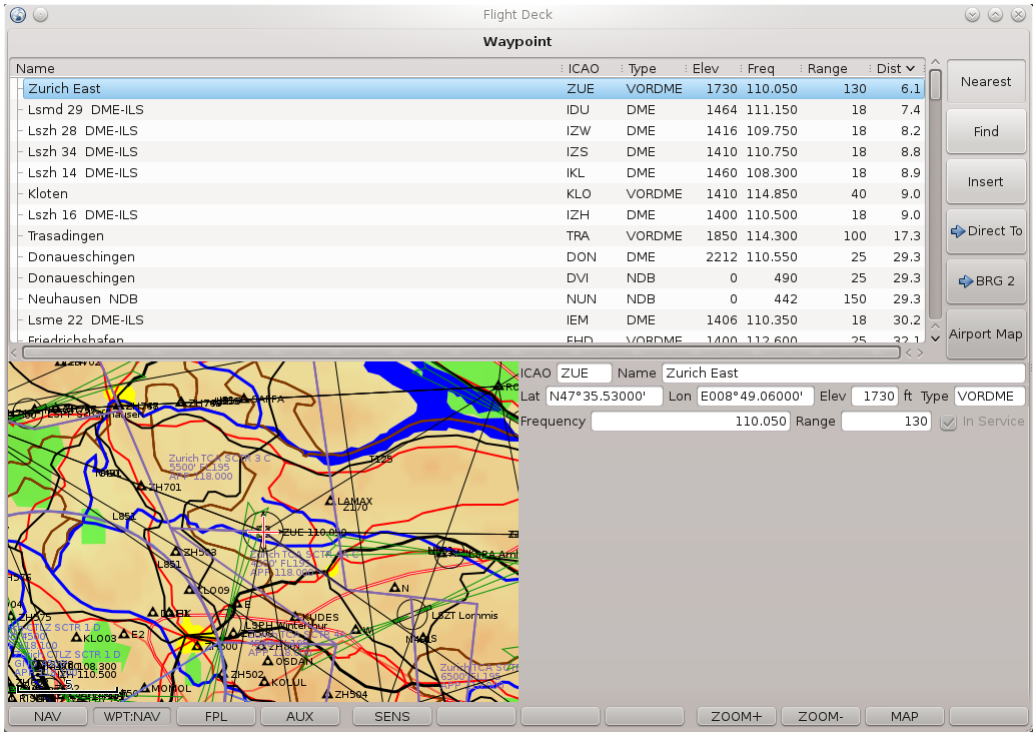

Figure 10: Waypoint Page: Navaid

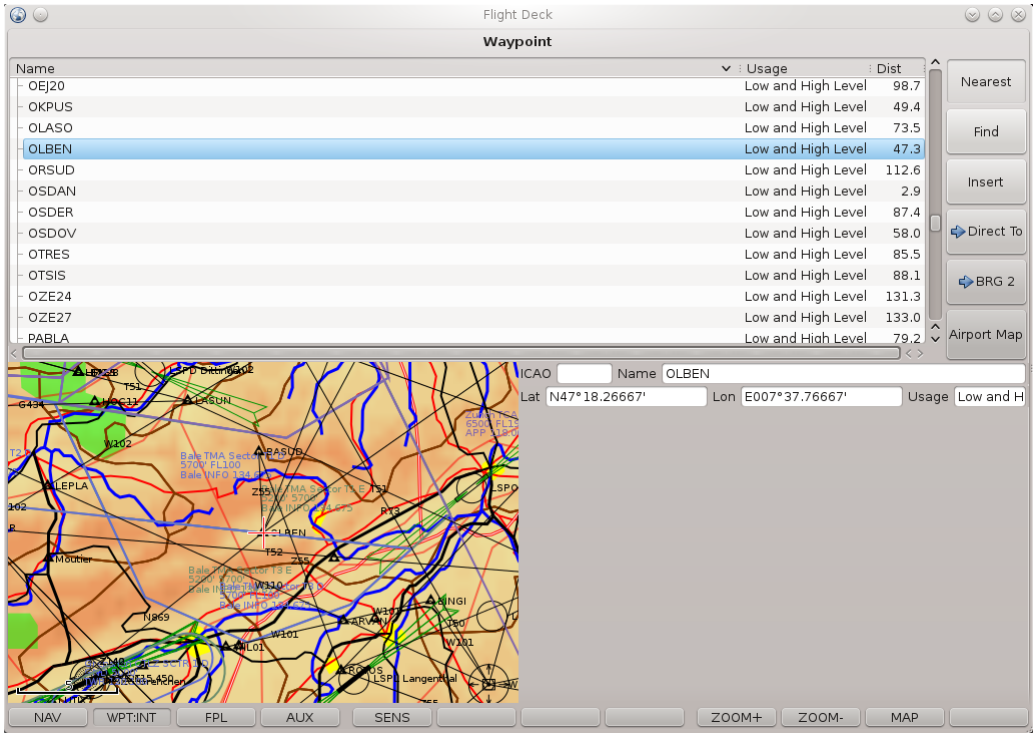

Figure 11: Waypoint Page: Intersection

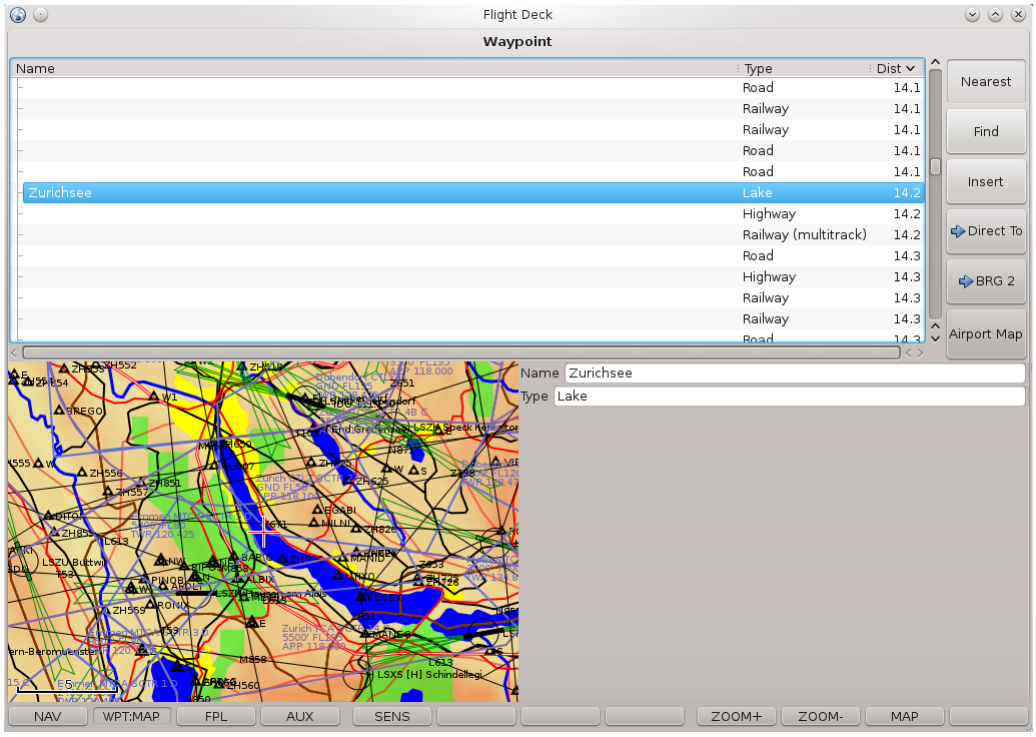

Figure 12: Waypoint Page: Map Element

MAP Change Map Mode (cycle through Vector Map, Terrain and Airport Map)

4 Flight Plan Page Group

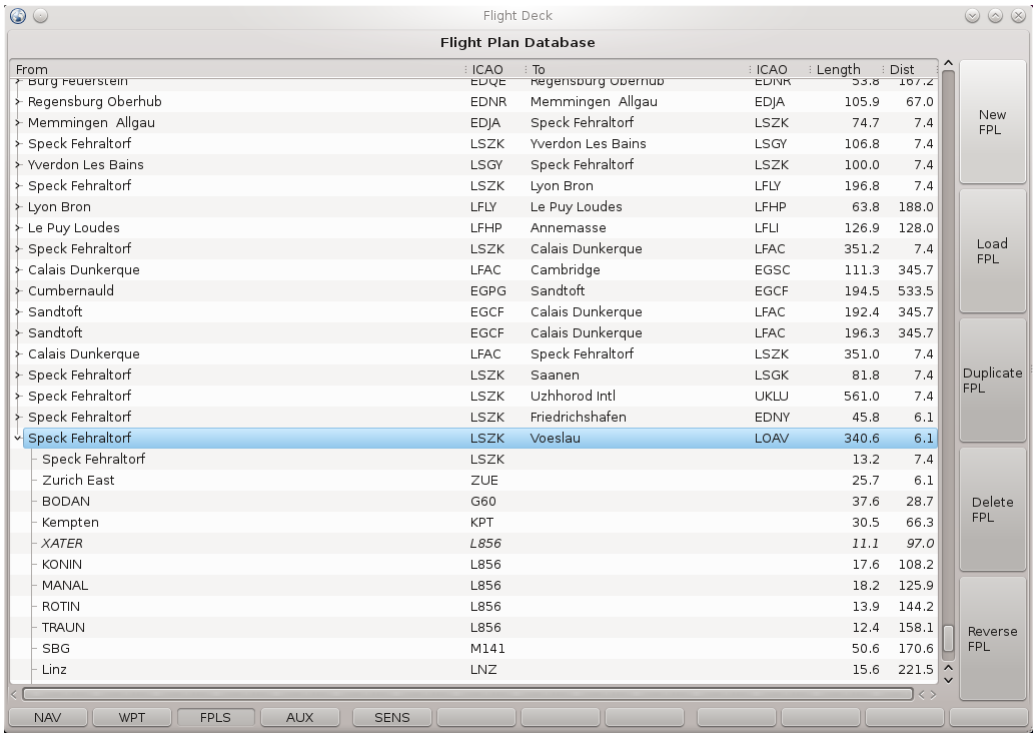

Figure 13: Flight Plan Browser Page

Figure 13 shows the Flight Plan Database Browser Page. It may be used to create a new flight plan, to load, delete, duplicate or reverse an existing flight plan.

To create a new flight plan, first select New FPL, then load the newly created empty flight plan.

4.1 Flight Plan Page

Figure 14 shows the flight plan editor. The top half displays the curent flight plan. The bottom left half displays the currently selected waypoint on a map. The bottom right half displays and allows to edit textual information about the currently selected waypoint.

Soft Keys

D:NORM Declutter Mode, same as in the main menu

ZOOM+ Zoom Map In

ZOOM− Zoom Map Out

SCRKBD Enable/Disable the on-screen keyboard (for touchscreen devices; Figure 15)

MAP Change Map Mode (cycle through Vector Map, Terrain and Airport Map)

Buttons

Insert WPT Duplicates the currently selected Waypoint, and opens the Waypoint Page in nearest mode, allowing to select a waypoint from the database

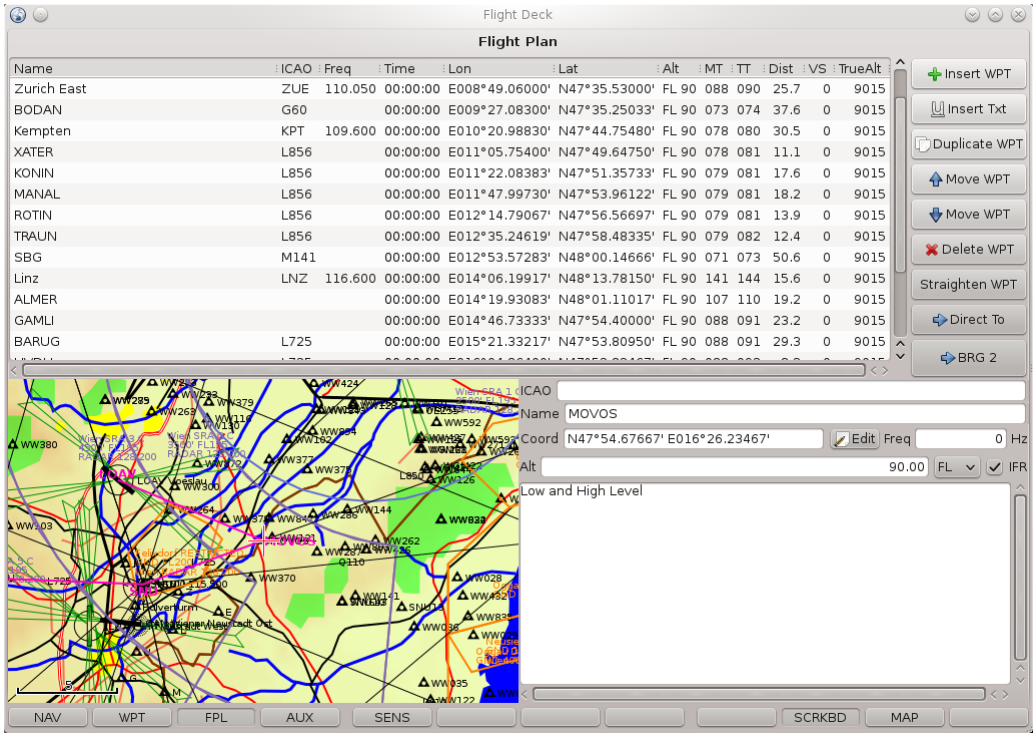

Figure 14: Flight Plan Editor Page

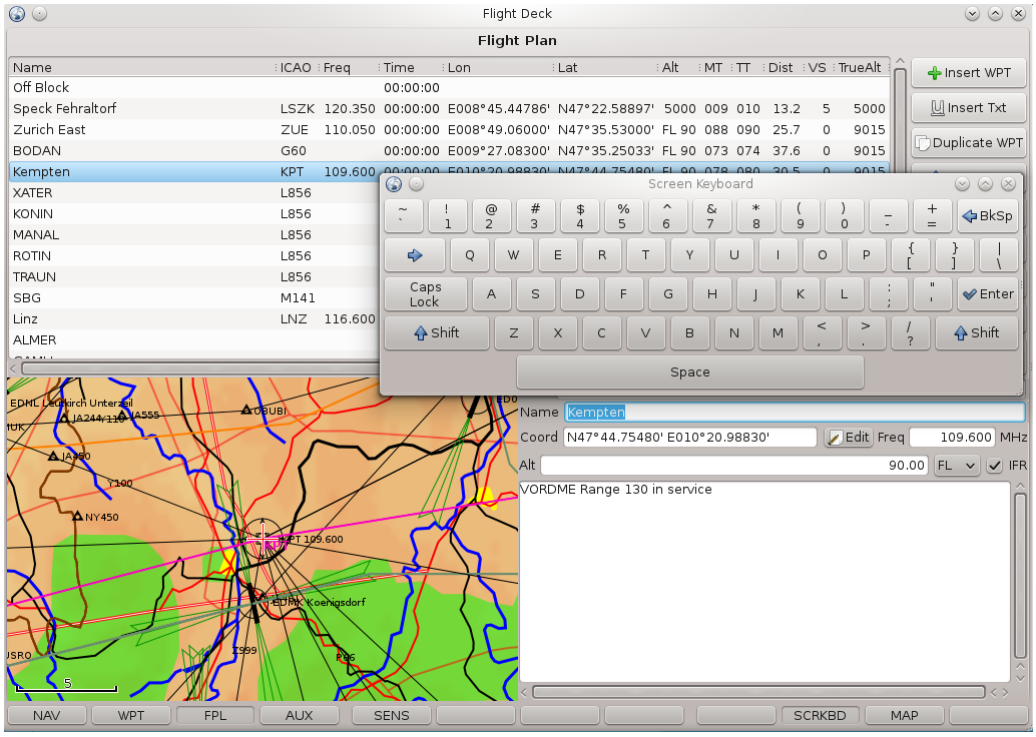

Figure 15: On Screen Keyboard

Figure 16: Flight Plan Text Entry

Insert Txt Opens the Flight Plan Text Entry Dialog (Figure 16), which allows multiple waypoints to be entered in "flight plan format", for example: "LSZK BARIG J51 WIL BINGI ARVAN LSZG". Points may include airports, intersections and navaids, or coordinates. Airways are also acceptable. It is not necessary to enter airway entry and exit points; if missing, the nearest point on the airway is searched and entered as well. This is usually the fastest method to enter a flight plan; some clean-up may be necessary though (mostly deleting unnecessary waypoints).

Duplicate WPT Duplicate the currently selected Waypoint

Move WPT Move the currently selected Waypoint up or down

Delete WPT Delete the currently selected Waypoint

Straighten WPT Shifts the currently selected Waypoint such that it lies on a straight line from the previous to the next Waypoint

Direct To Opens the Join dialog (Figure 17), which allows the user to select either Direct To the currently selected Waypoint, or Join the Leg between the previous and the currently selected Waypoint, and then start flight plan navigation

BRG 2 Point the second (cyan) HSI pointer to the currently selected Waypoint

Waypoint information may be edited directly in the lower right part of the page. Clicking on the Edit button opens the Coordinate Editor dialog (Figure 17), which offers additional options for entering coordinates (such as radial/distance from the current point, or even by clicking on the map).

5 Auxillary Page Group

The Auxillary Page Group contains an embedded document (PDF) reader suitable for quickly displaying approach charts, a performance calculator and sunrise/sunset information for the current flight plan.

5.1 Document Reader

Figure 18 shows the documents directory. FlightDeck searches user-selectable directories for displayable documents. It analyzes the file name of each document found, and determines which files may be relevant to each current flight plan waypoint. Furthermore, all documents found are also listed under the "all documents" heading.

Selecting a document and clicking on the AUX soft key leads to the document page.

Figure 19 shows the document page.

Soft Keys

FIT Toggles between Best Fit and Fit Width mode

ZOOM+ Zoom Document In

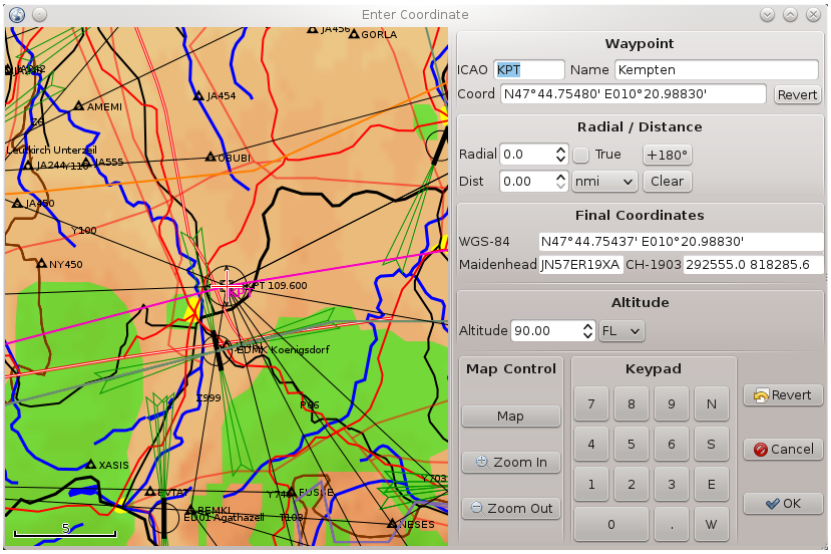

Figure 17: Coordinate Editor

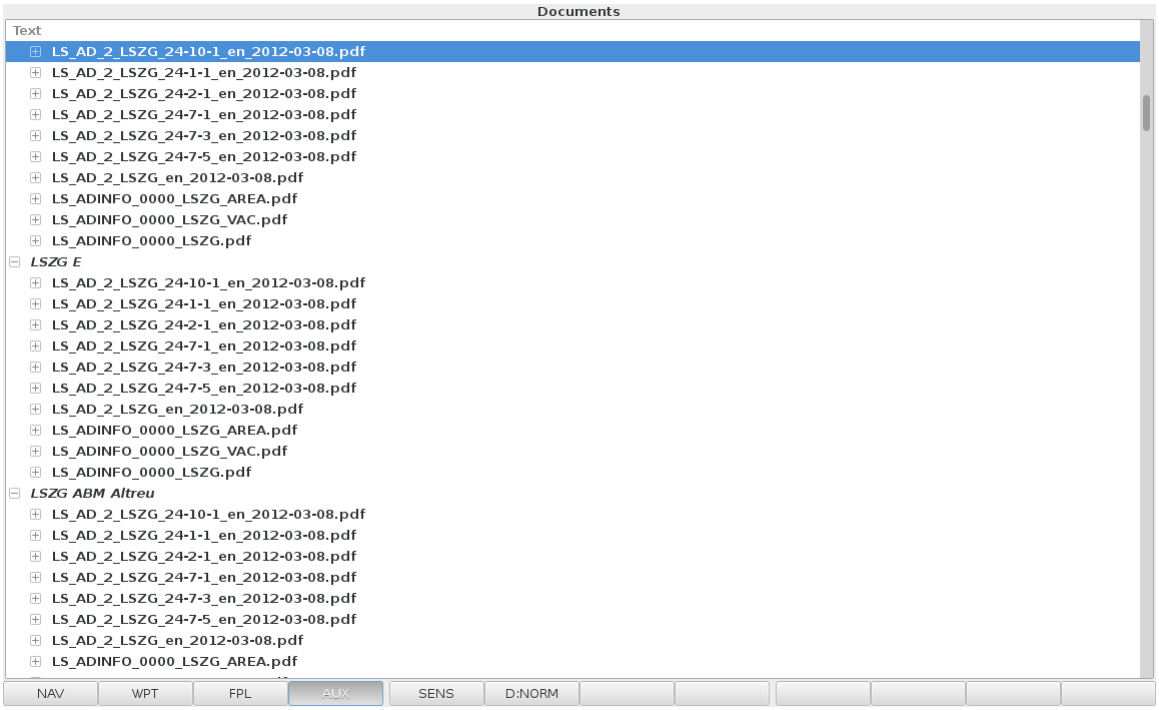

Figure 18: Documents Directory Page

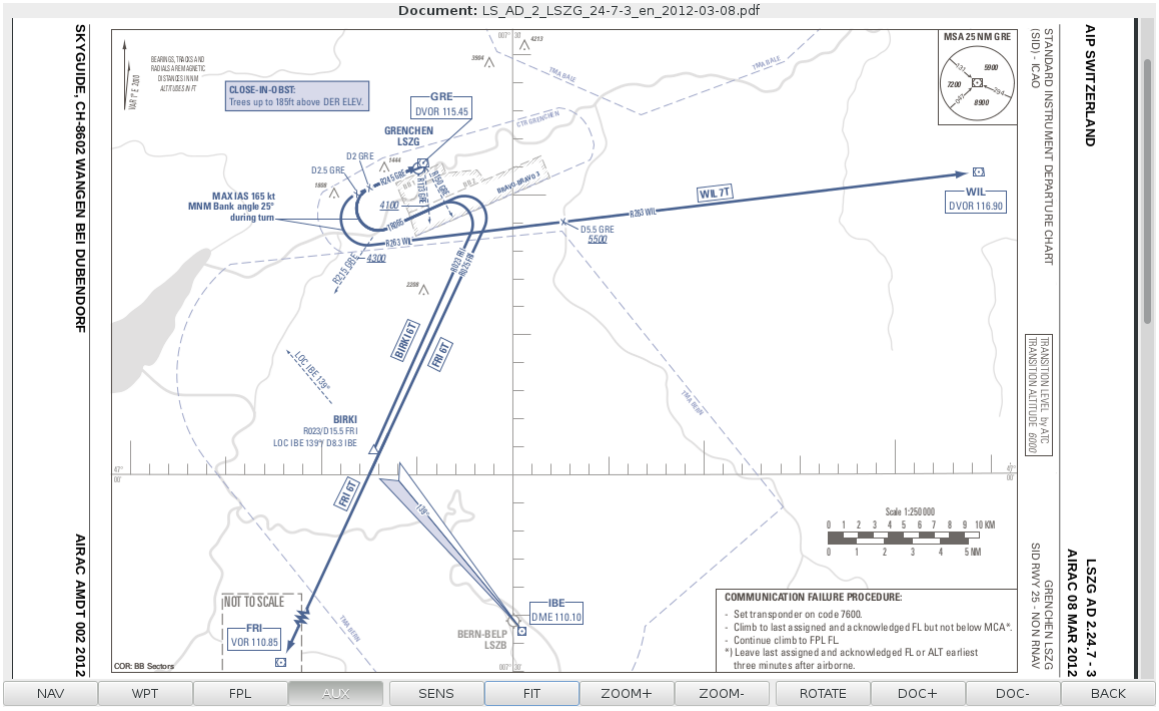

Figure 19: Document Page

ZOOM− Zoom Document Out

ROTATE Rotate Document by 90 degrees

DOC+ Advance to the next document in the list

DOC− Return to the previous document in the list

BACK Return to the Documents Directory Page

5.2 Performance Calculator

Figure 20 shows the performance calculator page. The left side computes takeoff and landing distances, while the right side computes the weight & balance graph.

Clicking on “From W&B” copies the masses from the Weight & Balance graph. The Takeoff mass is directly set from the Weight & Balance total mass, while the Landing mass has the total fuel (from the currently loaded flight plan) subtracted (but not more than sum total of the entered fuel in the Weight & Balance calculation).

Clicking on “From FPL” copies the takeoff and landing airfield elevations from the currently loaded Flight Plan.

5.3 Sunrise/Sunset Calculator

Figure 21 shows the Sunrise/Sunset calculator. The user may select a date, for which the calculator displays sunrise and sunset times (in UTC) for each waypoint of the currently loaded Flight Plan. Note that the calculator considers only geographical positions of the waypoints; the official day/night times may differ slightly due to country rules.

6 Sensors Page Group

Figure 22 shows the system log page.

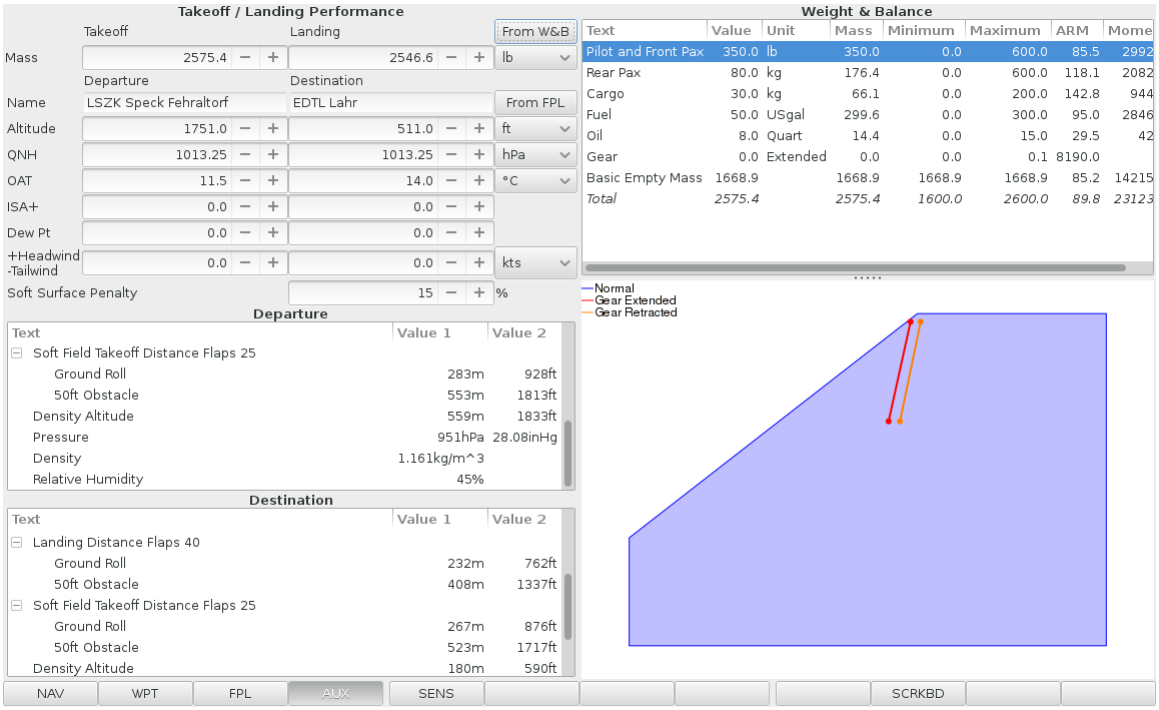

Figure 20: Performance Calculator Page

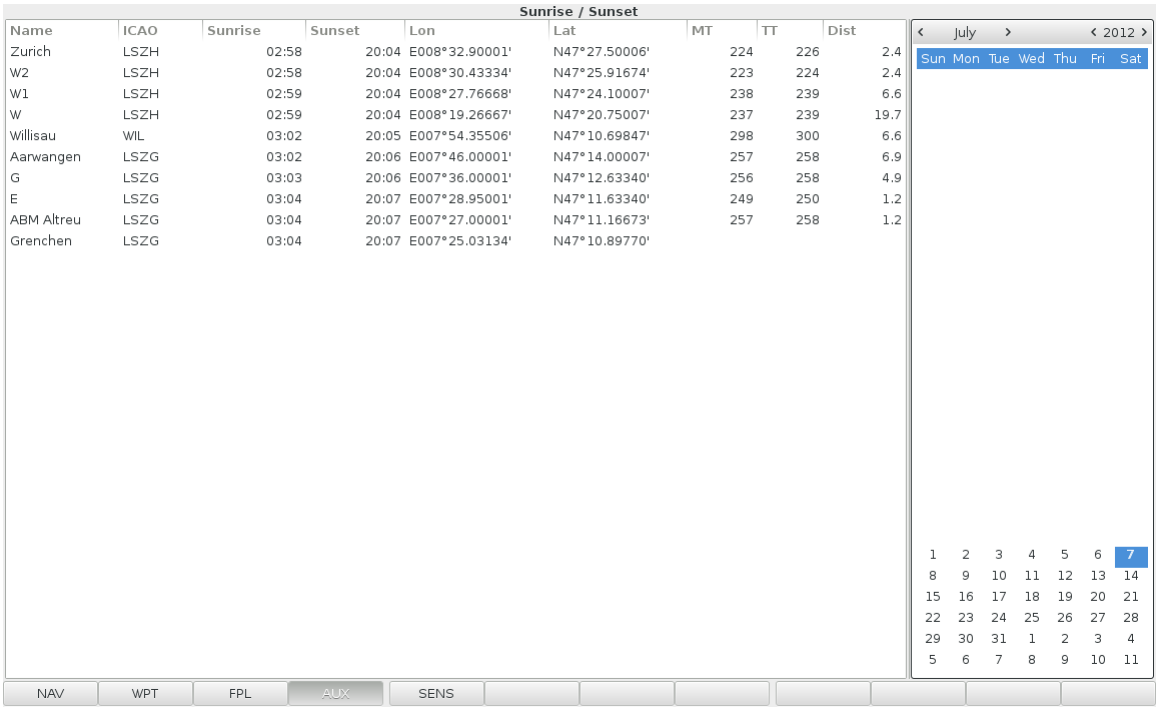

Figure 21: Page

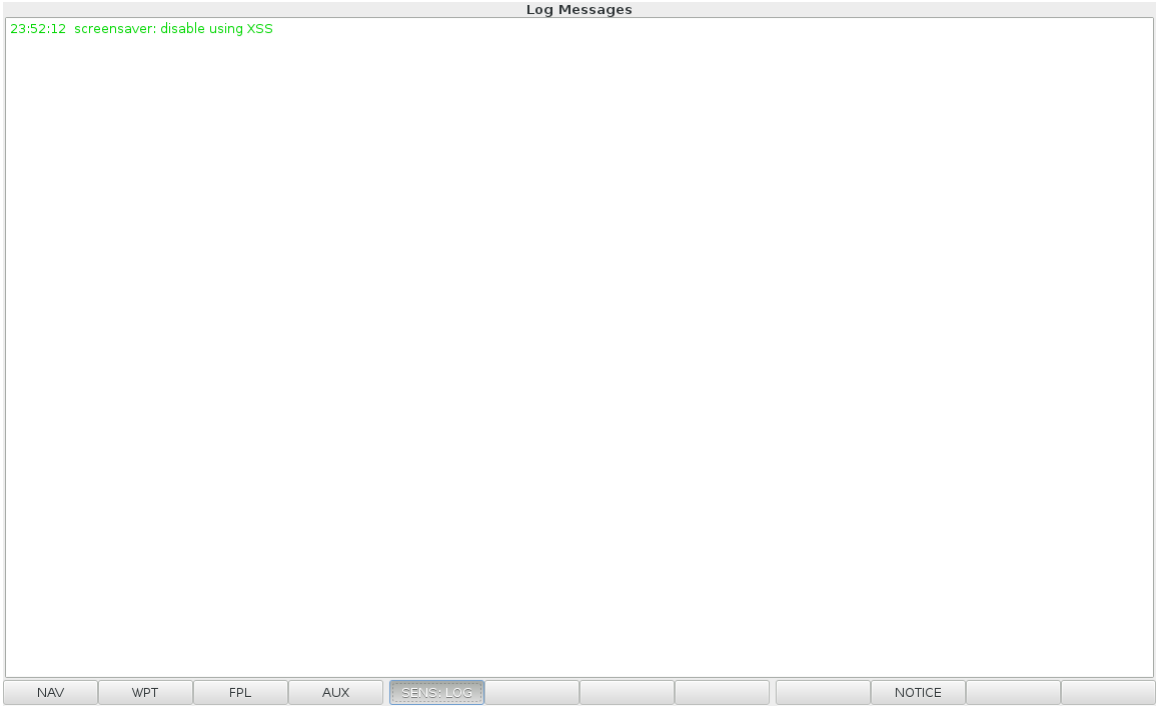

Figure 22: System Log Page

References

A Known Limitations

A.1 Windows Version

- Document Viewer is not available
- Only very limited I/O drivers available
- Lightly Tested

B Technical

B.1 IFR Autorouter

B.2 Introduction

IFR Flight planning in countries such as the United States is fairly simple. Given a RNAV equipped aircraft, flight plans between arbitrary waypoints may be filed with little restrictions.
Not so in the ECAC[1] region. An IFR flight plan must comply with many rules (more than 6000 early 2013) before it is accepted. When submitted to CFMU[2] in Bretigny or Brussels, a computer checks the flight plan and rejects it if any one of those rules is violated. IFR Flight Planning is even more complicated by the fact that the ECAC region is comprised by more than 20 states, each with sometimes significantly different rules.

IFR Flight Plans generally must follow the route network. Figure 23 shows an exceprt of the central Switzerland route network. The route network consists of Navigation Aids and Intersections. Intersections are

[1] European Civil Aviation Conference
[2] Central Flow Management Unit

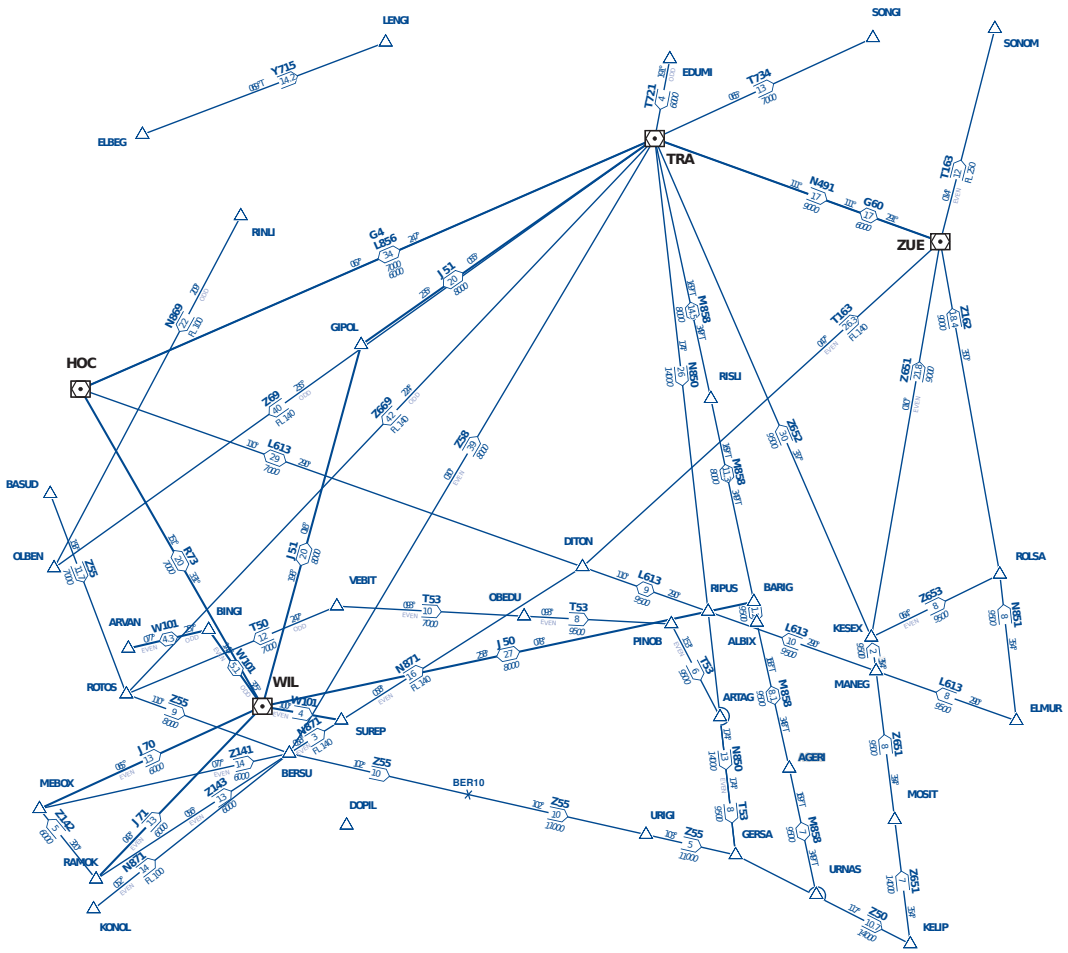

Figure 23: Central Switzerland Airway Network

specific coordinates that were given a 5 character identifier. Navaids and Intersections are connected by airway segment. An airway also has a name – for example G5 between WIL and FRI. Airways are often limited vertically. Furthermore, they may be unidirectional.
An IFR Flight Plan generally joins the route network at a point close to the departure aerodrome and leave the route network at a point close to the destination aerodrome. There are rules that govern which joining and leaving points are allowed.
Clearly, the complexity of finding an IFR Flight Plan that honours all rules, but also limitations of the aircraft, has become impractical to do by hand, especially for low flying aircraft and for the General Aviation community, where a Flight Plan is used only once. Flight Planning can easily exceed the flight time even for slow aircraft. There is therefore no way around automating construction of an acceptable IFR flight plan.
An autorouter should have the following desirable properties:

1. Minimal user input; ideally it should only require the departure and destination aerodrome, and the aircraft to be flown
2. Additional altitude restrictions, for example due to weather (icing)
3. Find the optimal route between the given aerodromes for the given aircraft; optimality criteria should include flight time and fuel consumption and be user selectable

The router descibed in this document achieves these properties. Additionally, it would be desirable to have the following additional properties:

1. Offline operation
2. Consider winds aloft

Offline operation is currently infeasible, unfortunately, as the rules are apparently not available completely in an electronically useable format.
Winds aloft awareness should be easy to add to the general algorithm structure.
The autorouter algorithm performs the following steps:

1. Construct Routing Graph
   (a) Add Navaid and Intersection vertices
   (b) Add Airway edges
   (c) Remove Intersections with non-flightplannable names
   (d) Add Direct-To (DCT) edges
   (e) Add Departure and Destination Aerodromes, and SID and STAR edges
2. Router Iteration
   (a) Find the (k-)shortest path in the Routing Graph from Departure to Destination
   (b) Check the path against the locally available rules
   (c) If the local check passes, submit it to the CFMU flight plan validation website
   (d) If it passes the CFMU test as well, we are done
   (e) (Try to) interpret the error messages; if an edge is clearly forbidden for all possible flight plans between these aerodromes, remove the edge from the Routing Graph and compute the shortest path during the next iteration, otherwise compute the next shortest path during the next iteration

B.3 Routing Graph Construction

Operations research provides us with a great many publications on algorithms for finding paths in graphs.
A graph consists of vertices and edges. Each edge connects two vertices. A directed graph (digraph) is a graph with directed edges (i.e. each edge may only be travelled in one direction). Parallel edges are allowed – there may be multiple airways between two intersections. Each edge has a “weight” – for example the distance, flight time, or fuel consumption when crossing the edge. A path through the graph from one vertex to another vertex may only follow edges; the weight of the path is the sum of the weights of the edges crossed. There are

efficient algorithms for computing the shortest path (minimum weight path) in a graph, for example the Dijkstra algorithm. Unfortunately, computing the second best or kth best path is significantly harder (for example the Yen algorithm).
The digraph concept matches the airway network well. Navaids and Intersections correspond to vertices, and airway segments to edges.
What weight should the edges be given? Distance might be chosen, but usually, the user is not interested in the shortest route, as the shortest route may require a high flight level and a long climb. A slightly longer route on a lower flight level may be faster, especially on aircraft equipped with normally aspirated engines. So the weight is set to either the travel time on the leg, or the fuel consumption, depending on user selection.
What altitude should be chosen for a flight plan? Often, no compliant route exists between two aerodromes on a single flight level, or large detours would have to be flown. Therefore, the autorouter should be able to handle level changes on every flight plan leg. On the other hand, the user should not need to select the altitude; the router should automatically select the best altitude from an aircraft model and the terrain. It should be possible, however, to restrict the altitude range, for example because of icing. So how can flight levels be mapped to the graph concept?

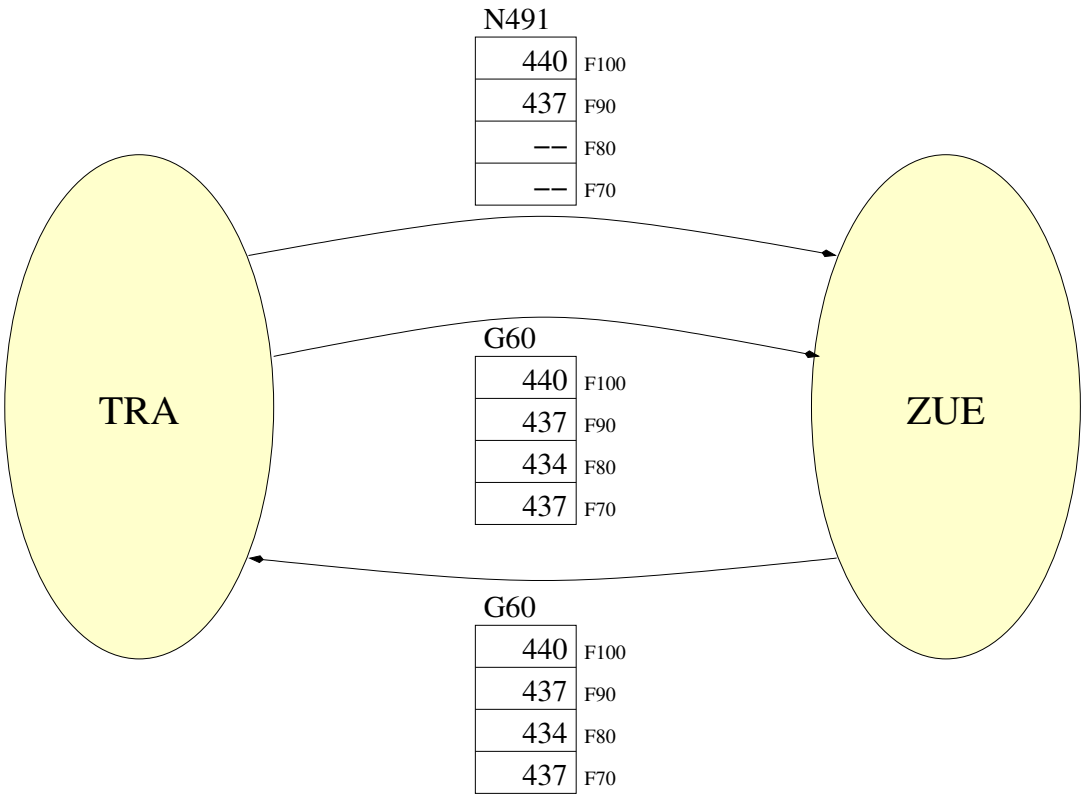

Figure 24: Routing Graph

Figure 24 shows the solution. Consider flight planning on four levels from FL70 to FL100, for simplicity. Navaids and Intersections map to vertices.
Each airway edge carries not just one "weight", but a table of "weights" for each flight level, in this case travel time in seconds. Figure 24 also shows level and directionality constraints, see N491 which only exists at FL090 and higher, and only in the direction TRA→ZUE. Nonexisting levels are marked with NaN (not a number).
Level changes are handled by using a modified version of the Dijkstra algorithm, that does not just keep track of vertices, but also of levels. If the algorithm tries a level change, it adjusts the edge weight. For climbs, it adds the additional time or fuel needed for the climb. This figure is computed using the aircraft performance model. In descent, no adjustment is made. It could theoretically be negative; however, in my experience, in practice, I am seldom allowed to fly an optimal descent towards the destination, I almost always arrive at close

to the cruise level in the vincinity of the destination, and then need additional track miles for the descent. Therefore, I have chosen to not give credits for descent.
Increasingly, airways contain points that are not flight-plannable (i.e. may not be submitted in a flight plan). An example above is BER10 between BERSU and URIGI. These points need to be removed; all edges incident on such vertices need to be replaced by edges between predecessor and successor vertices, with the weight set to the sum of the weight of the inbound and the outbound edge. Only pairs of inbound and outbound edges belonging to the same flight level and the same airway should be considered.
Besides airway segments, direct routes may be allowed under some conditions, for example BERSU to WIL in the graph above. The conditions where direct-to segments (DCT) are allowed differ greatly from country to country. Switzerland and Austria are very restrictive, in Germany and parts of France they are allowed for low level IFR up to a certain leg length, while in Poland it is often the only possibility due to the thin low level route network. Clearly, the router has to support direct-to segments.
DCT edges are added on all (super-)vertex pairs up to a configurable maximum. DCT edges are not added if an airway route that is not significantly longer (currently 1%) than the DCT is available. Furthermore, DCT edges are only added for altitudes 1000ft above terrain (or 2000ft if the terrain is higher than 5000ft). Terrain altitudes are computed in a corridor ±5 nautical miles around the center line.
Finally, the departure and destination aerodrome vertex needs to be added. These are simple vertices, as the aerodrome has a fixed altitude. From the departure aerodrome vertex, an SID edge is added to every flight level of every possible entry point. Similarily, STAR edges are added to the destination aerodrome vertex. Entry and exit points may either be specified, or every point with a maximum configurable distance is tried. Since procedure databases with exact routings are not available to me and the actual runway used is not known at flight planning time, the direct distance between the aerodrome and the entry/exit point is computed. The weight is then the time or fuel needed to travel that distance at the flight level at the entry/exit point. For SID edges, the weight is increased by the additional time or fuel needed to climb from aerodrome elevation to the given flight level; for STAR edges, the weight is not reduced by the descent, for the reasons given above.
Due to the flight plan format and the way the CFMU checker works, the flight level must not be changed immediately after the SID or before the STAR. This is enforced by duplicating the entry and exit supervertex without level change edges, and duplicating all other incident edges.

B.4 Waypoint Sequencing

Waypoint sequencing switches to the next waypoint whenever it determines that the turn must be initiated to smoothly reach the next track (it assumes all waypoints are fly-by waypoints at the moment!).

$\alpha = \text{OutboundTrack} - \text{InboundRadial}$ is the angle describing the course change.
$r = \frac{v \cdot 2\text{min}}{2\pi}$ is the radius of a standard rate turn.
$d = \frac{r}{\tan\frac{\alpha}{2}}$ is the distance from the waypoint where the turn must be initiated.
$\tau = (\frac{\pi}{2} - \frac{\alpha}{2}) \cdot 2 \cdot \frac{r}{v} = (\pi - \alpha)\frac{r}{v} = (\pi - \alpha)\frac{2\text{min}}{2\pi} = (1 - \frac{\alpha}{\pi})1\text{min}$ is the time needed to fly half the arc between inbound radial and outbound track.

B.5 MS5534 Interface

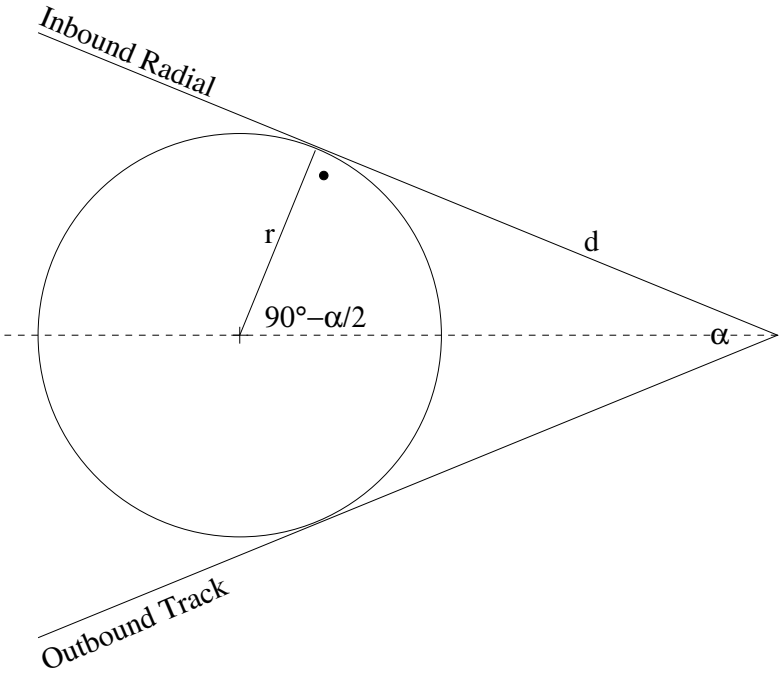

Figure 25: Waypoint Sequencing Geometry

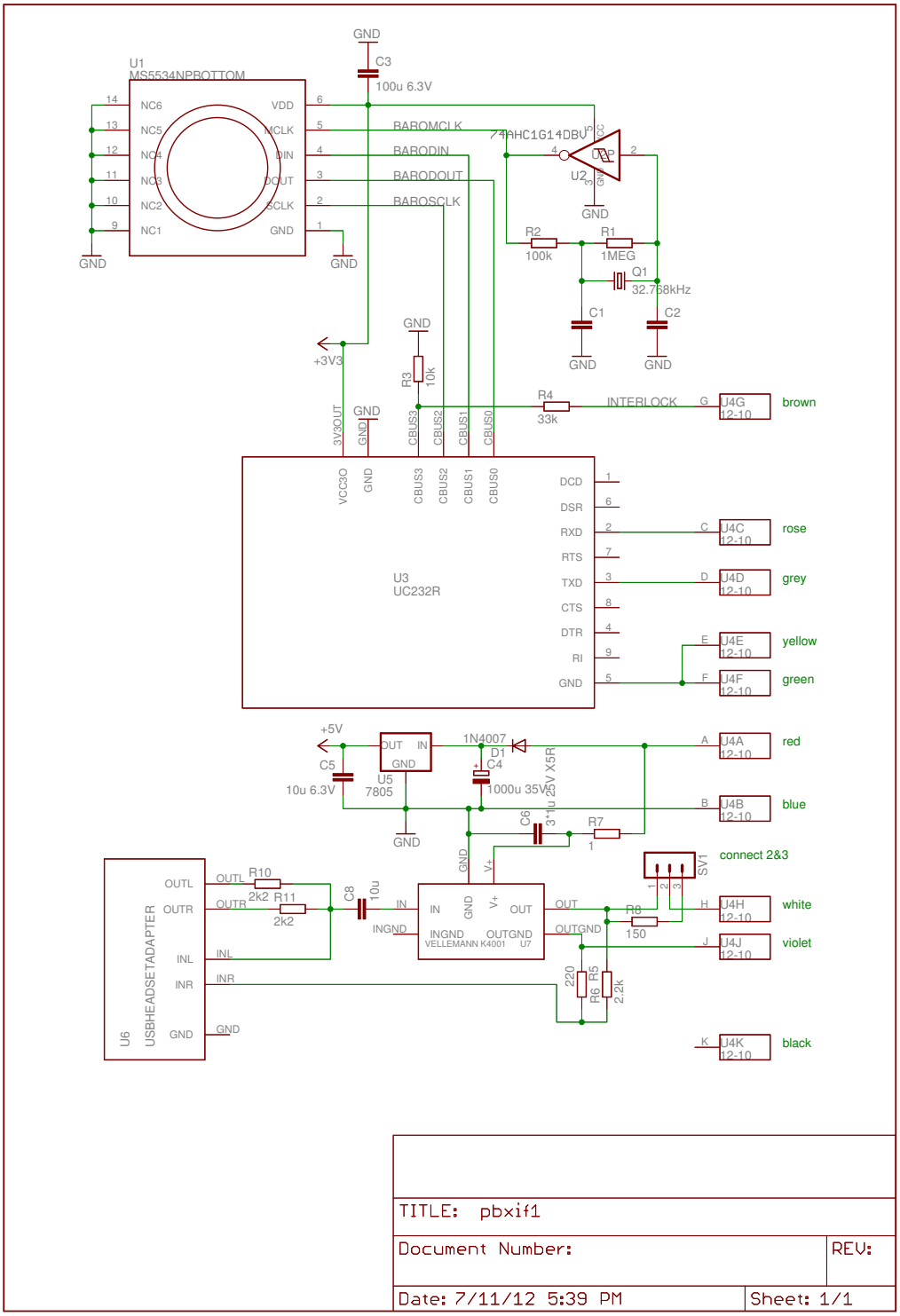

Figure 26: MS5534 Interface

B.6 Weather Charts

B.6.1 Barycentric Interpolation

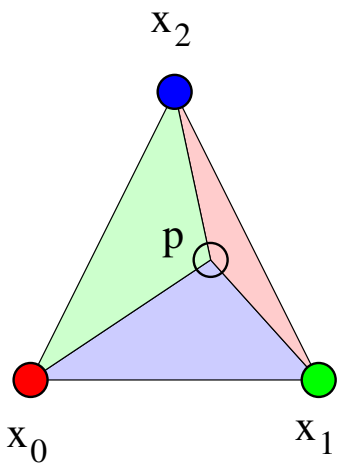

Figure 27: Barycentric Coordinates in a Triangle

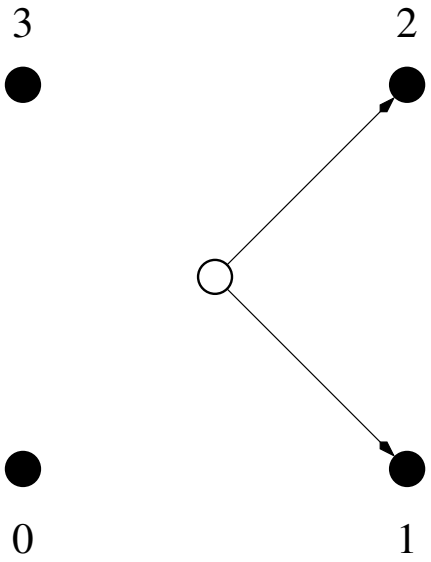

Figure 28: Barycentric Coordinates in a Triangle

The barycentric coordinates are given by

$$(a_0 + a_1 + a_2) \cdot \vec{p} = a_0 \cdot \vec{x_0} + a_1 \cdot \vec{x_1} + a_2 \cdot \vec{x_2} \tag{1}$$

Additionally, $a_0 + a_1 + a_2 = 1$ to make them unique.
The ratio between barycentric coordinates is the same as the ratio of the correspondingly coloured triangles.
The interpolated value for $\vec{p}$ is the sum of the triangle vertex values weighted by their correspondic barycentric coordinate.
In order to interpolate within a rectangle, the rectangle is decomposed into four triangles each consisting of the center point (whose value is the average of all four corner points) and two of the corner points.
Assume $x_0 = x_2$, $x_1 = x_3$, $y_0 = y_1$ and $y_2 = y_3$.
Set:

$$a_3 = \frac{x_p - x_0}{x_1 - x_0} \frac{y_p - y_0}{y_2 - y_0} \tag{2}$$

$$a_2 = \frac{x_p - x_1}{x_0 - x_1}\frac{y_p - y_0}{y_2 - y_0} \tag{3}$$

$$a_1 = \frac{x_p - x_0}{x_1 - x_0}\frac{y_p - y_2}{y_0 - y_2} \tag{4}$$

$$a_0 = \frac{x_p - x_1}{x_0 - x_1}\frac{y_p - y_2}{y_0 - y_2} \tag{5}$$

$$\begin{aligned}\sum_{i=0}^{3} a_i &= \frac{x_p - x_0}{x_1 - x_0}\frac{y_p - y_0}{y_2 - y_0} + \frac{x_p - x_1}{x_0 - x_1}\frac{y_p - y_0}{y_2 - y_0} + \frac{x_p - x_0}{x_1 - x_0}\frac{y_p - y_2}{y_0 - y_2} + \frac{x_p - x_1}{x_0 - x_1}\frac{y_p - y_2}{y_0 - y_2} \\ &= \frac{x_p - x_0 - x_p + x_1}{x_1 - x_0}\frac{y_p - y_0}{y_2 - y_0} + \frac{x_p - x_0 - x_p + x_1}{x_1 - x_0}\frac{y_p - y_2}{y_0 - y_2} \\ &= \frac{y_p - y_0}{y_2 - y_0} + \frac{y_p - y_2}{y_0 - y_2} = \frac{y_p - y_0 - y_p + y_2}{y_2 - y_0} = 1\end{aligned} \tag{6}$$

$$\begin{aligned}\sum_{i=0}^{3} a_i x_i &= \frac{x_p - x_1}{x_0 - x_1}\frac{y_p - y_2}{y_0 - y_2}x_0 + \frac{x_p - x_0}{x_1 - x_0}\frac{y_p - y_2}{y_0 - y_2}x_1 + \frac{x_p - x_1}{x_0 - x_1}\frac{y_p - y_0}{y_2 - y_0}x_0 + \frac{x_p - x_0}{x_1 - x_0}\frac{y_p - y_0}{y_2 - y_0}x_1 \\ &= \frac{x_p - x_1}{x_0 - x_1}x_0 + \frac{x_p - x_0}{x_1 - x_0}x_1 = \frac{x_0 x_p - x_0 x_1 + x_1 x_0 - x_1 x_p}{x_0 - x_1} = x_p\frac{x_0 - x_1}{x_0 - x_1} = x_p\end{aligned} \tag{7}$$

$$\begin{aligned}\sum_{i=0}^{3} a_i y_i &= \frac{x_p - x_1}{x_0 - x_1}\frac{y_p - y_2}{y_0 - y_2}y_0 + \frac{x_p - x_0}{x_1 - x_0}\frac{y_p - y_2}{y_0 - y_2}y_0 + \frac{x_p - x_1}{x_0 - x_1}\frac{y_p - y_0}{y_2 - y_0}y_2 + \frac{x_p - x_0}{x_1 - x_0}\frac{y_p - y_0}{y_2 - y_0}y_2 \\ &= \frac{y_p - y_2}{y_0 - y_2}y_0 + \frac{y_p - y_0}{y_2 - y_0}y_2 = \frac{y_0 y_p - y_0 y_2 + y_2 y_0 - y_2 y_p}{y_0 - y_2} = y_p\frac{y_0 - y_2}{y_0 - y_2} = y_p\end{aligned} \tag{8}$$

B.6.2 Contour Extraction

Contour Extraction works clockwise around points "inside" (i.e. whose value is greater than the contour line value). There are 5 cases (and rotational symmetric variants) to consider.

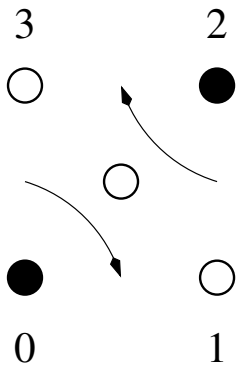

Figure 29: Contour 1–1

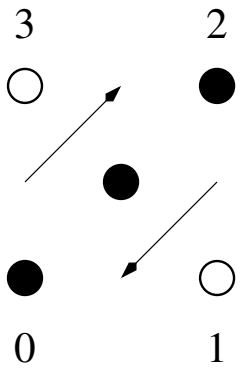

Figure 30: Contour 1–1

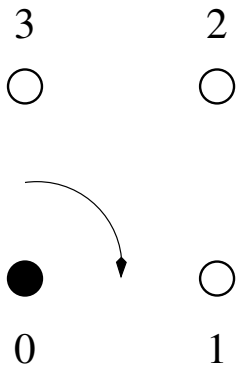

Figure 31: Contour 1

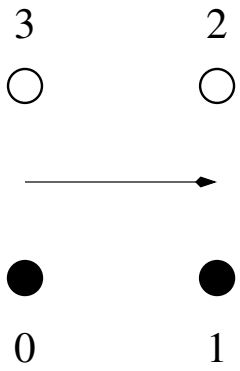

Figure 32: Contour 2

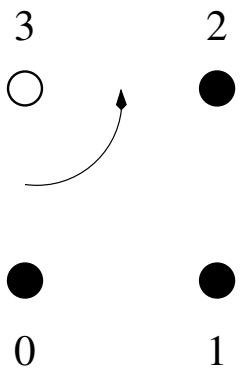

Figure 33: Contour 3

B.7 Physical Airframe / Engine Model

B.7.1 Propeller

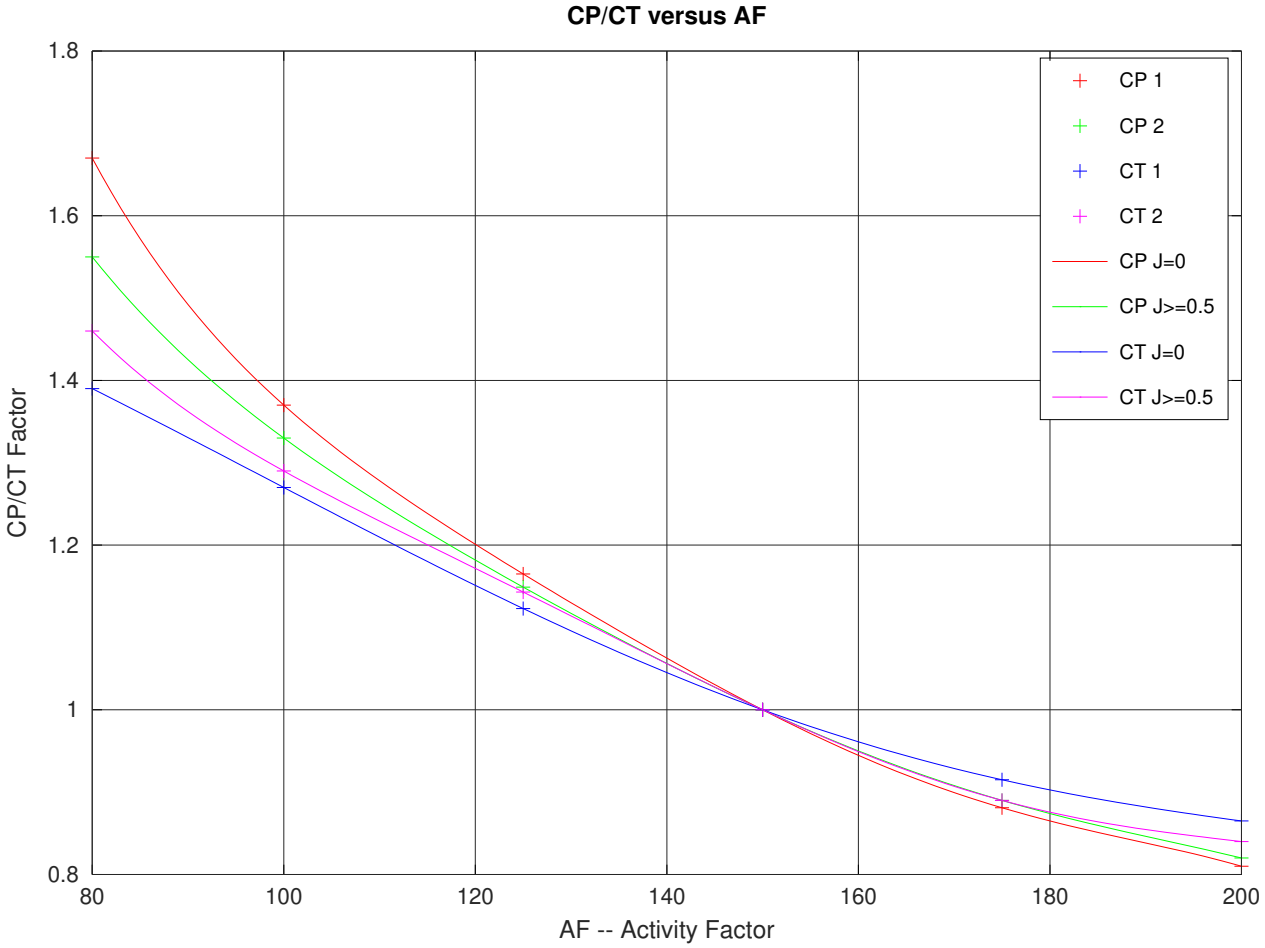

Figure 34: P_{CP}/P_{CT} versus Propeller Activity Factor AF

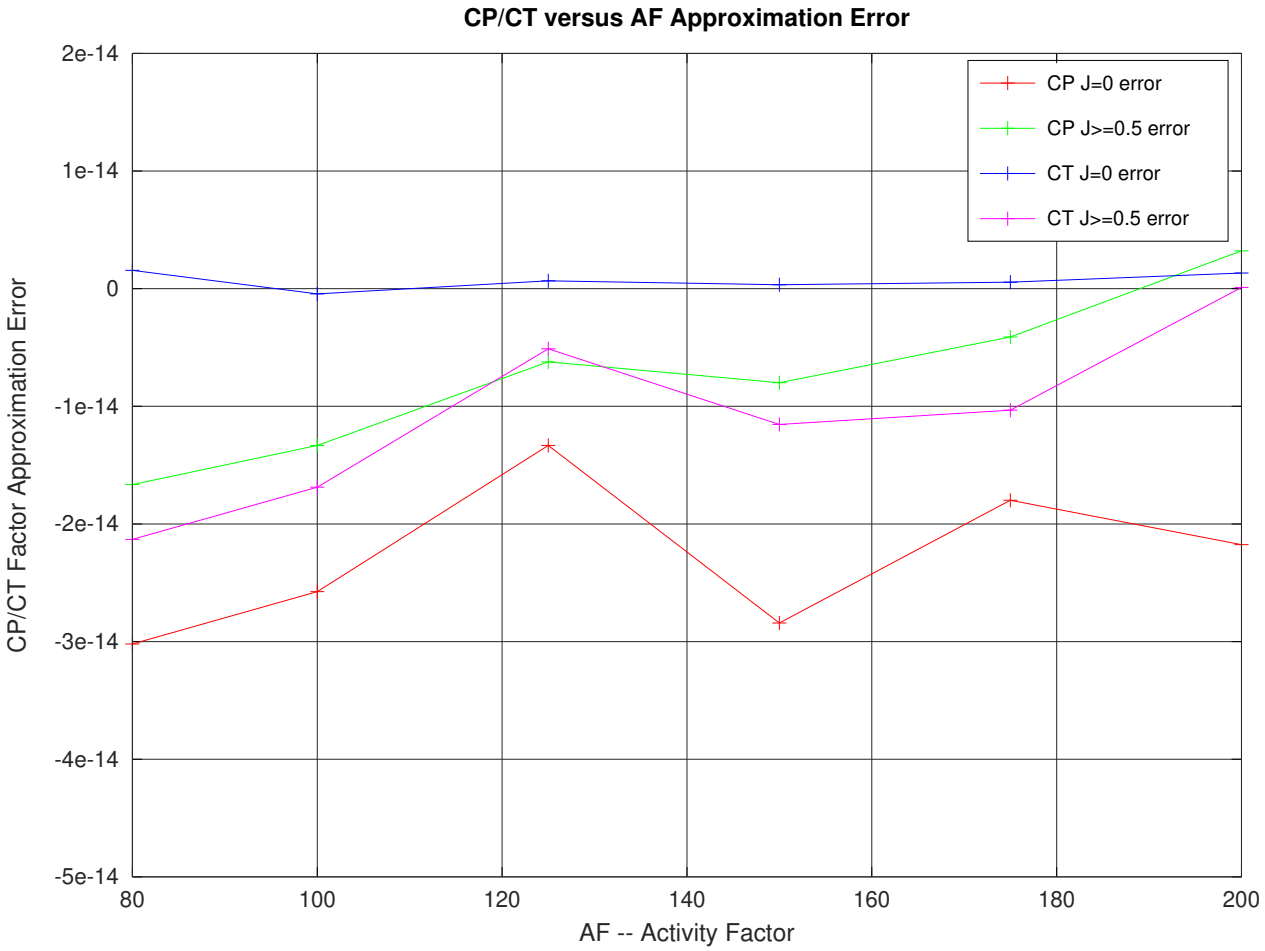

Figure 35: P_{CP}/P_{CT} versus Propeller Activity Factor AF Approximation Error

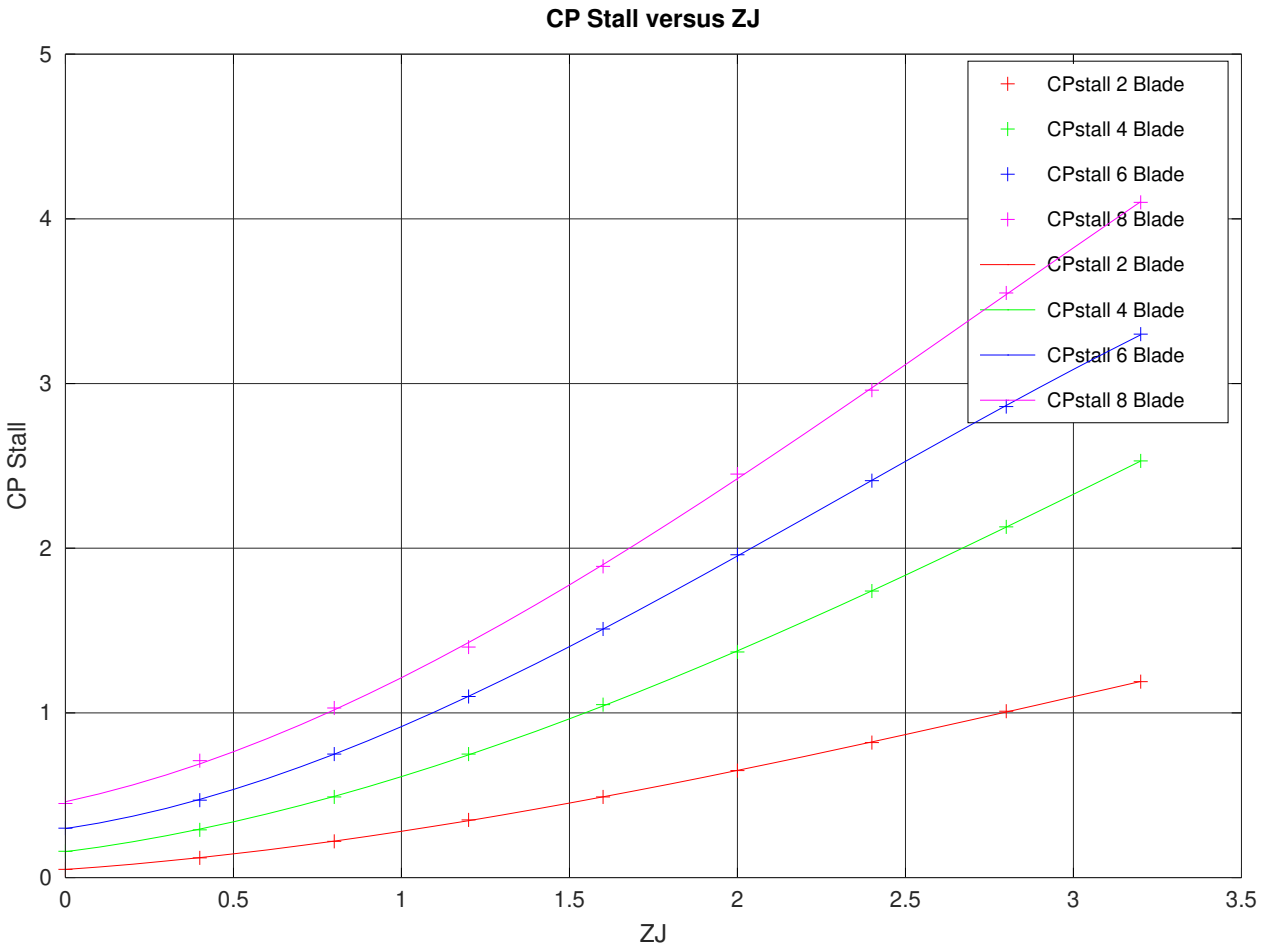

Figure 36: C_P where 50% of the propeller is stalled versus J

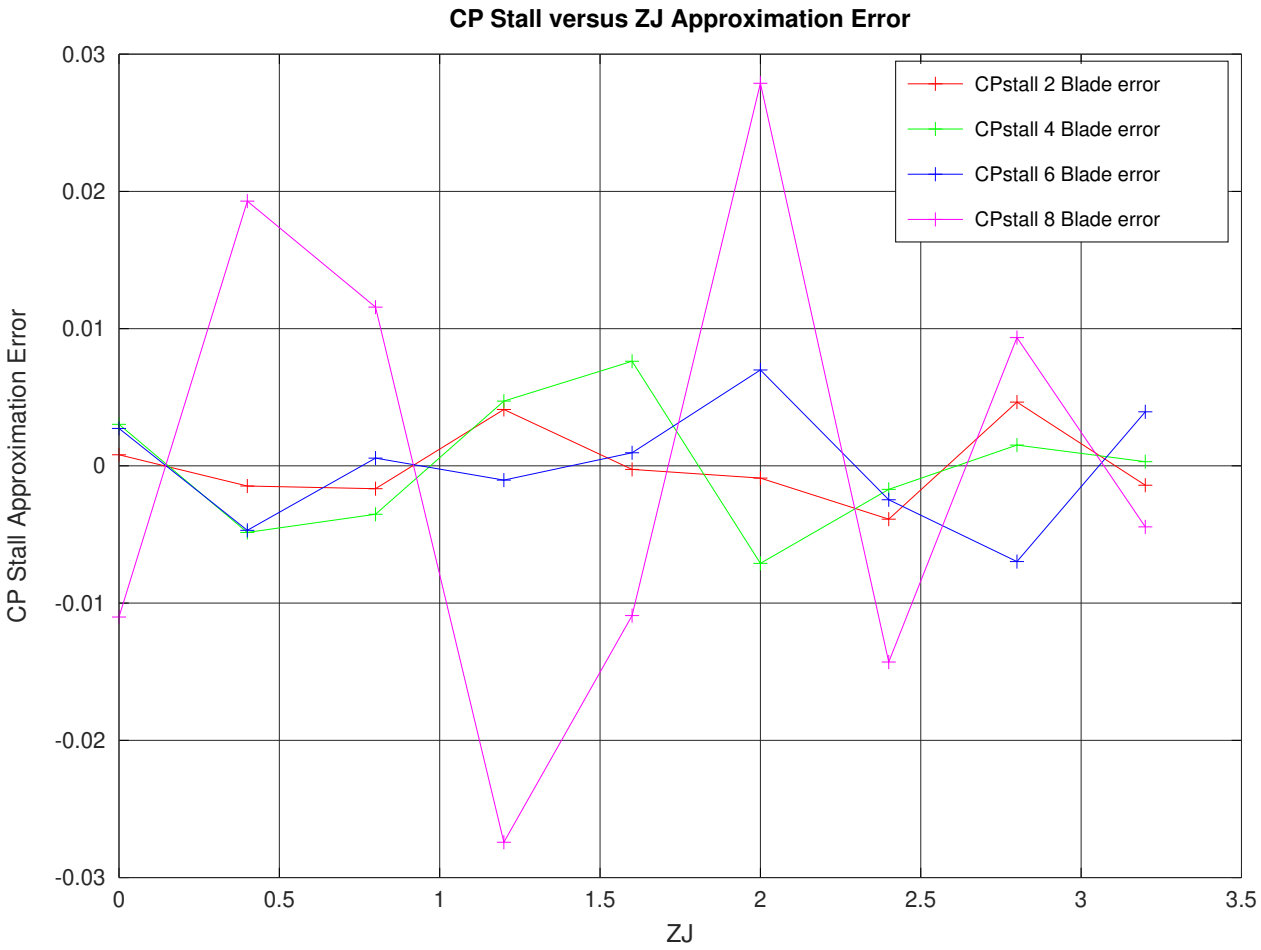

Figure 37: C_P where 50% of the propeller is stalled versus J Approximation Error

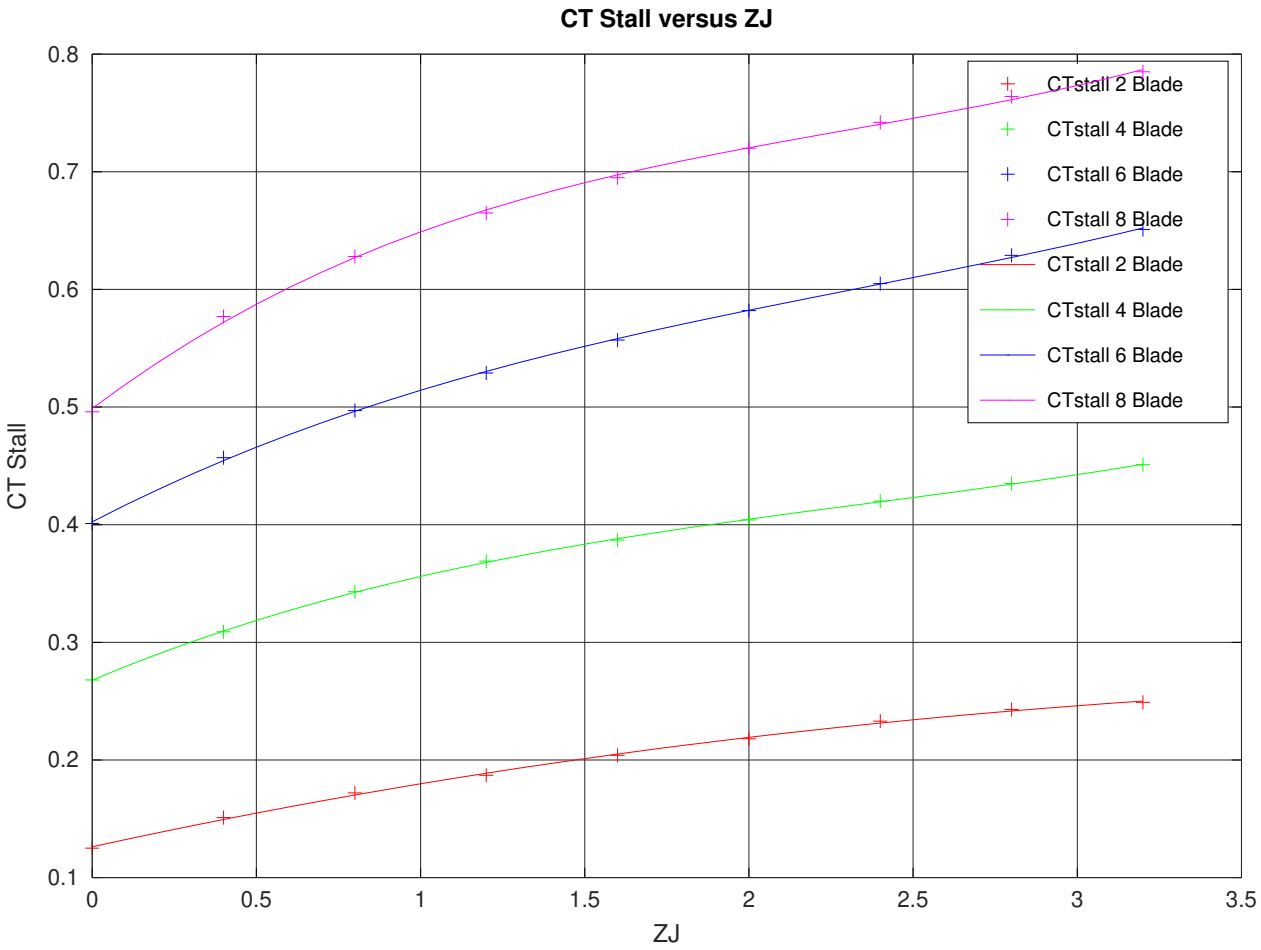

Figure 38: C_T where 50% of the propeller is stalled versus J

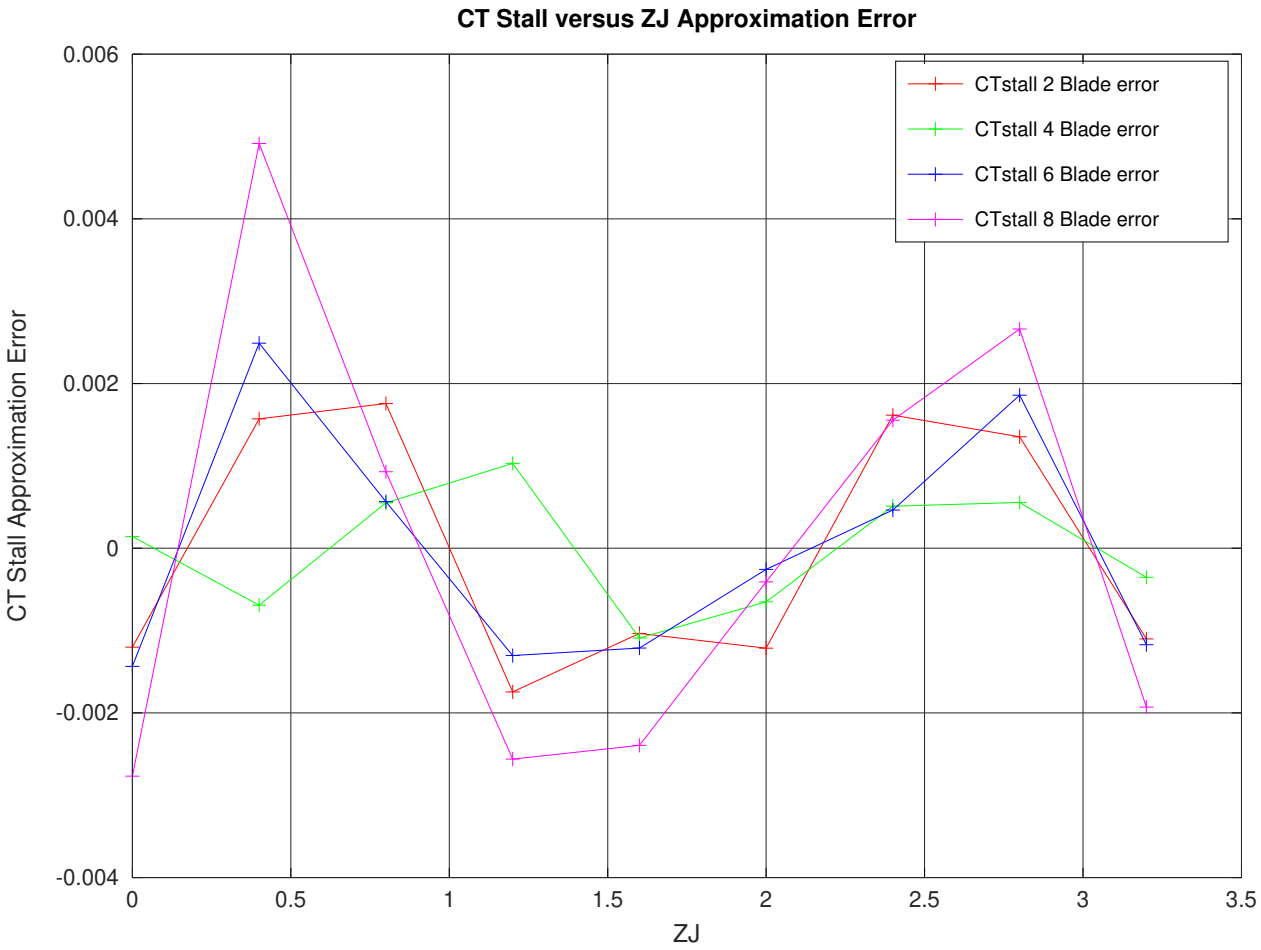

Figure 39: C_T where 50% of the propeller is stalled versus J Approximation Error

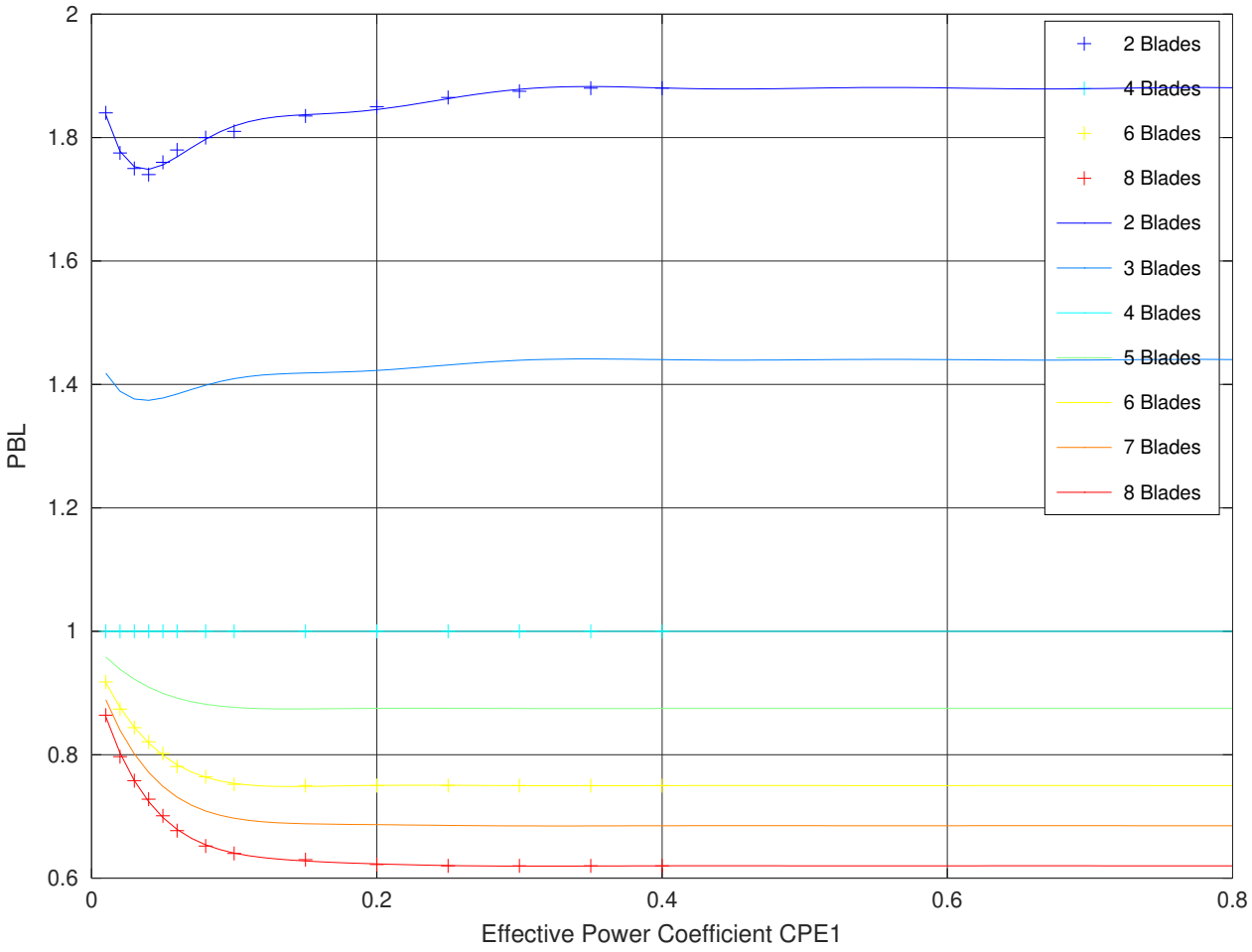

Figure 40: P_{BL}

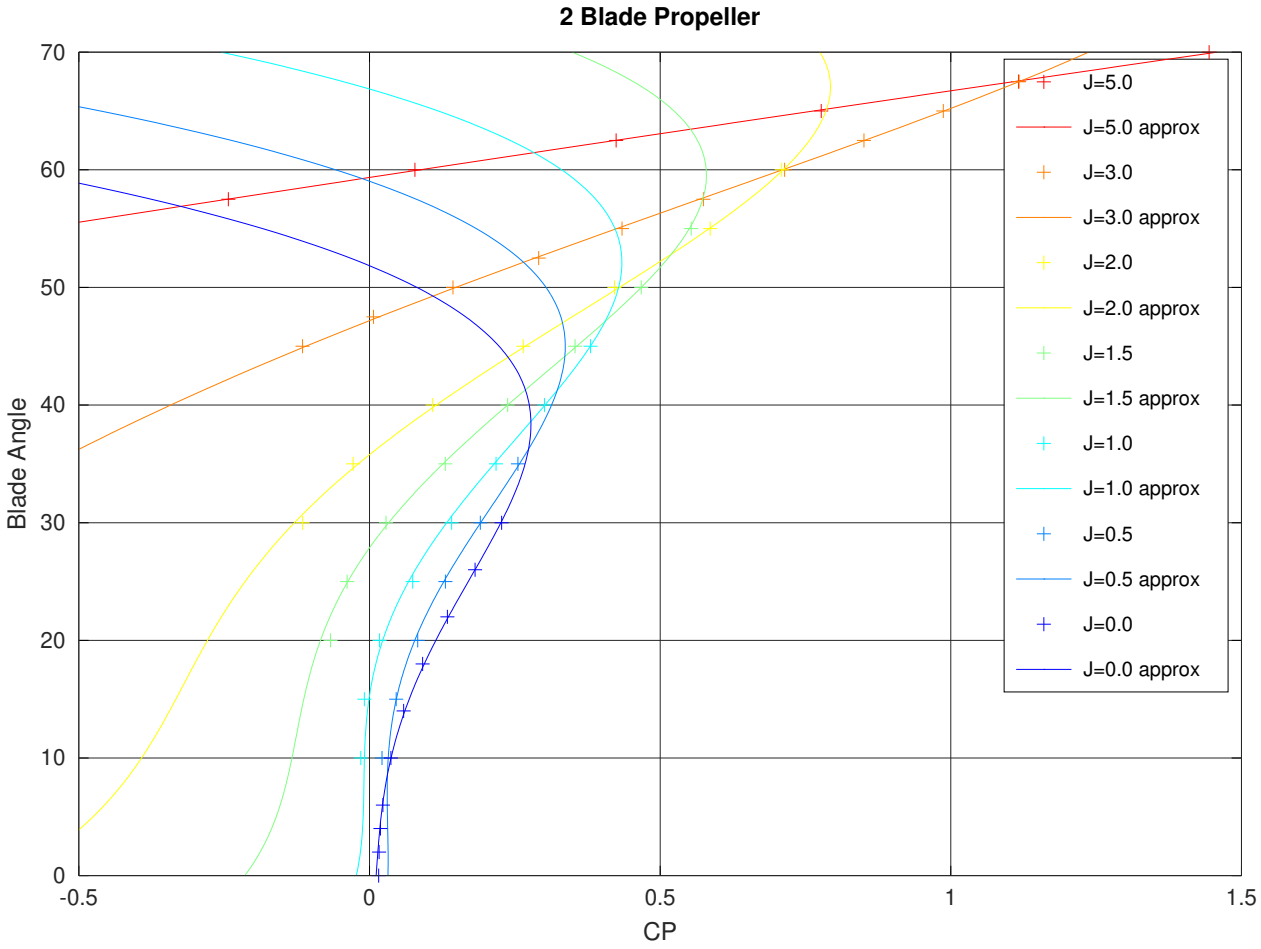

Figure 41: C_P versus Blade Angle $\beta_{3/4}$ for a 2 Blade Propeller

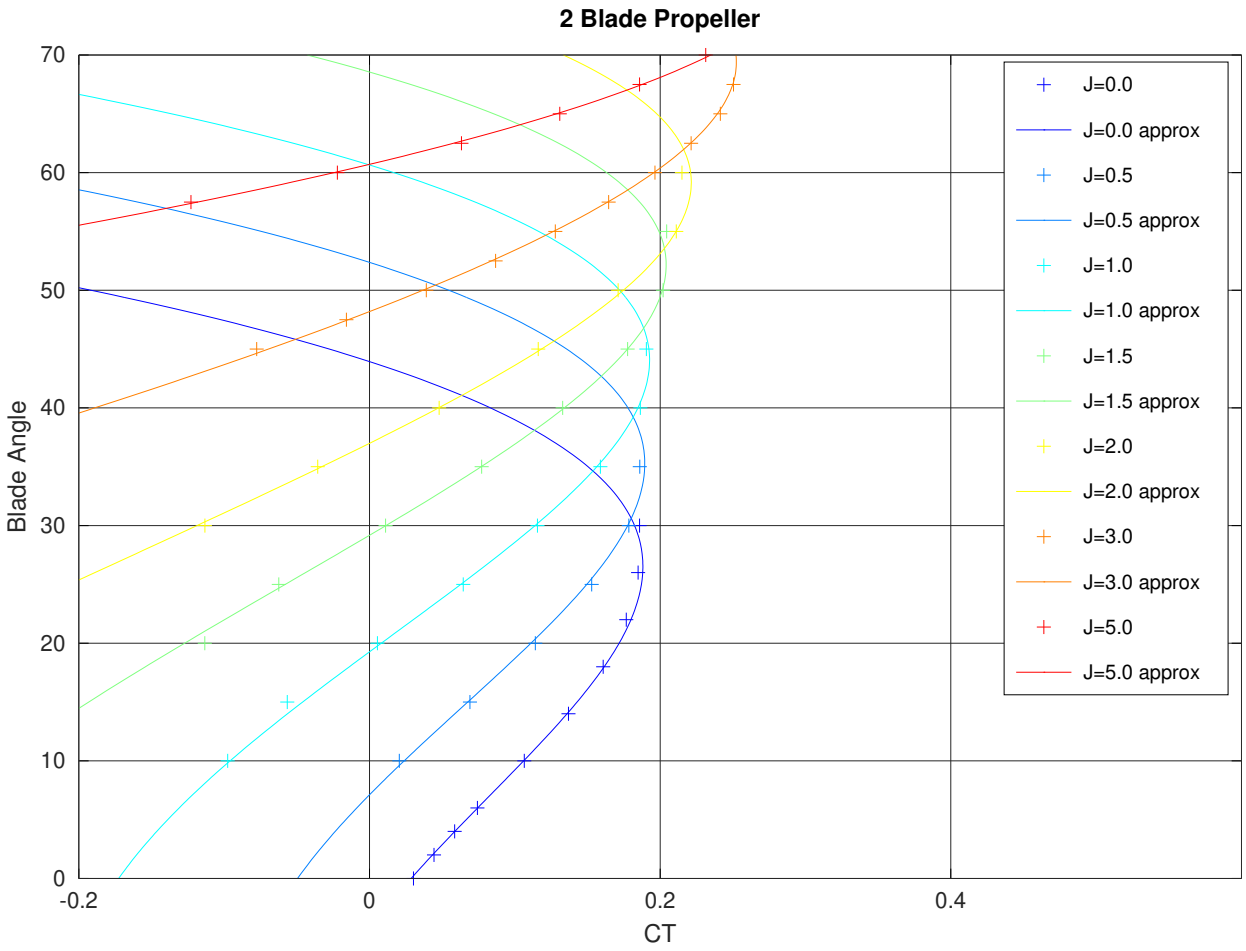

Figure 42: C_T versus Blade Angle $\beta_{3/4}$ for a 2 Blade Propeller

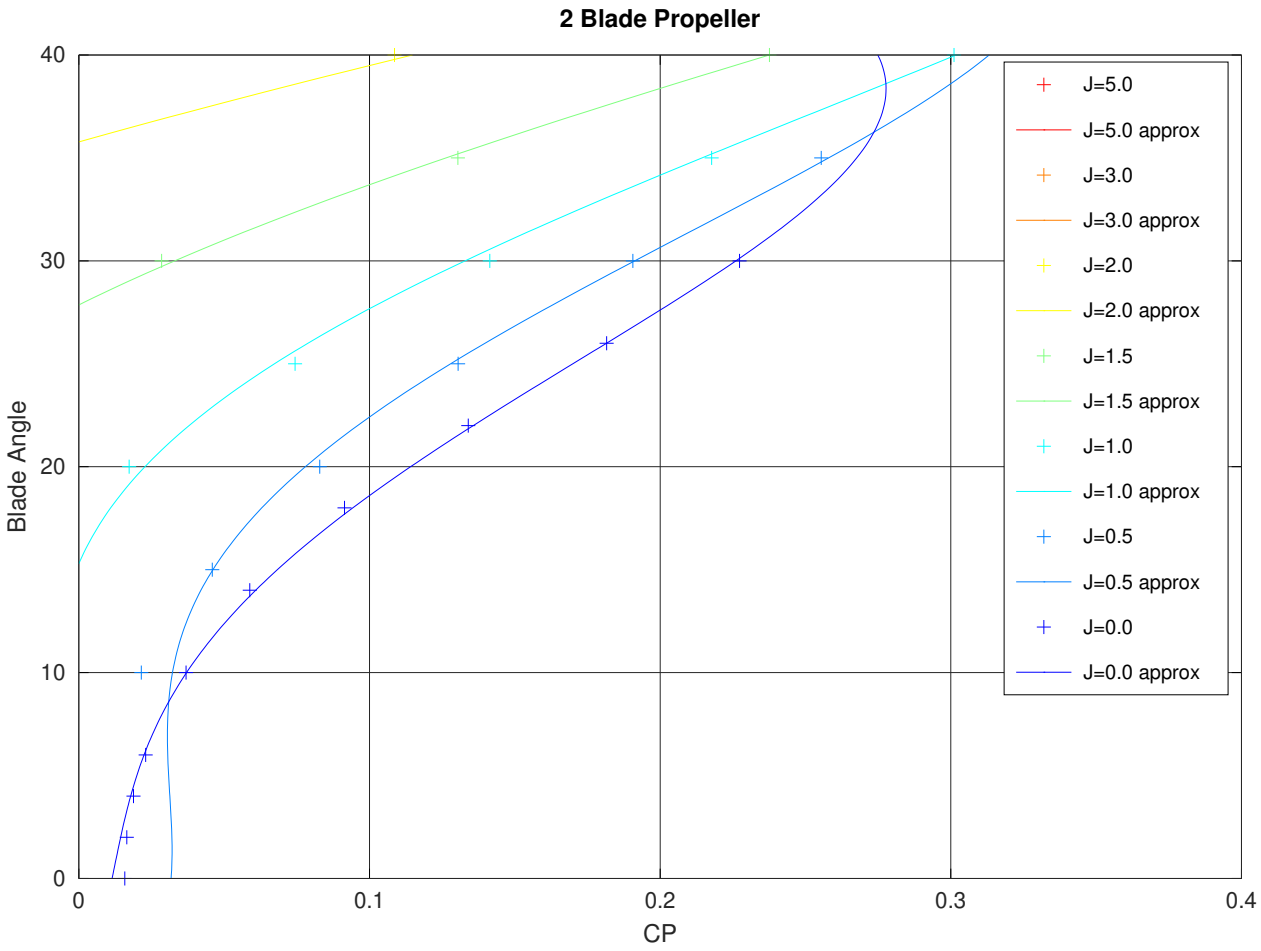

Figure 43: C_P versus Blade Angle $\beta_{3/4}$ for a 2 Blade Propeller

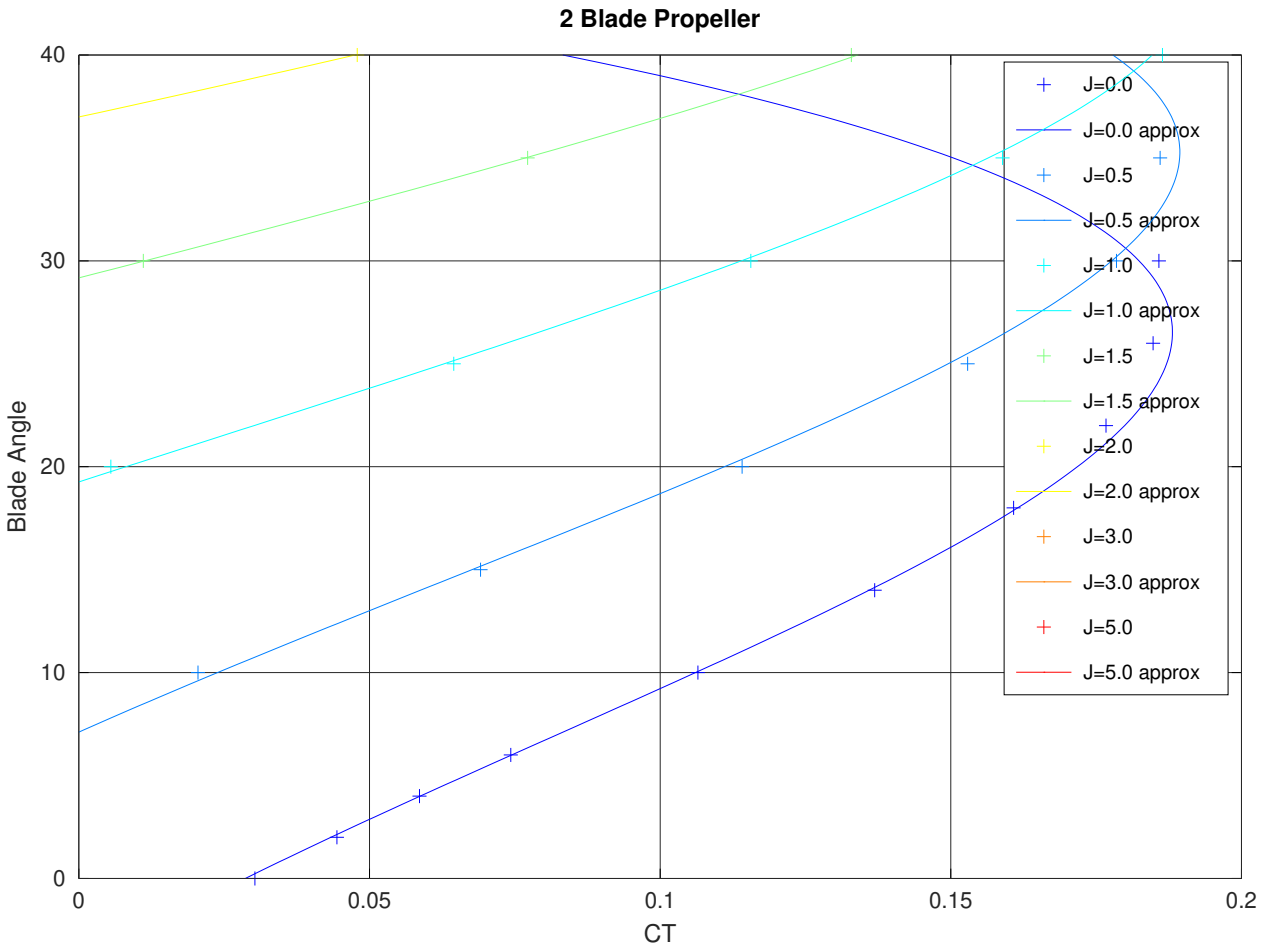

Figure 44: C_T versus Blade Angle $\beta_{3/4}$ for a 2 Blade Propeller

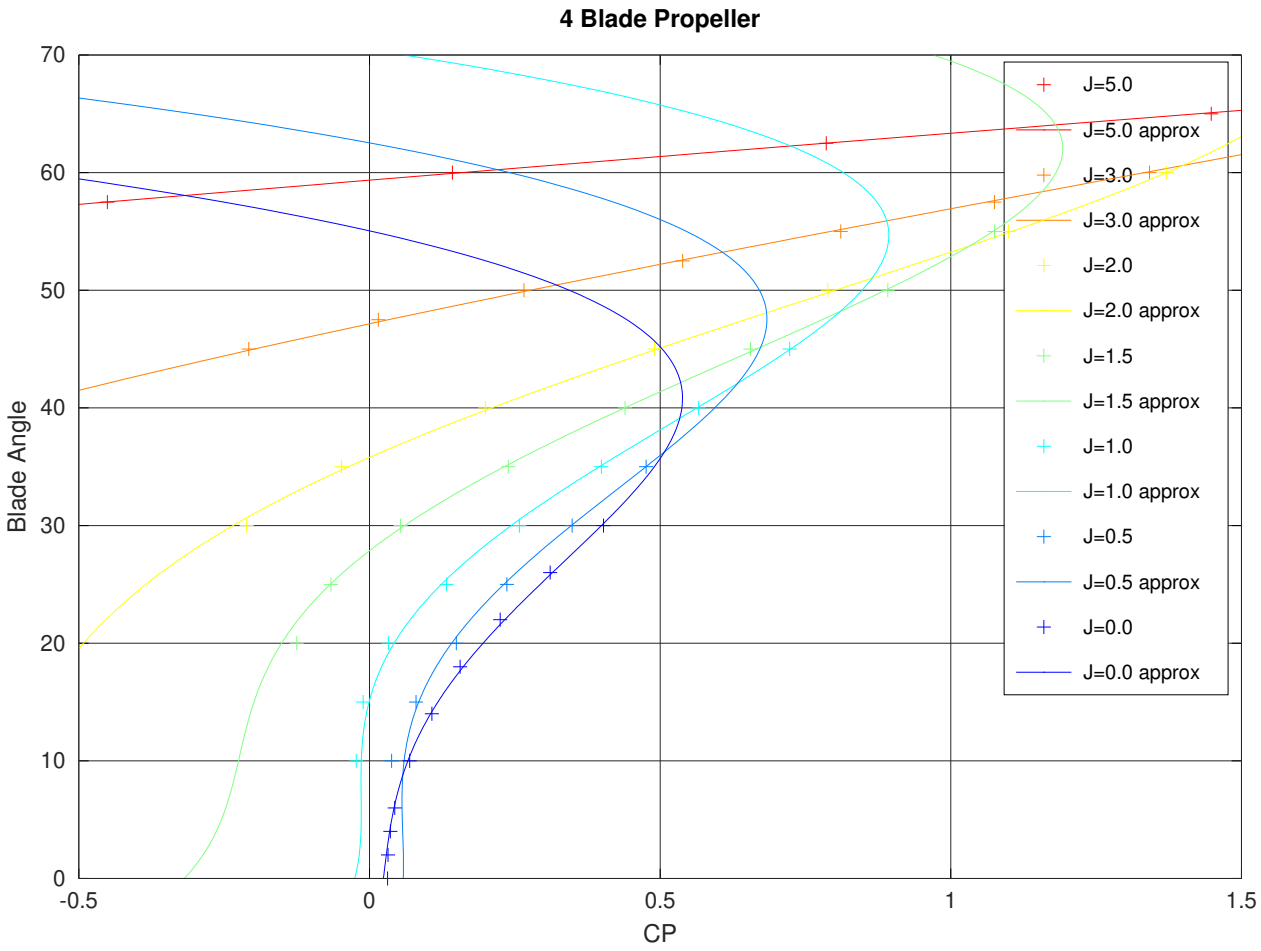

Figure 45: C_P versus Blade Angle $\beta_{3/4}$ for a 4 Blade Propeller

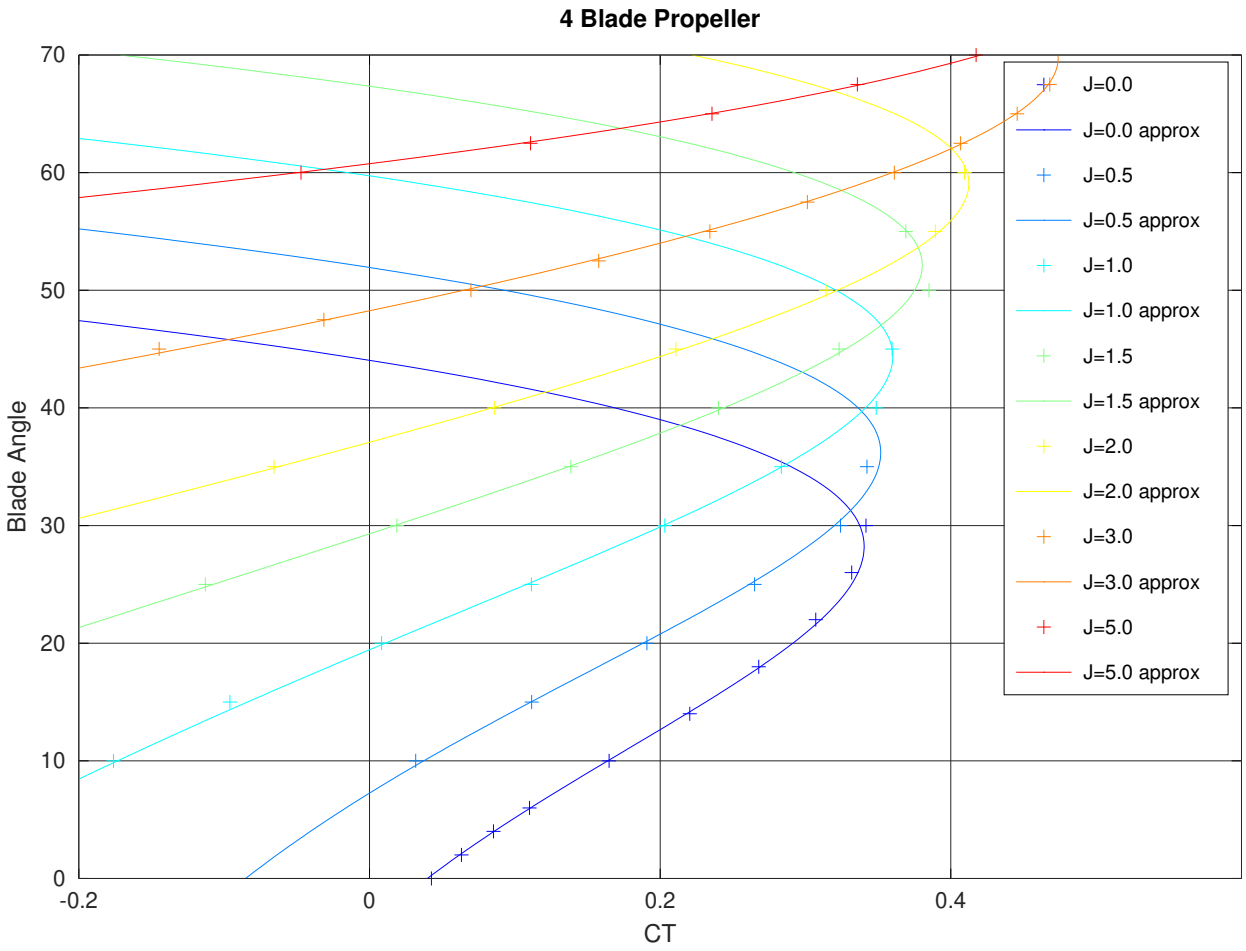

Figure 46: C_T versus Blade Angle $\beta_{3/4}$ for a 4 Blade Propeller

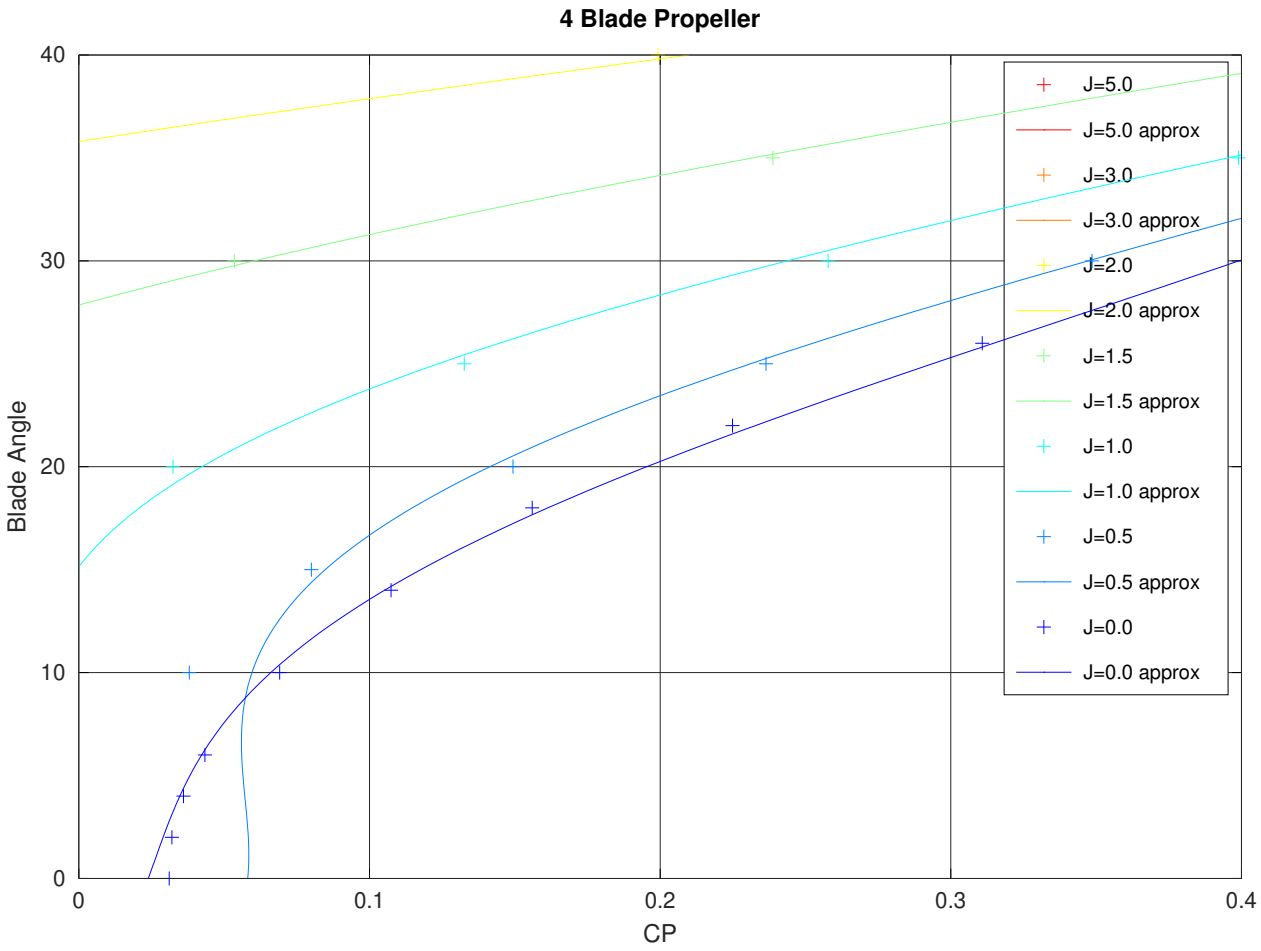

Figure 47: C_P versus Blade Angle $\beta_{3/4}$ for a 4 Blade Propeller

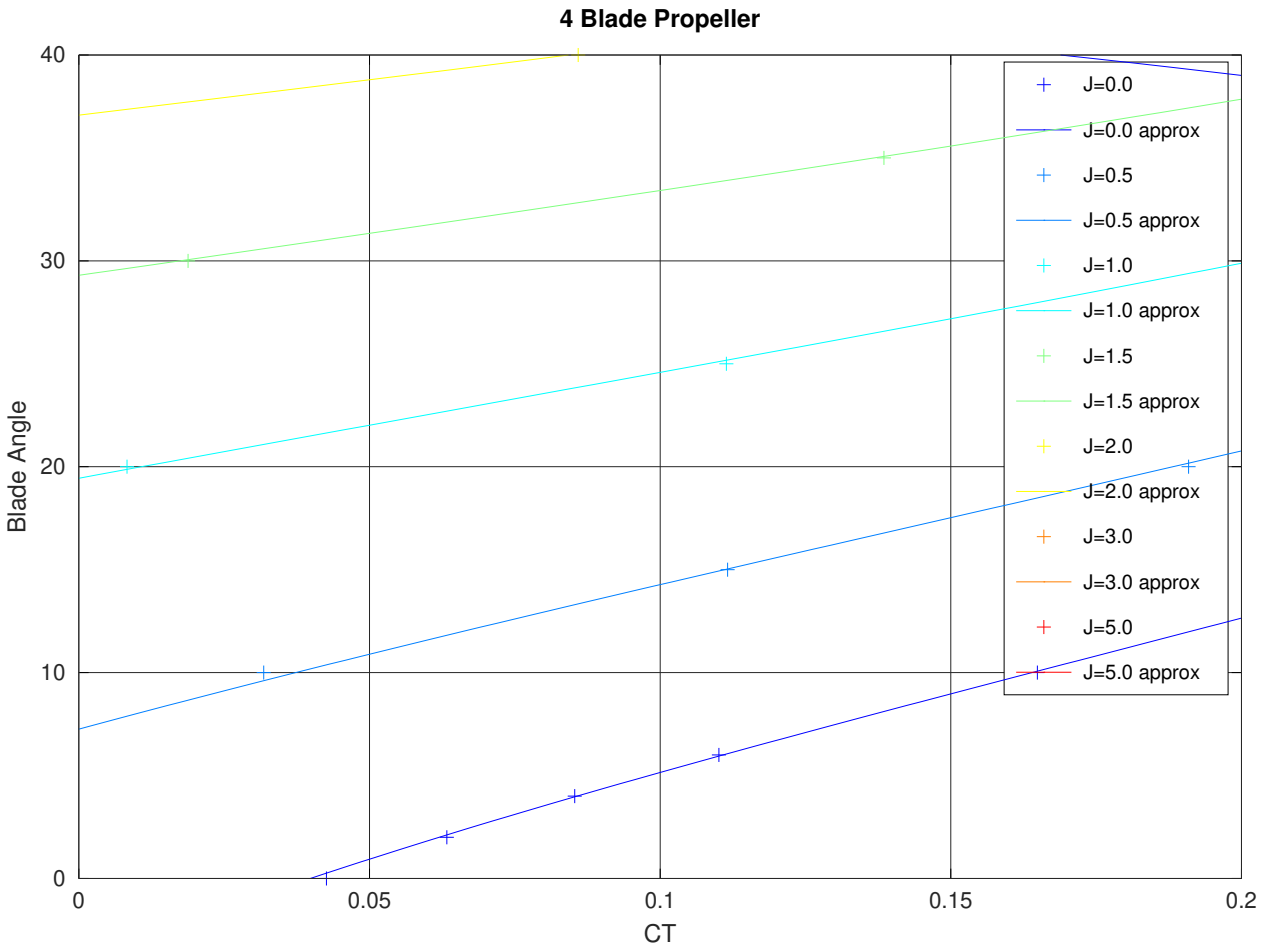

Figure 48: C_T versus Blade Angle $\beta_{3/4}$ for a 4 Blade Propeller

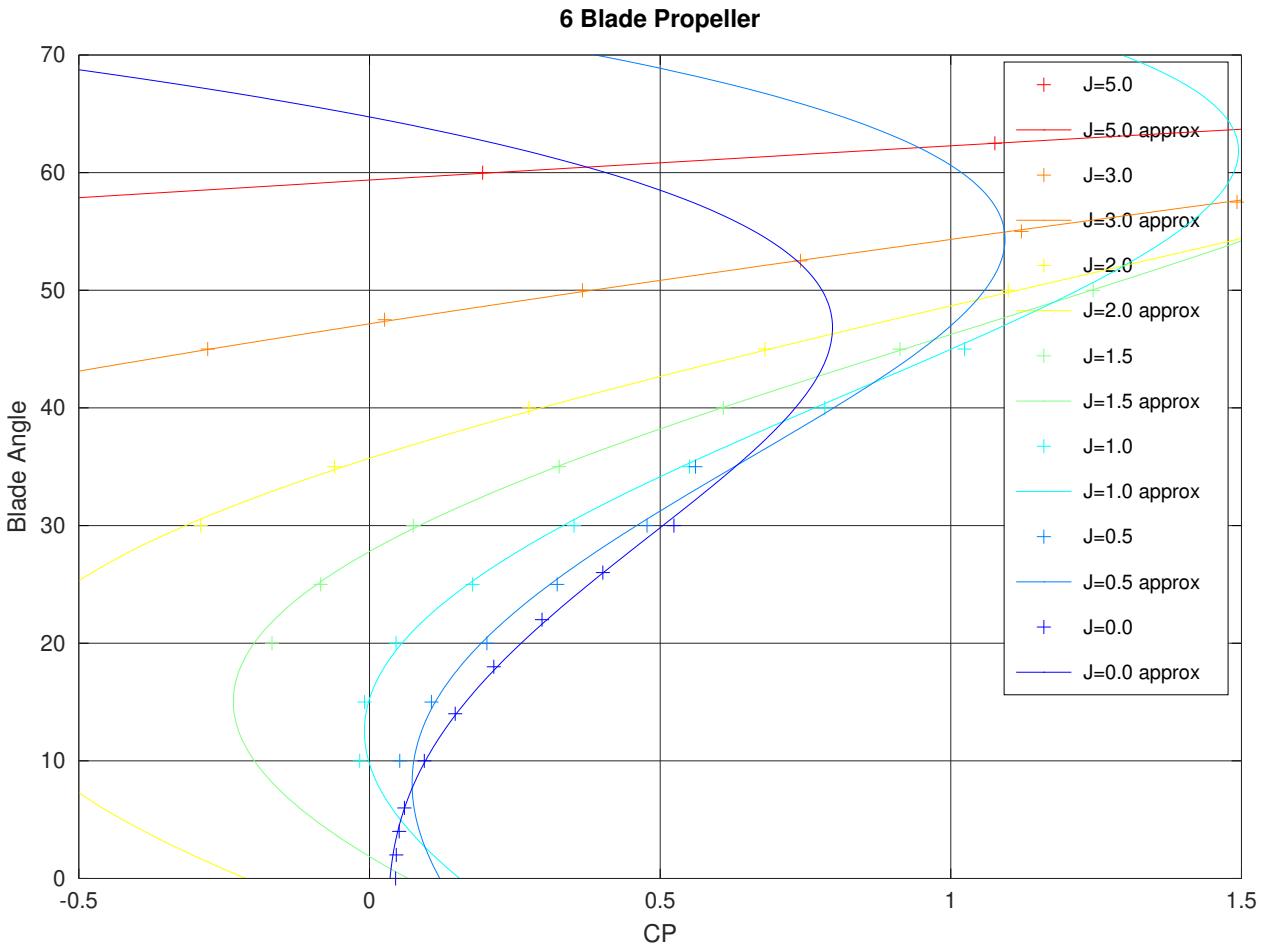

Figure 49: C_P versus Blade Angle $\beta_{3/4}$ for a 6 Blade Propeller

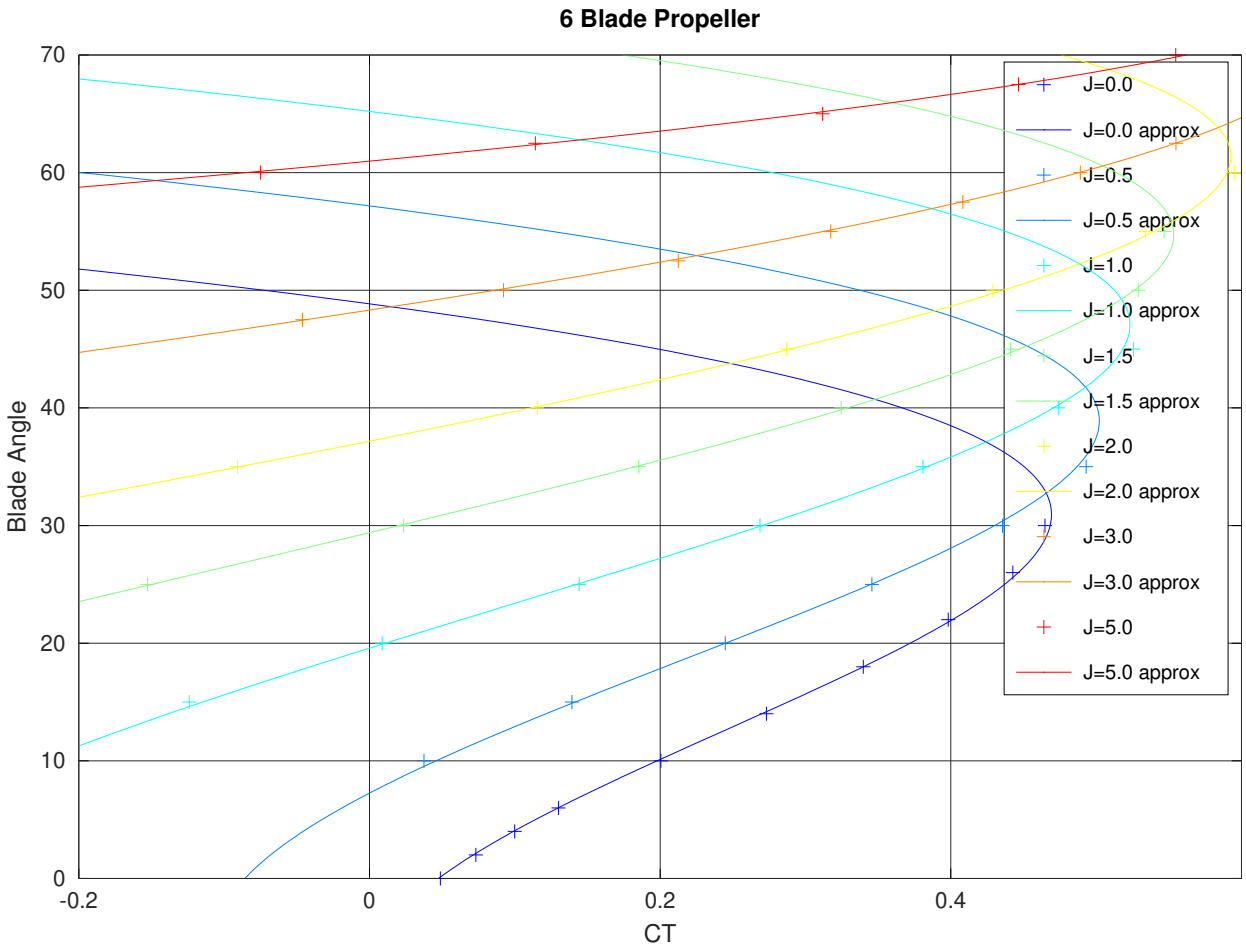

Figure 50: C_T versus Blade Angle $\beta_{3/4}$ for a 6 Blade Propeller

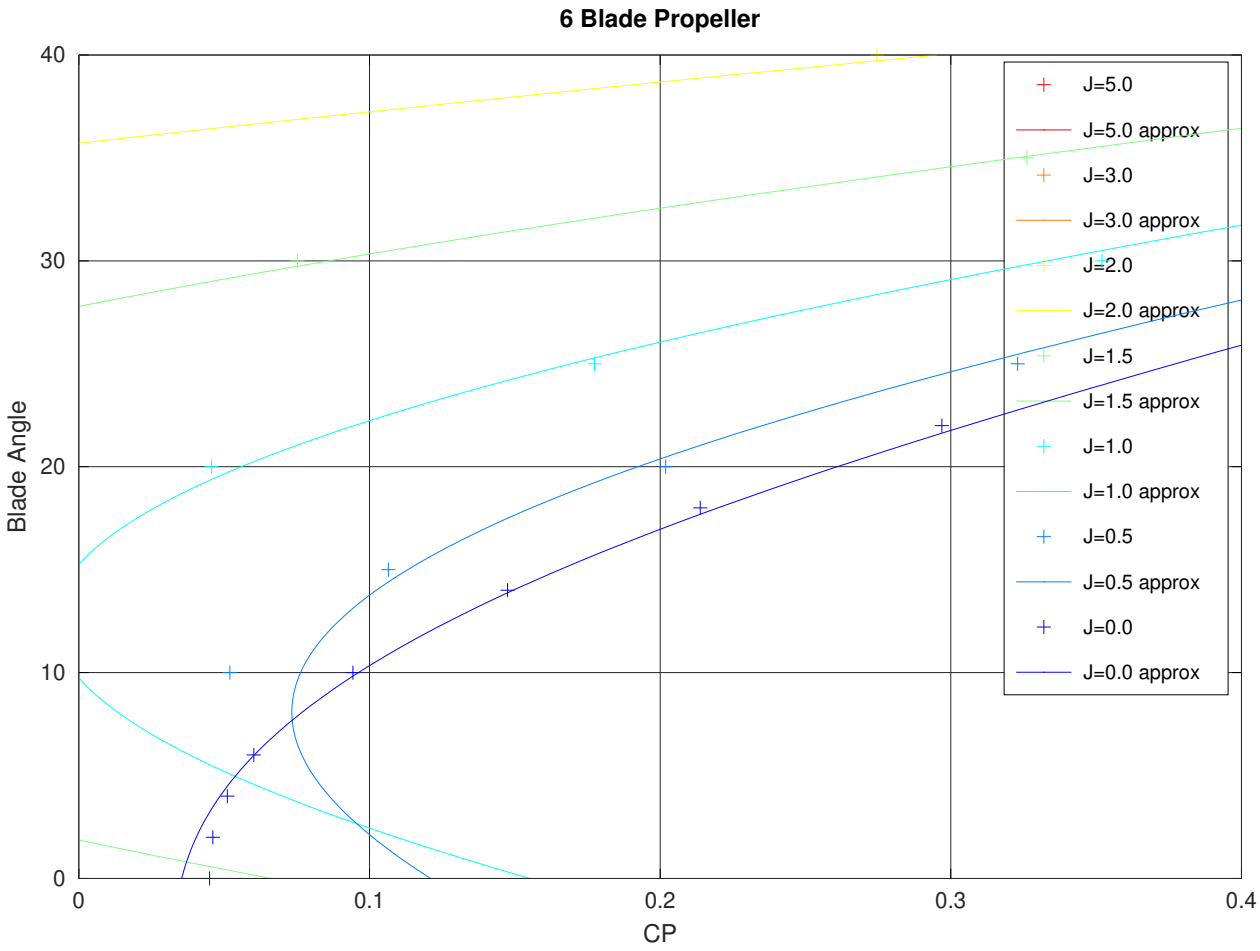

Figure 51: C_P versus Blade Angle $\beta_{3/4}$ for a 6 Blade Propeller

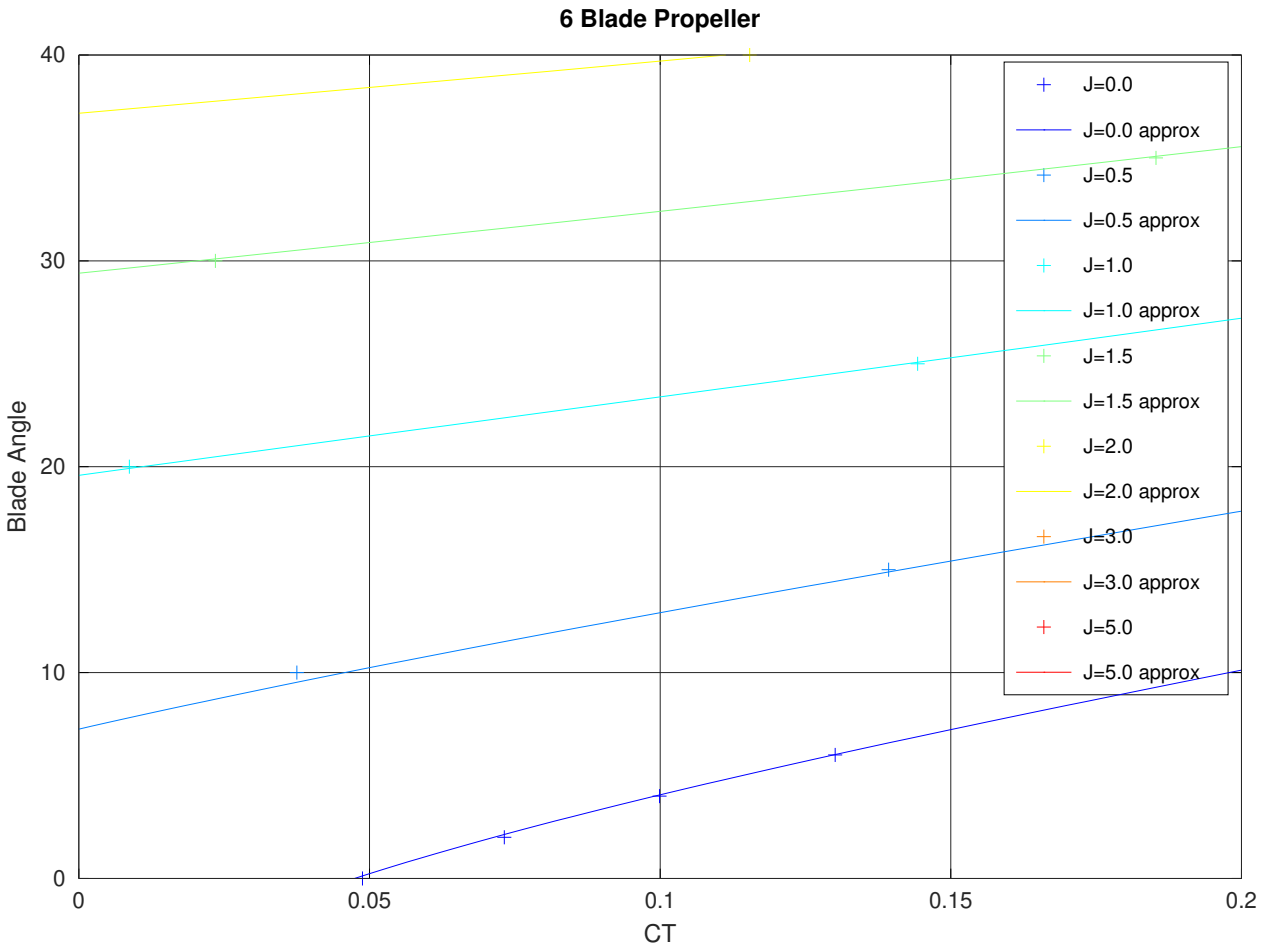

Figure 52: C_T versus Blade Angle $\beta_{3/4}$ for a 6 Blade Propeller

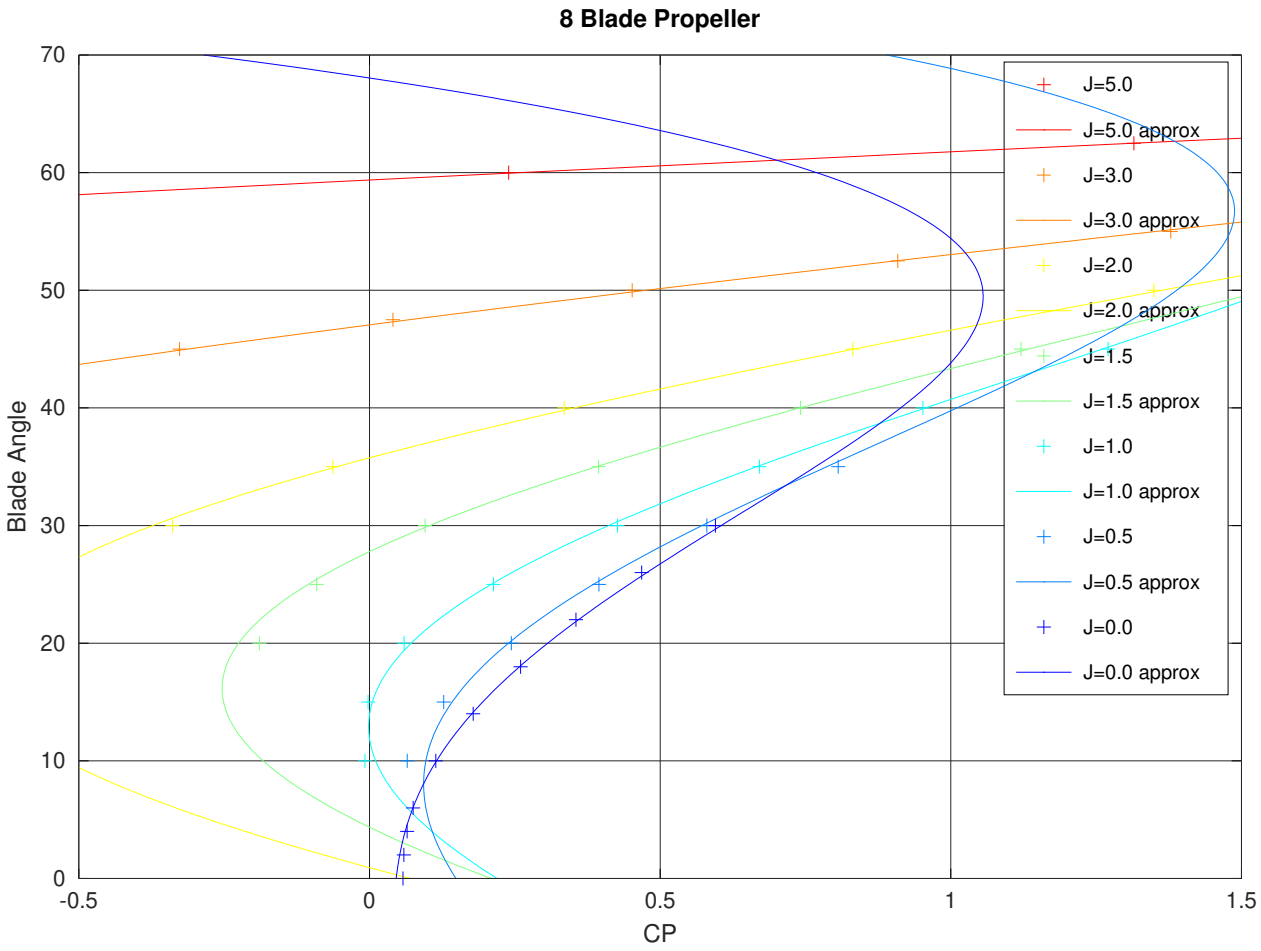

Figure 53: C_P versus Blade Angle $\beta_{3/4}$ for a 8 Blade Propeller

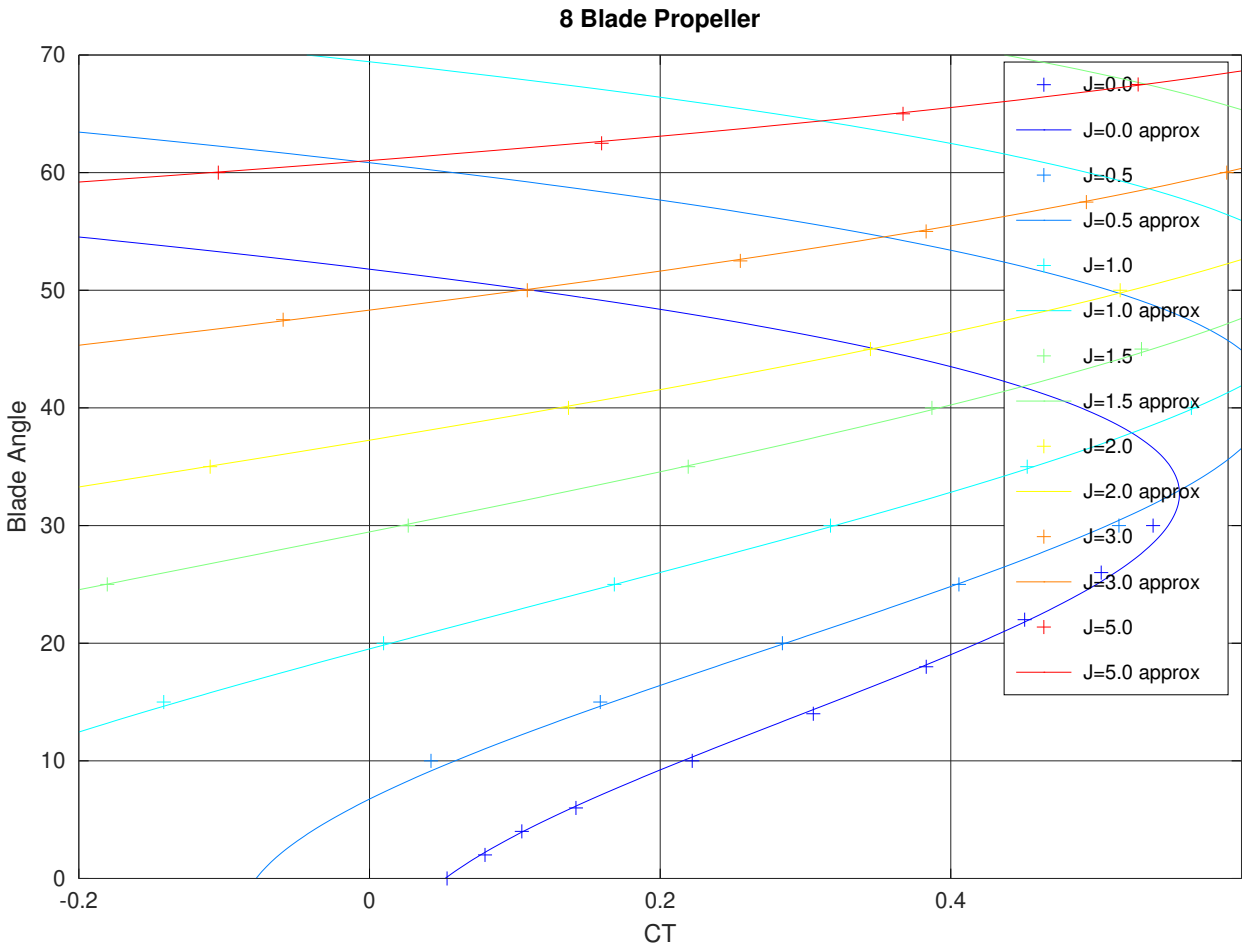

Figure 54: C_T versus Blade Angle $\beta_{3/4}$ for a 8 Blade Propeller

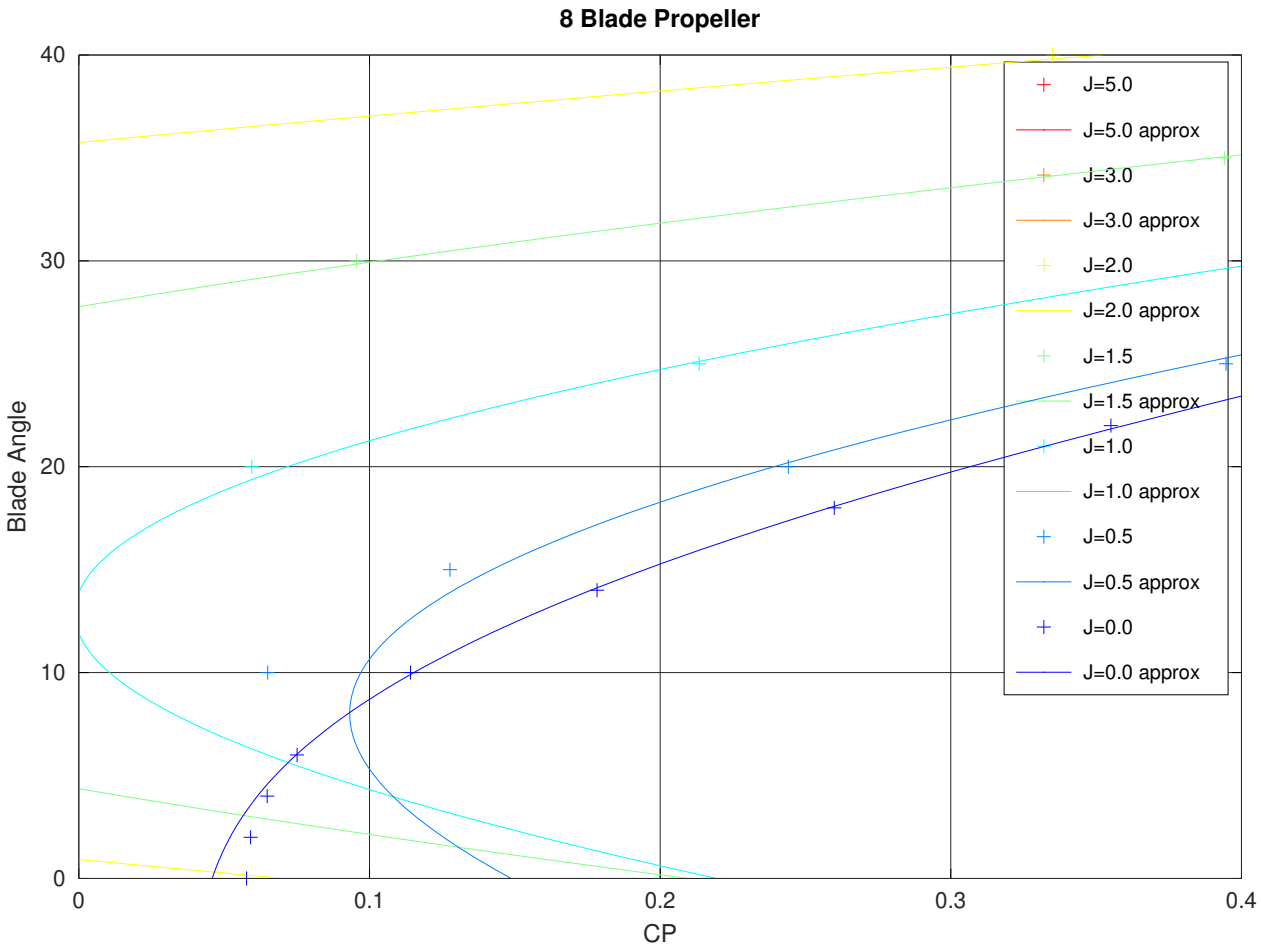

Figure 55: C_P versus Blade Angle $\beta_{3/4}$ for a 8 Blade Propeller

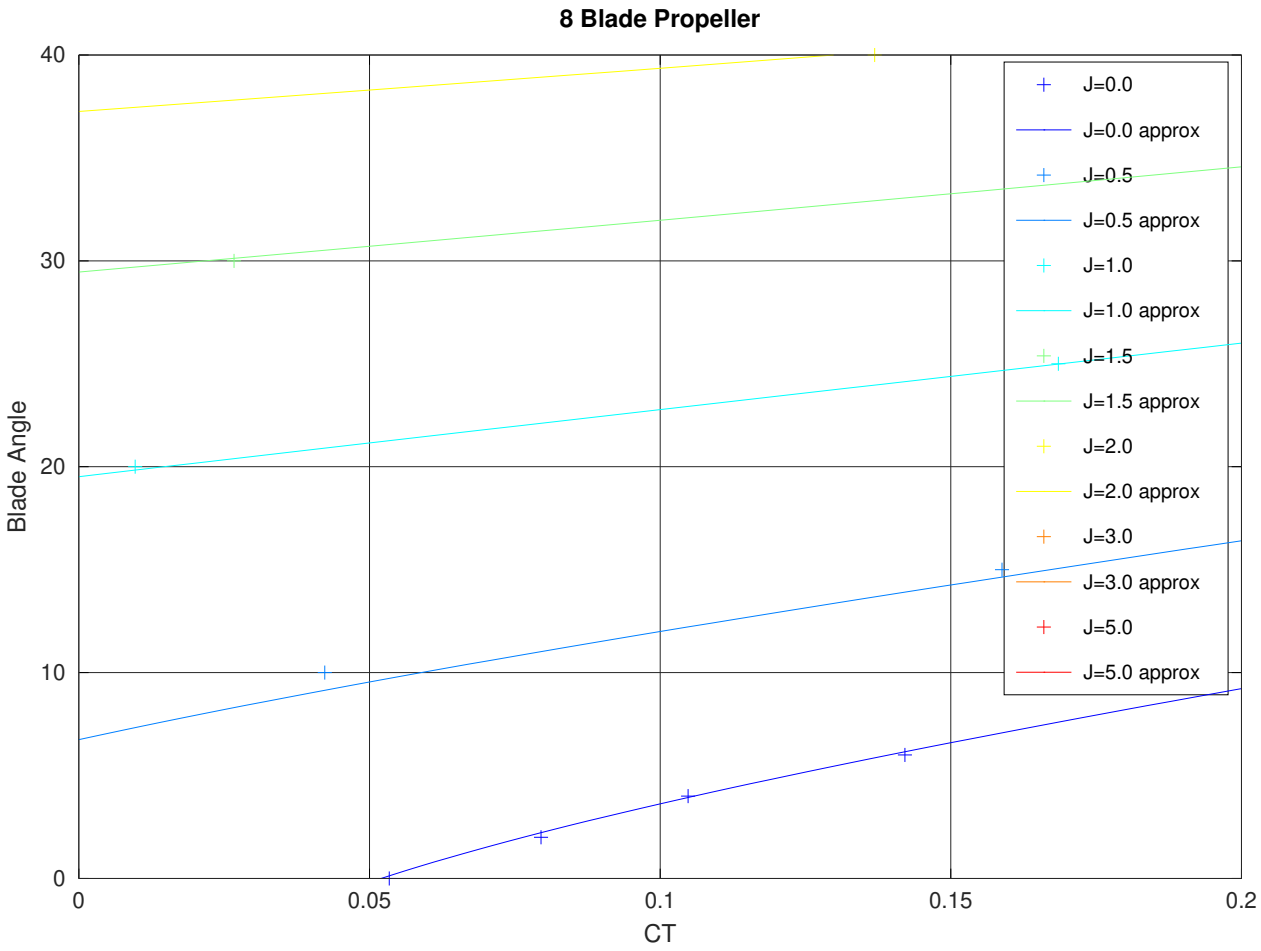

Figure 56: C_T versus Blade Angle $\beta_{3/4}$ for a 8 Blade Propeller

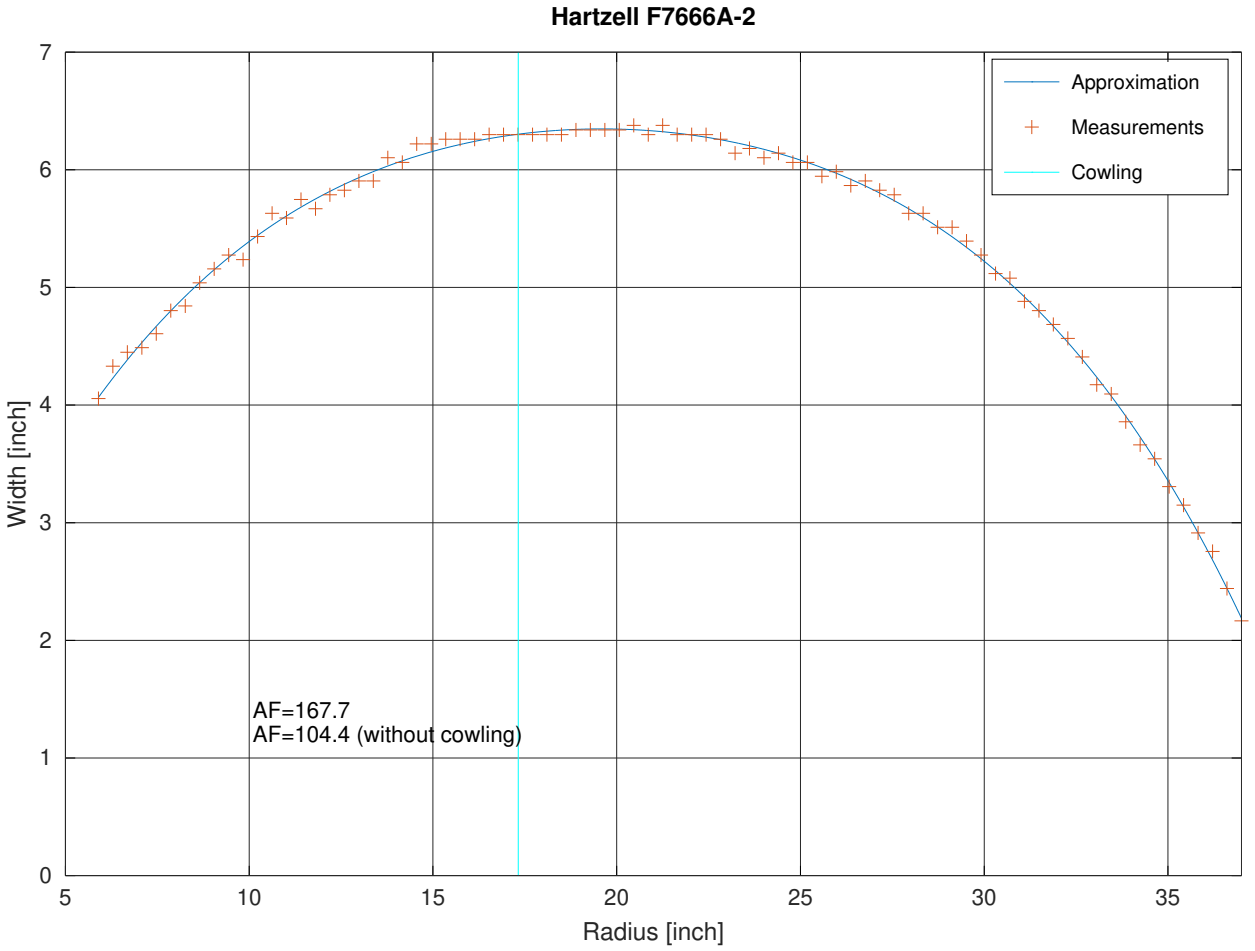

Figure 57: Hartzell F7666A-2 Activity Factor

1. ρ_0/ρ Density Ratio
2. N_0 Rated Engine RPM (RPM at which SHP is given) (in min^{-1})
3. N Engine RPM (in min^{-1})
4. D Propeller Diameter (in ft)
5. $C_P = \frac{\frac{N}{N_0} \cdot \text{SHP} \cdot \rho_0/\rho \cdot 10^{11}}{2 \cdot N^3 \cdot D^5}$
6. $J = \frac{101.4 \cdot V_K}{N \cdot D}$ (V_K free stream velocity in kts)
7. $P_{AF} = f_{PAF}(AF)$ activity factor correction (Figure 34)
8. $C_{P_E} = C_P \cdot P_{AF}$
9. $\beta_{3/4} = f^{-1}_{\beta_{3/4} \to C_{P_E}}(J, C_{P_E})$ ($\beta_{3/4}$ is the blade angle) (Figures 41, 45, 49, 53)
10. $C_{T_E} = f_{\beta_{3/4} \to C_{T_E}}(J, \beta_{3/4})$ (Figures 42, 46, 50, 54)
11. $T_{AF} = f_{TAF}(AF)$ activity factor correction (Figure 34)
12. $C_T = \frac{C_{T_E}}{T_{AF}}$

13. $T = \frac{0.661 \cdot 10^{-6} \cdot C_T \cdot N^2 \cdot D^4}{\rho_0/\rho}$ (Thrust in lbf)

14. $\eta = \frac{C_T}{C_P} \cdot J$ Propeller efficiency

Fixed Pitch Propeller

$$\epsilon = \frac{\text{SHP} \cdot \rho_0/\rho \cdot 10^{11}}{2 \cdot N_0 \cdot N^2 \cdot D^5} \cdot P_{AF} - f_{\beta_{3/4} \to C_{P_E}} \left(\frac{101.4 \cdot V_K}{N \cdot D}, \beta_{3/4} \right) \tag{9}$$

Solve N for $\epsilon = 0$.

$$\frac{\partial}{\partial N}\epsilon = -\frac{\text{SHP} \cdot \rho_0/\rho \cdot 10^{11}}{N_0 \cdot N^3 \cdot D^5} \cdot P_{AF} + \frac{\partial}{\partial C_{P_E}} f_{\beta_{3/4} \to C_{P_E}} \left(\frac{101.4 \cdot V_K}{N \cdot D}, \beta_{3/4} \right) \cdot \frac{101.4 \cdot V_K}{N^2 \cdot D} \tag{10}$$

B.7.2 Bootstrap Method

See `http://www.allstar.fiu.edu/aero/airper-ba.htm`.
Bootstrap data plate for Piper Cherokee Arrow 200.

Bootstrap Data Plate Item	Value	Units	Aircraft Subsystem
Wing area, S	160	ft^2	Airframe
Wing aspect ratio, A	5.625		Airframe
Rated MSL torque, M_0	389.05	$\text{ft} \cdot \text{lbf}$	Engine
Altitude drop-off parameter, C	0.12		Engine
Propeller diameter, d	6.333	ft	Propeller
Parasite drag coefficient, C_{D_0}	0.030662		Airframe
Airplane efficiency factor, e	0.60648		Airframe
Propeller polar slope, m	2.073704		Propeller
Propeller polar intercept, b	-0.054411		Propeller

Wing aspect ratio: $A = B^2/S$, where B is the wing span.
Mean sea level (MSL) full–throttle rated torque $M_0 = \frac{P_0}{2\pi n_0}$, where P_0 is the rated power, n_0 is the rated propeller revolutions per second.
For the Arrow 200, $P_0 = 200\text{HP} = 110000\frac{\text{ft}\cdot\text{lbf}}{\text{s}}$, and $n_0 = \frac{\text{RPM}}{60\text{s}} = \frac{2700}{60\text{s}} = 45\text{s}^{-1}$.
The proportional mechanical power loss independent of altitude, C, can almost always be taken as 0.12.
$M(\sigma) = \Phi(\sigma) \cdot M_0$. $\Phi(\sigma) = \frac{\sigma - C}{1 - C}$. σ is the relative density.
Parasite drag and efficiency. $V_T \cdot \sqrt{\sigma} = V_C$. $\gamma_{bg} = \tan^{-1}(\frac{1}{r_{bg}})$. r_{bg} is the glide ratio, γ_{bg} the glide angle, W the aircraft weight. $\rho_0 = 0.002377\frac{\text{slug}}{\text{ft}^3}$. $C_{D_0} = \frac{W \cdot \sin(\gamma_{bg})}{\rho_0 \cdot V_{Cbg}^2 \cdot S}$. $e = \frac{4 \cdot C_{D_0}}{\pi \cdot A \cdot \tan^2(\gamma_{bg})}$.
For the Arrow 200, $W = 2600\text{lbf}$, $r_{bg} = \frac{20\text{nmi}}{13000\text{ft}} = 9.3479$, $\gamma_{bg} = 6.1061$, $V_{Cbg} = 105\text{MPH} = 154\frac{\text{ft}}{\text{s}}$,
$C_{D_0} = 0.030662$, $e = 0.60648$.
Propeller polars. V_{Tx} true speed for best glide angle. $b = \frac{S \cdot C_{D_0}}{2 \cdot d^2} - \frac{2 \cdot W^2}{\rho^2 \cdot d^2 \cdot S \cdot \pi \cdot e \cdot A \cdot V_{Cx}^4}$.
$m = \frac{2 \cdot n_0 \cdot d \cdot W^2}{\Phi(\sigma) \cdot P_0 \cdot \rho \cdot S \cdot \pi \cdot e \cdot A} \cdot \left(\frac{1}{V_{CM}^2} - \frac{V_{CM}^2}{V_{Cx}^4} \right)$.
For the Arrow 200, $V_{Cx} = 80\text{MPH} = 117.33333\frac{\text{ft}}{\text{s}}$, $V_{CM} = 174\text{MPH} = 255.2\frac{\text{ft}}{\text{s}}$ @ 5000ft,
$V_{CM} = 168\text{MPH} = 246.4\frac{\text{ft}}{\text{s}}$ @ 10000ft, $\sigma = 0.73875$, $\Phi(\sigma) = 0.70312$, $b = -0.12241$, $m = 5.5720$.

Alt	Density ρ
ft	$10^{-4}\frac{\text{slugs}}{\text{ft}^3}$
-5000	27.45
0	23.77
5000	20.48
10000	17.56
15000	14.96

Thrust / Power Propeller Advance $J = \frac{V_T}{n \cdot d}$, V_T (true) speed, n revolutions per second, d propeller diameter.
Propeller Thrust $T = C_T \cdot \rho \cdot n^2 \cdot d^4$.
Propeller Power $P = C_P \cdot \rho \cdot n^3 \cdot d^5$.

Propeller Efficiency $\eta = J \cdot \frac{C_T}{C_P} = \frac{V_T \cdot T}{P}$.
Propeller Polar $\frac{C_T}{J^2} = m \cdot \frac{C_P}{J^2} + b$.
$C_P = \frac{P}{\rho \cdot n^3 \cdot d^5}$.
$C_T = m \cdot C_P + J^2 \cdot b = m \cdot \frac{P}{\rho \cdot n^3 \cdot d^5} + J^2 \cdot b$.
$T = \frac{m \cdot P}{n \cdot d} + J^2 \cdot b \cdot \rho \cdot n^2 \cdot d^4 = \frac{m \cdot P}{n \cdot d} + V_T^2 \cdot b \cdot \rho \cdot d^2 = \frac{m \cdot P}{n \cdot d} + V_C^2 \cdot b \cdot \rho_0 \cdot d^2$.
$P = \frac{n \cdot d}{m} \cdot \left(T - V_C^2 \cdot b \cdot \rho_0 \cdot d^2\right)$.

Drag / Lift $C_D = C_{D_0} + \frac{C_L^2}{\pi \cdot A \cdot e}$.
$L = \frac{1}{2} \cdot C_L \cdot \rho \cdot V_T^2 \cdot S$.
$D = \frac{1}{2} \cdot C_D \cdot \rho \cdot V_T^2 \cdot S$.
$C_L = \frac{W}{\frac{1}{2} \cdot \rho \cdot V_T^2 \cdot S}$

$$\begin{aligned} D &= \frac{1}{2} \cdot C_{D_0} \cdot \rho \cdot V_T^2 \cdot S + \frac{1}{2} \cdot \frac{W^2}{(\frac{1}{2} \cdot \rho \cdot V_T^2 \cdot S)^2 \cdot \pi \cdot A \cdot e} \cdot \rho \cdot V_T^2 \cdot S \\ &= \frac{1}{2} \cdot C_{D_0} \cdot \rho \cdot V_T^2 \cdot S + \frac{W^2}{\frac{1}{2} \cdot \rho \cdot V_T^2 \cdot S \cdot \pi \cdot A \cdot e} \\ &= \frac{1}{2} \cdot C_{D_0} \cdot \rho_0 \cdot V_C^2 \cdot S + \frac{W^2}{\frac{1}{2} \cdot \rho_0 \cdot V_C^2 \cdot S \cdot \pi \cdot A \cdot e} \end{aligned} \tag{11}$$

$$0 = \frac{1}{2} \cdot C_{D_0} \cdot \rho_0^2 \cdot V_C^4 \cdot S - D \cdot \rho_0 \cdot V_C^2 + \frac{W^2}{\frac{1}{2} \cdot S \cdot \pi \cdot A \cdot e} \tag{12}$$

$$\rho_0 \cdot V_C^2 = \rho \cdot V_T^2 = \frac{D}{C_{D_0} \cdot S} \pm \sqrt{\frac{D^2}{C_{D_0}^2 \cdot S^2} - \frac{4 \cdot W^2}{C_{D_0} \cdot S^2 \cdot \pi \cdot A \cdot e}} \tag{13}$$

Unaccelerated Level Flight

$$\rho \cdot V_{T,max}^2 = \frac{\frac{m \cdot P}{n \cdot d} + \rho \cdot V_{T,max}^2 \cdot b \cdot d^2}{C_{D_0} \cdot S} + \sqrt{\frac{\left(\frac{m \cdot P}{n \cdot d} + \rho \cdot V_{T,max}^2 \cdot b \cdot d^2\right)^2}{C_{D_0}^2 \cdot S^2} - \frac{4 \cdot W^2}{C_{D_0} \cdot S^2 \cdot \pi \cdot A \cdot e}} \tag{14}$$

$$\rho \cdot V_{T,min}^2 = \frac{\frac{m \cdot P}{n \cdot d} + \rho \cdot V_{T,min}^2 \cdot b \cdot d^2}{C_{D_0} \cdot S} - \sqrt{\frac{\left(\frac{m \cdot P}{n \cdot d} + \rho \cdot V_{T,min}^2 \cdot b \cdot d^2\right)^2}{C_{D_0}^2 \cdot S^2} - \frac{4 \cdot W^2}{C_{D_0} \cdot S^2 \cdot \pi \cdot A \cdot e}} \tag{15}$$

Initial Guess:

$$\rho \cdot \hat{V}_{T,max}^2 = \frac{m \cdot P}{n \cdot d \cdot C_{D_0} \cdot S} + \sqrt{\frac{m^2 \cdot P^2}{n^2 \cdot d^2 \cdot C_{D_0}^2 \cdot S^2} - \frac{4 \cdot W^2}{C_{D_0} \cdot S^2 \cdot \pi \cdot A \cdot e}} \tag{16}$$

$$\rho \cdot \hat{V}_{T,min}^2 = \frac{m \cdot P}{n \cdot d \cdot C_{D_0} \cdot S} - \sqrt{\frac{m^2 \cdot P^2}{n^2 \cdot d^2 \cdot C_{D_0}^2 \cdot S^2} - \frac{4 \cdot W^2}{C_{D_0} \cdot S^2 \cdot \pi \cdot A \cdot e}} \tag{17}$$

Error:

$$\epsilon = \frac{\frac{m \cdot P}{n \cdot d} + \rho \cdot \hat{V}_{T,max}^2 \cdot b \cdot d^2}{C_{D_0} \cdot S} - \rho \cdot \hat{V}_{T,max}^2 + \sqrt{\frac{\left(\frac{m \cdot P}{n \cdot d} + \rho \cdot \hat{V}_{T,max}^2 \cdot b \cdot d^2\right)^2}{C_{D_0}^2 \cdot S^2} - \frac{4 \cdot W^2}{C_{D_0} \cdot S^2 \cdot \pi \cdot A \cdot e}} \tag{18}$$

$$\epsilon = \frac{\frac{m \cdot P}{n \cdot d} + \rho \cdot \hat{V}_{T,max}^2 \cdot b \cdot d^2}{C_{D_0} \cdot S} - \rho \cdot \hat{V}_{T,max}^2 - \sqrt{\frac{\left(\frac{m \cdot P}{n \cdot d} + \rho \cdot \hat{V}_{T,max}^2 \cdot b \cdot d^2\right)^2}{C_{D_0}^2 \cdot S^2} - \frac{4 \cdot W^2}{C_{D_0} \cdot S^2 \cdot \pi \cdot A \cdot e}} \tag{19}$$

$$\frac{\partial}{\partial \rho \cdot \hat{V}_{T,max}^2}\epsilon = \frac{b \cdot d^2}{C_{D_0} \cdot S} - 1 + \frac{b \cdot d^2 \cdot \left(\frac{m \cdot P}{n \cdot d} + \rho \cdot \hat{V}_{T,max}^2 \cdot b \cdot d^2\right)}{C_{D_0} \cdot S \cdot \sqrt{\left(\frac{m \cdot P}{n \cdot d} + \rho \cdot \hat{V}_{T,max}^2 \cdot b \cdot d^2\right)^2 - \frac{4 \cdot W^2 \cdot C_{D_0}}{\pi \cdot A \cdot e}}} \tag{20}$$

$$\frac{\partial}{\partial \rho \cdot \hat{V}_{T,min}^2}\epsilon = \frac{b \cdot d^2}{C_{D_0} \cdot S} - 1 - \frac{b \cdot d^2 \cdot \left(\frac{m \cdot P}{n \cdot d} + \rho \cdot \hat{V}_{T,min}^2 \cdot b \cdot d^2\right)}{C_{D_0} \cdot S \cdot \sqrt{\left(\frac{m \cdot P}{n \cdot d} + \rho \cdot \hat{V}_{T,min}^2 \cdot b \cdot d^2\right)^2 - \frac{4 \cdot W^2 \cdot C_{D_0}}{\pi \cdot A \cdot e}}} \tag{21}$$

Rate of Climb

$$\frac{m \cdot P}{n \cdot d} + V_C^2 \cdot b \cdot \rho_0 \cdot d^2 = \frac{1}{2} \cdot C_{D_0} \cdot \rho_0 \cdot V_C^2 \cdot S + \frac{W^2 \cdot \cos^2(\alpha)}{\frac{1}{2} \cdot \rho_0 \cdot V_C^2 \cdot S \cdot \pi \cdot A \cdot e} + W \sin(\alpha) \tag{22}$$

$$\frac{m \cdot P}{n \cdot d} + V_C^2 \cdot \rho_0 \cdot \left(b \cdot d^2 - \frac{1}{2} \cdot C_{D_0} \cdot S\right) = \frac{W^2 \cdot \cos^2(\alpha)}{\frac{1}{2} \cdot \rho_0 \cdot V_C^2 \cdot S \cdot \pi \cdot A \cdot e} + W \sin(\alpha) \tag{23}$$

$$\frac{m \cdot P}{n \cdot d} + V_C^2 \cdot \rho_0 \cdot \left(b \cdot d^2 - \frac{1}{2} \cdot C_{D_0} \cdot S\right) - \frac{W^2}{\frac{1}{2} \cdot \rho_0 \cdot V_C^2 \cdot S \cdot \pi \cdot A \cdot e} = W \sin(\alpha) - \frac{W^2 \cdot \sin^2(\alpha)}{\frac{1}{2} \cdot \rho_0 \cdot V_C^2 \cdot S \cdot \pi \cdot A \cdot e} \tag{24}$$

$$\sin(\alpha) = \frac{\rho_0 \cdot V_C^2 \cdot S \cdot \pi \cdot A \cdot e}{4 \cdot W^2} \cdot \left(W \pm \sqrt{W^2 - \frac{8 \cdot W^2}{\rho_0 \cdot V_C^2 \cdot S \cdot \pi \cdot A \cdot e} \cdot \left(\frac{m \cdot P}{n \cdot d} + V_C^2 \cdot \rho_0 \cdot \left(b \cdot d^2 - \frac{1}{2} \cdot C_{D_0} \cdot S\right) - \frac{W^2}{\frac{1}{2} \cdot \rho_0 \cdot V_C^2 \cdot S \cdot \pi \cdot A \cdot e}\right)}\right) \tag{25}$$

$$\sin(\alpha) \approx \frac{1}{W} \cdot \left(\frac{m \cdot P}{n \cdot d} + V_C^2 \cdot \rho_0 \cdot \left(b \cdot d^2 - \frac{1}{2} \cdot C_{D_0} \cdot S\right) - \frac{W^2}{\frac{1}{2} \cdot \rho_0 \cdot V_C^2 \cdot S \cdot \pi \cdot A \cdot e}\right) \tag{26}$$

$$\begin{aligned} \text{ROC} &= V_T \cdot \sin(\alpha) = V_C \cdot \sqrt{\frac{\rho_0}{\rho}} \cdot \sin(\alpha) \\ &\approx V_C \cdot \sqrt{\frac{\rho_0}{\rho}} \cdot \frac{1}{W} \cdot \left(\frac{m \cdot P}{n \cdot d} + V_C^2 \cdot \rho_0 \cdot \left(b \cdot d^2 - \frac{1}{2} \cdot C_{D_0} \cdot S\right) - \frac{W^2}{\frac{1}{2} \cdot \rho_0 \cdot V_C^2 \cdot S \cdot \pi \cdot A \cdot e}\right) \end{aligned} \tag{27}$$

Rate of Climb 2

$$\text{ROC} = \frac{V_T}{W}(T - D) \tag{28}$$

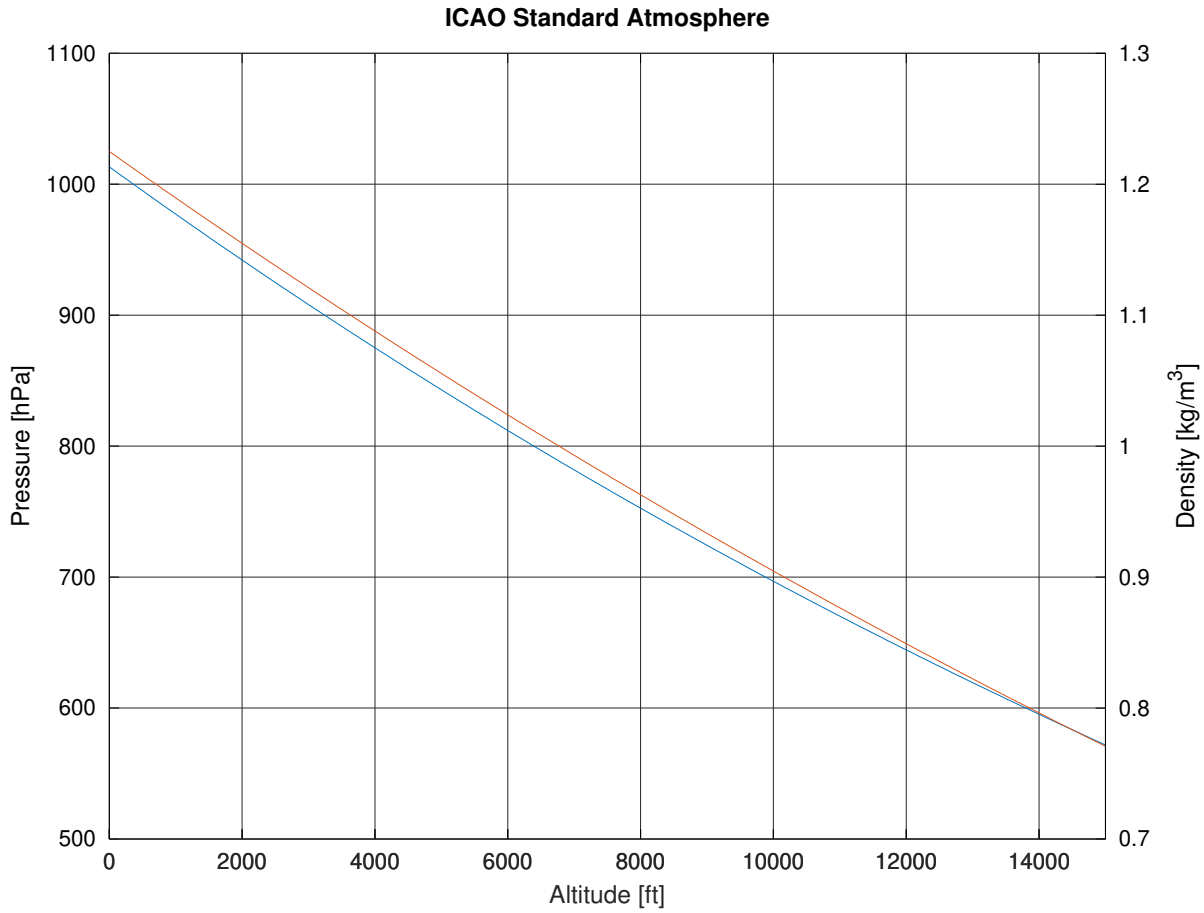

Figure 58: ICAO Standard Atmosphere

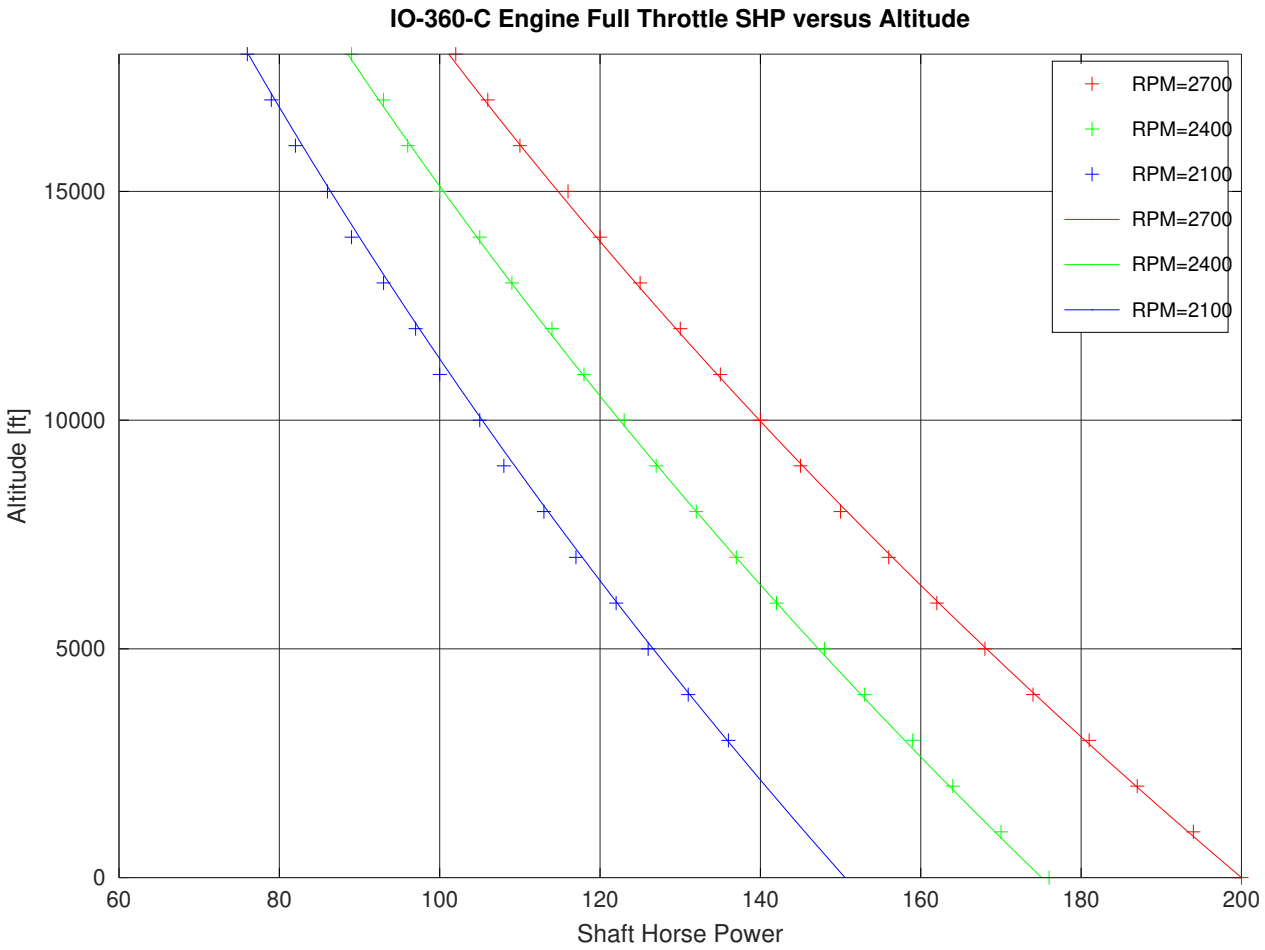

Figure 59: IO-360-C Engine Performance versus Altitude

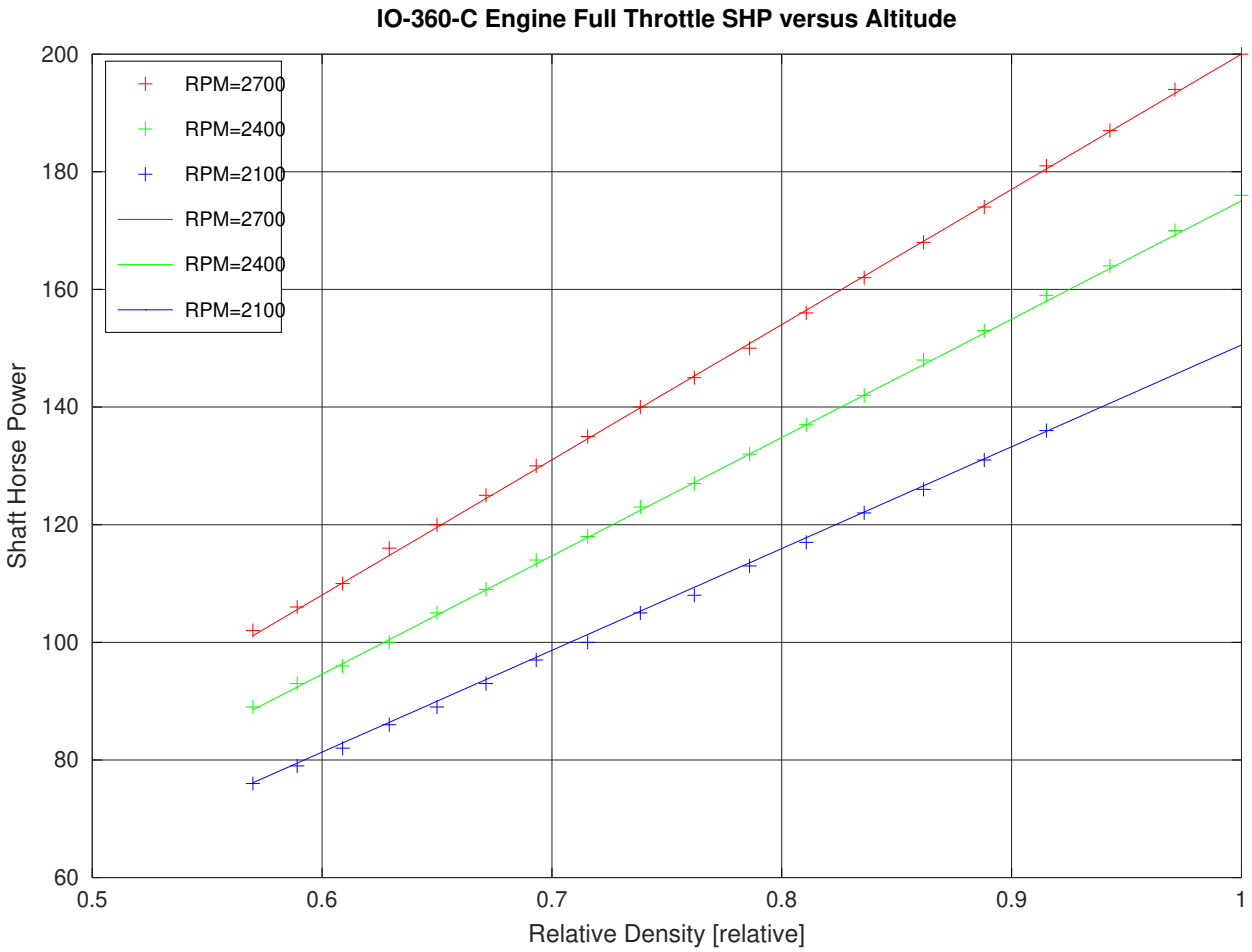

Figure 60: IO-360-C Engine Performance versus Altitude

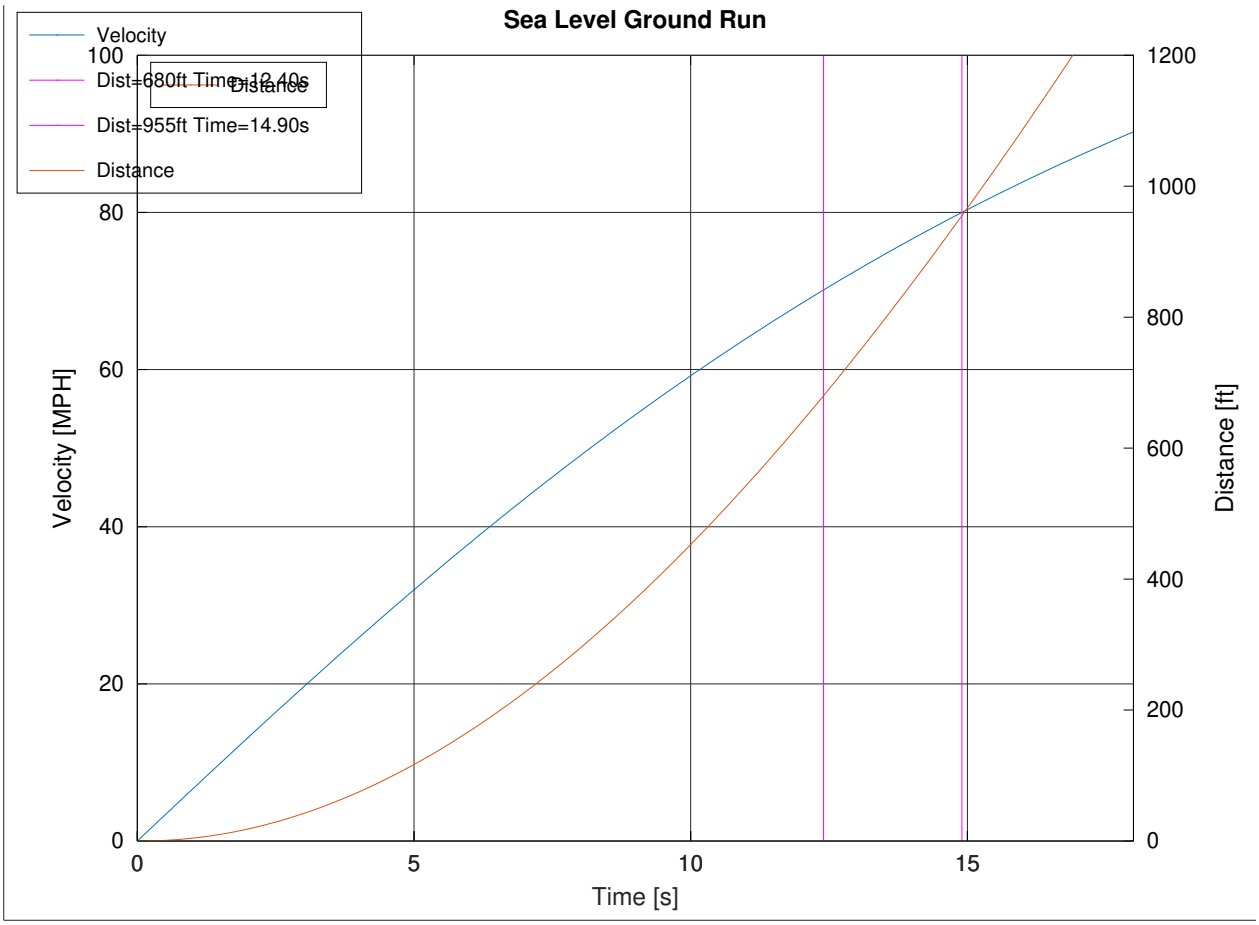

Figure 61: P28R-200B Sea Level Ground Run

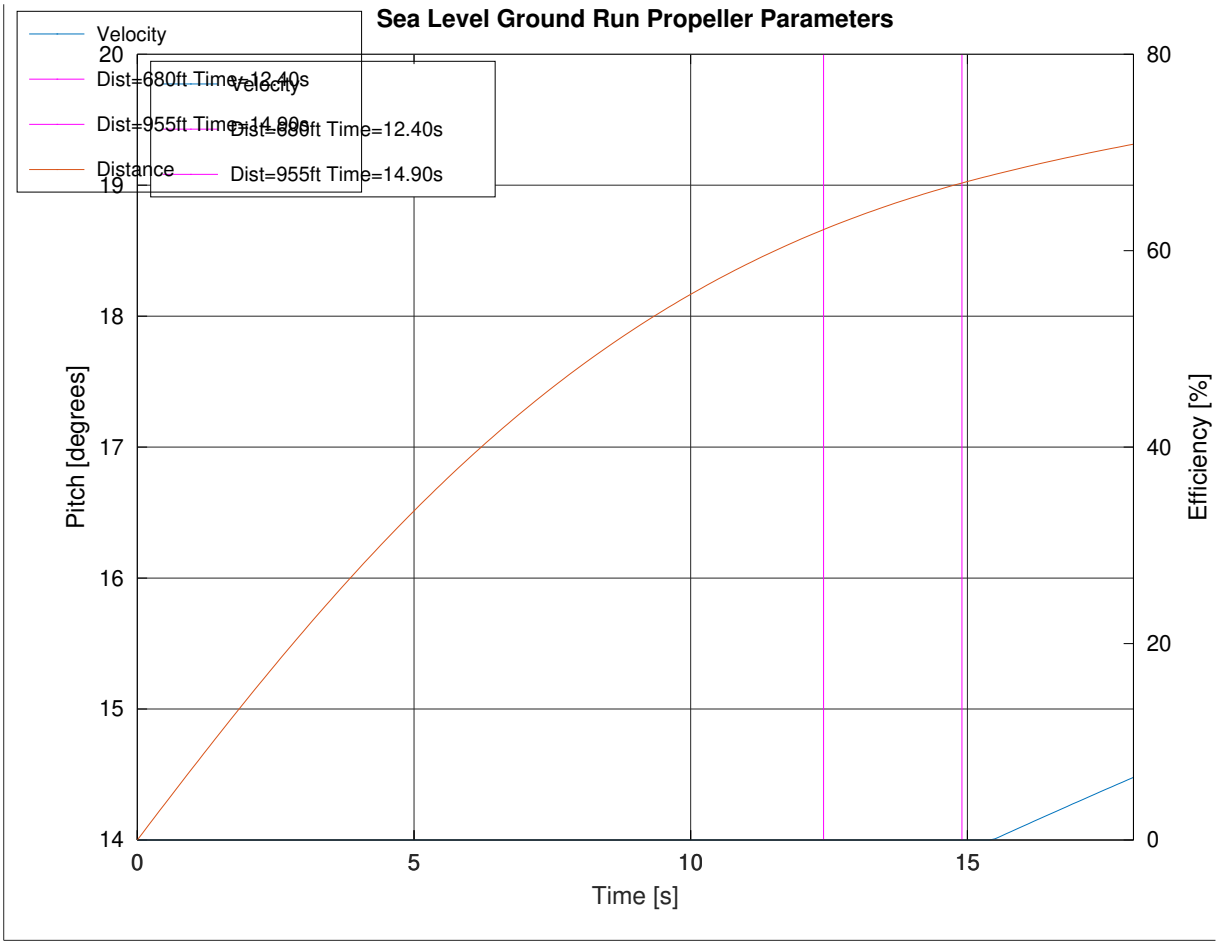

Figure 62: P28R-200B Sea Level Ground Run

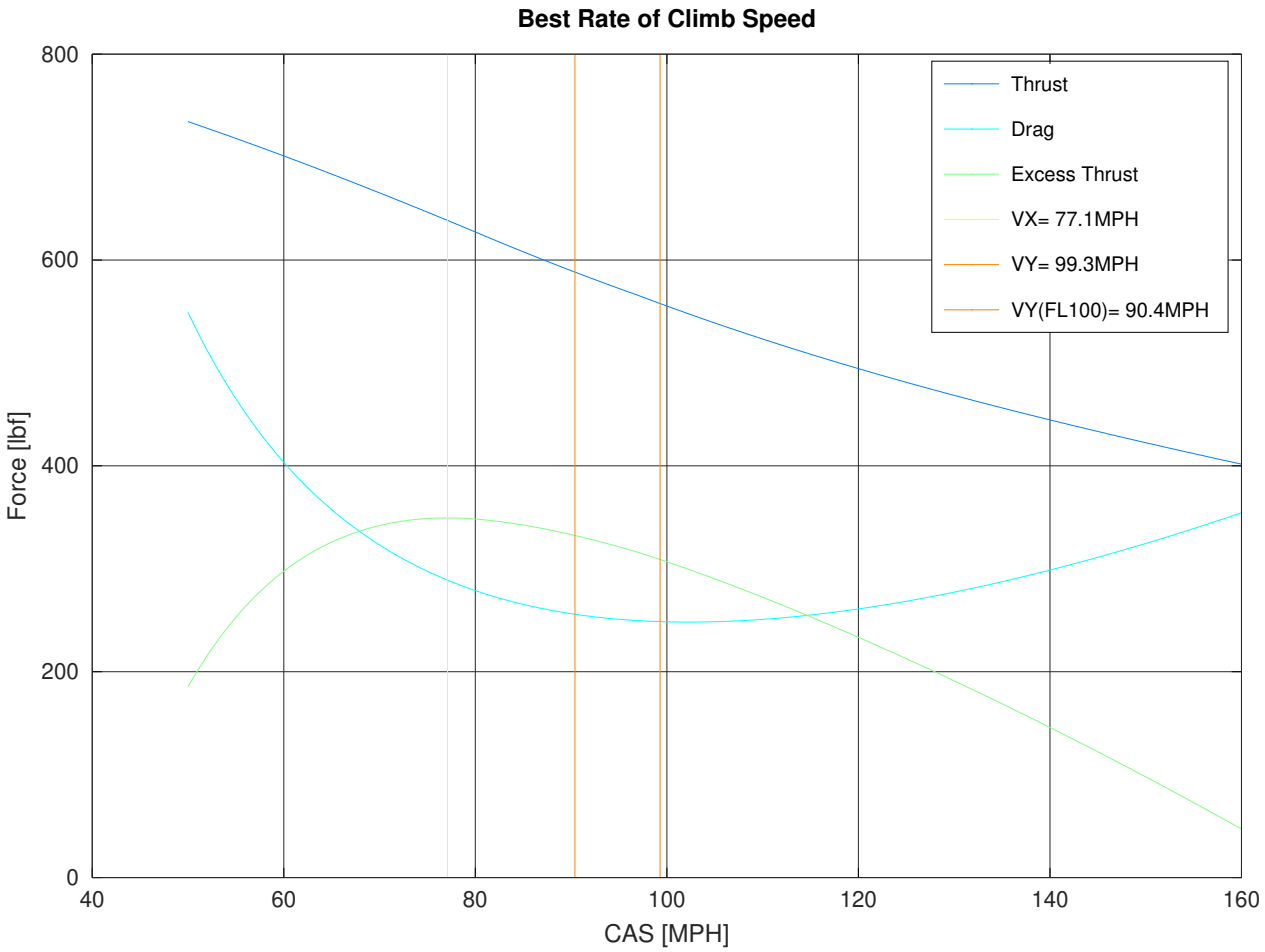

Figure 63: P28R-200B Climb Performance

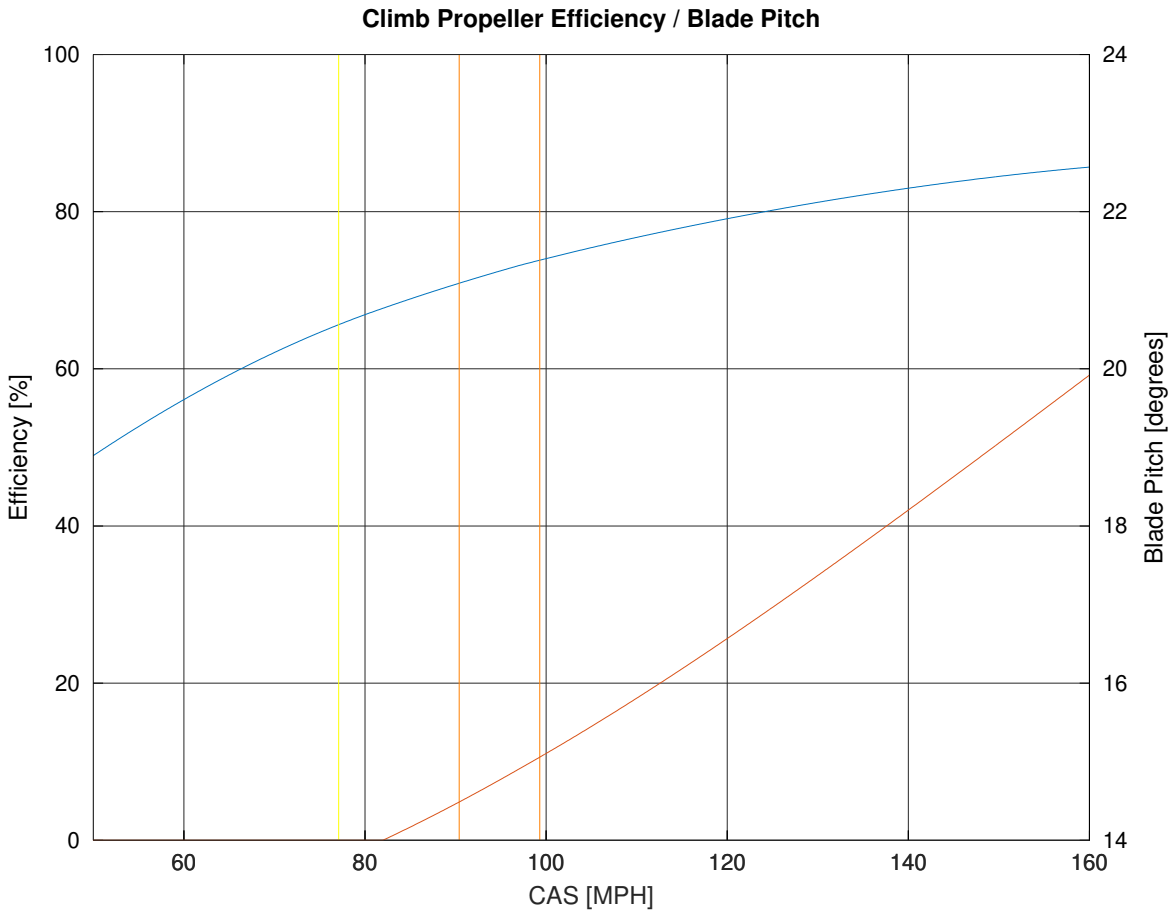

Figure 64: P28R-200B Climb Propeller Efficiency / Pitch

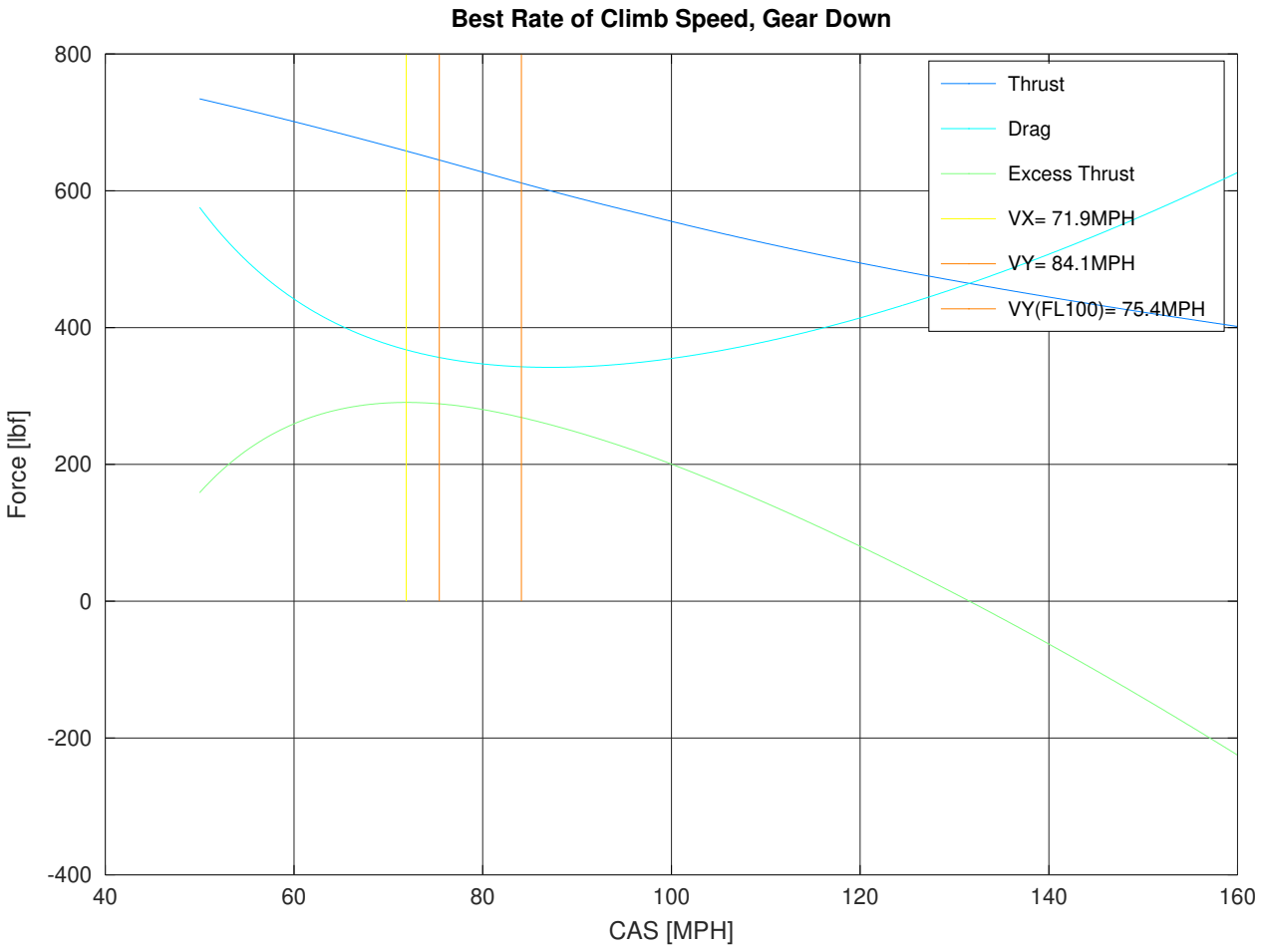

Figure 65: P28R-200B Climb Performance

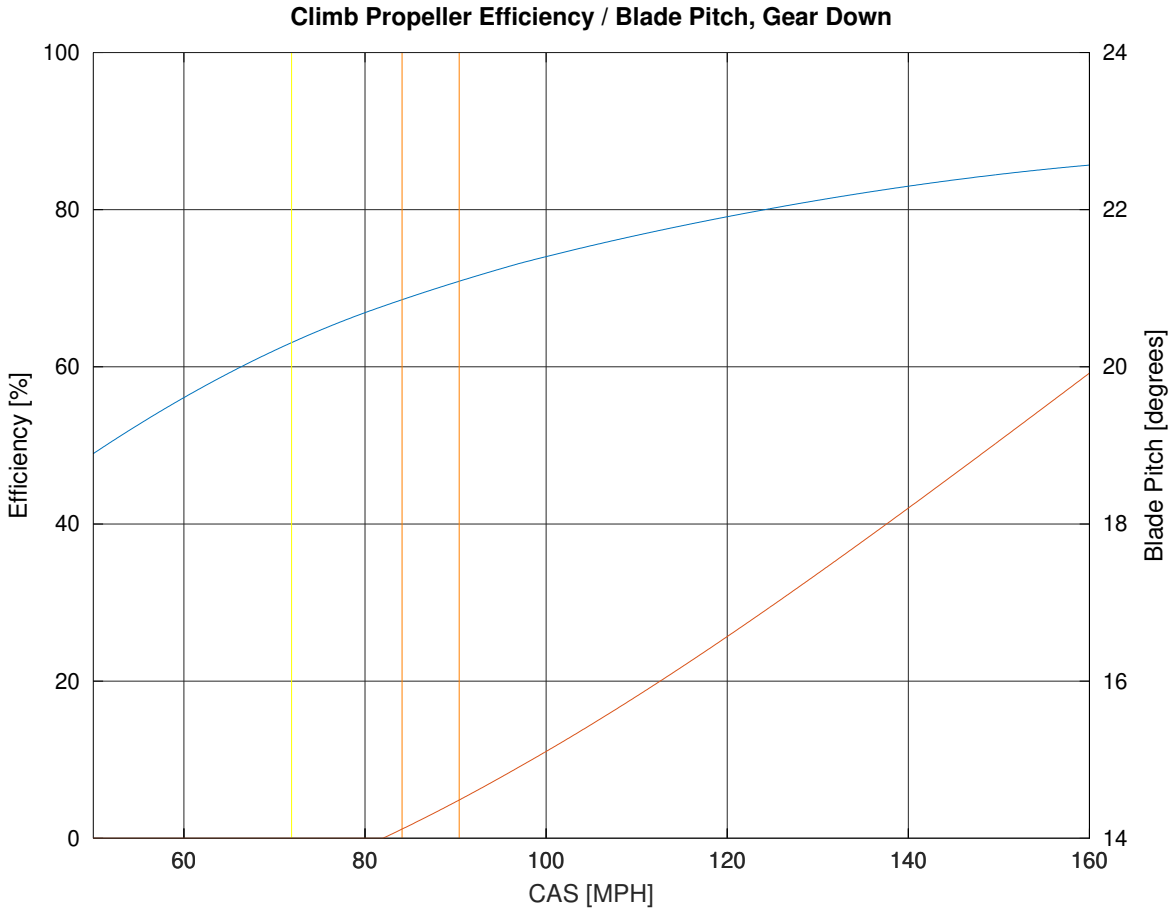

Figure 66: P28R-200B Climb Propeller Efficiency / Pitch

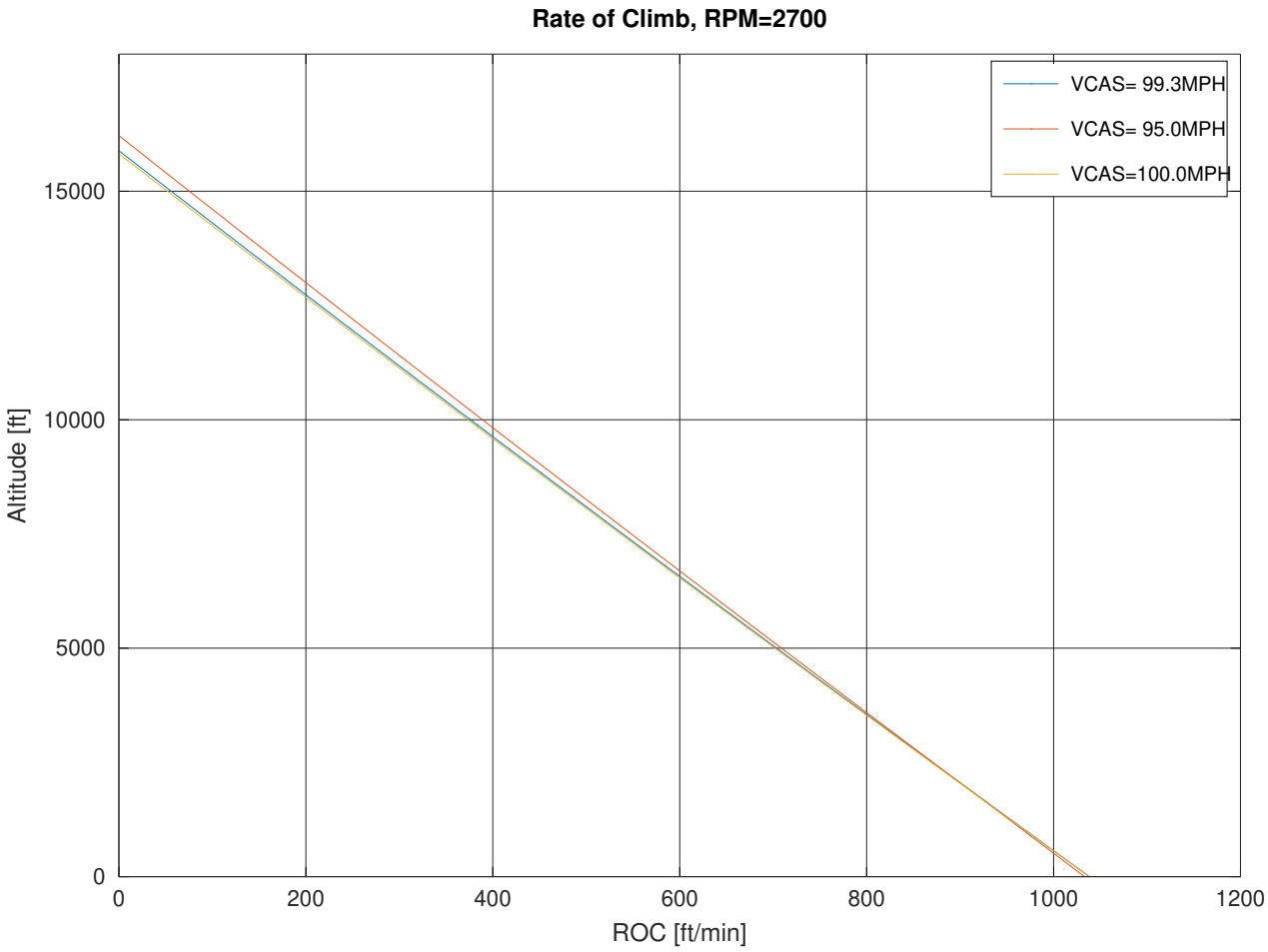

Figure 67: P28R-200B Rate of Climb, 2700 RPM

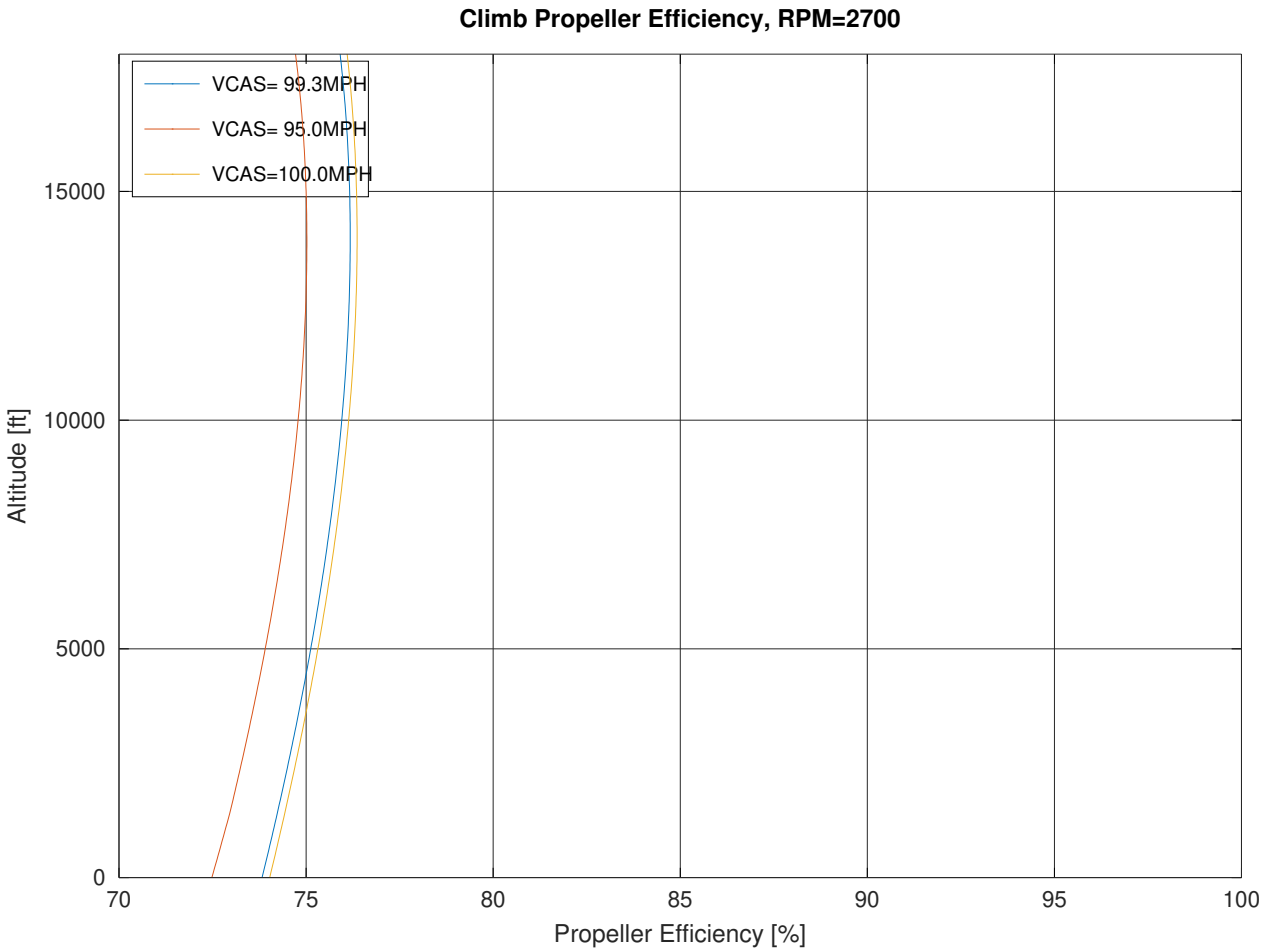

Figure 68: P28R-200B Climb Propeller Efficiency, 2700 RPM

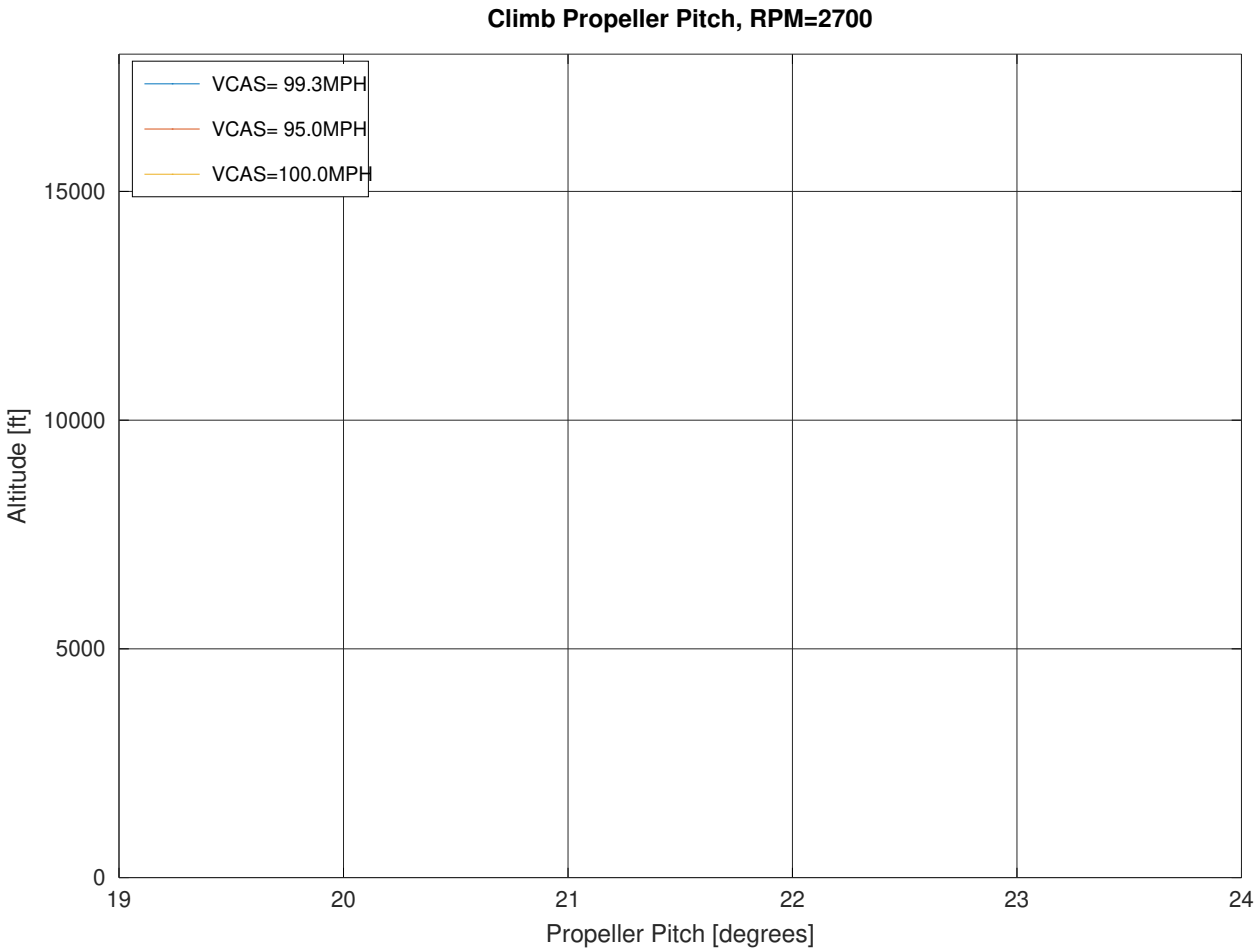

Figure 69: P28R-200B Climb Propeller Pitch, 2700 RPM

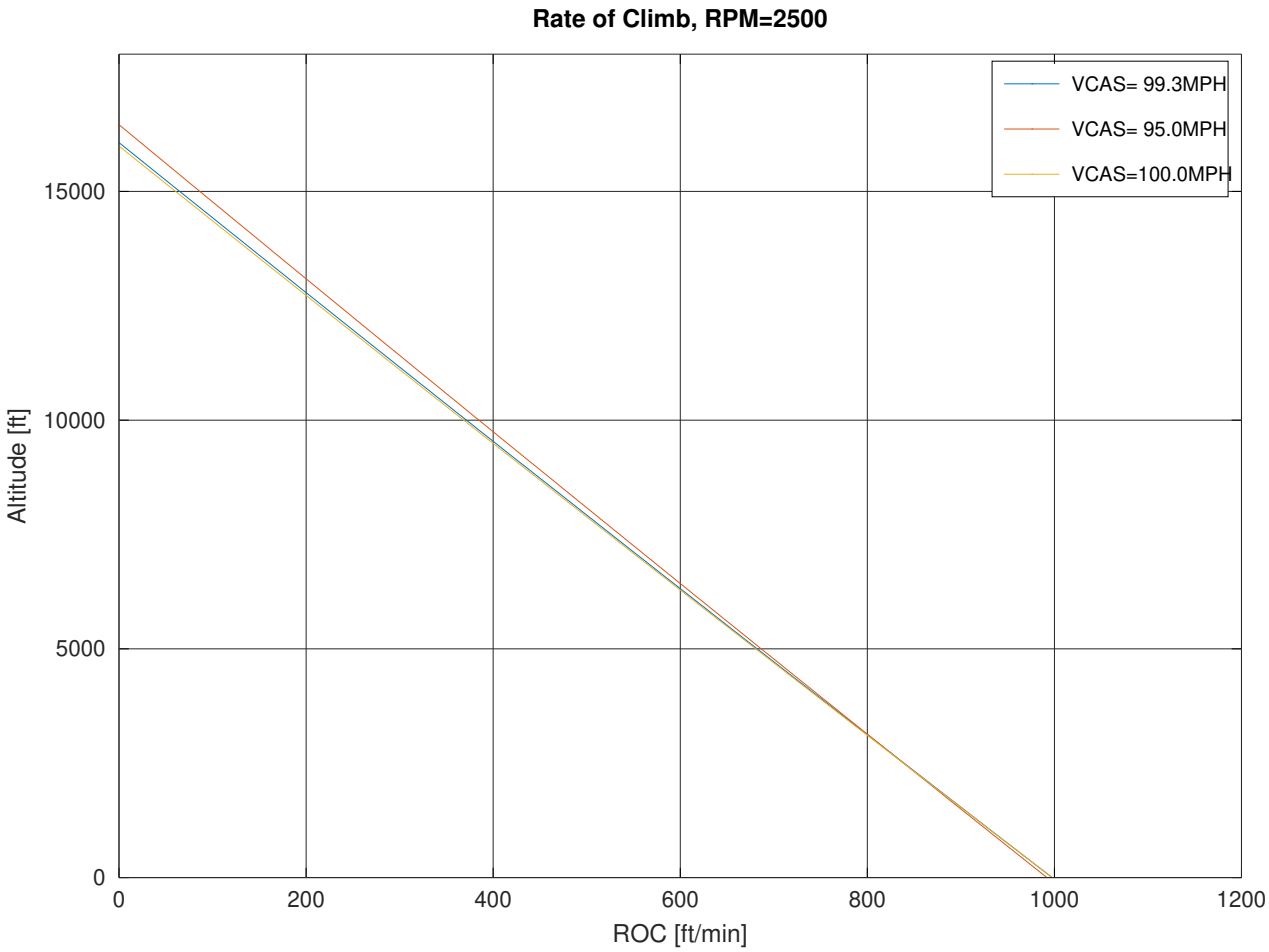

Figure 70: P28R-200B Rate of Climb, 2500 RPM

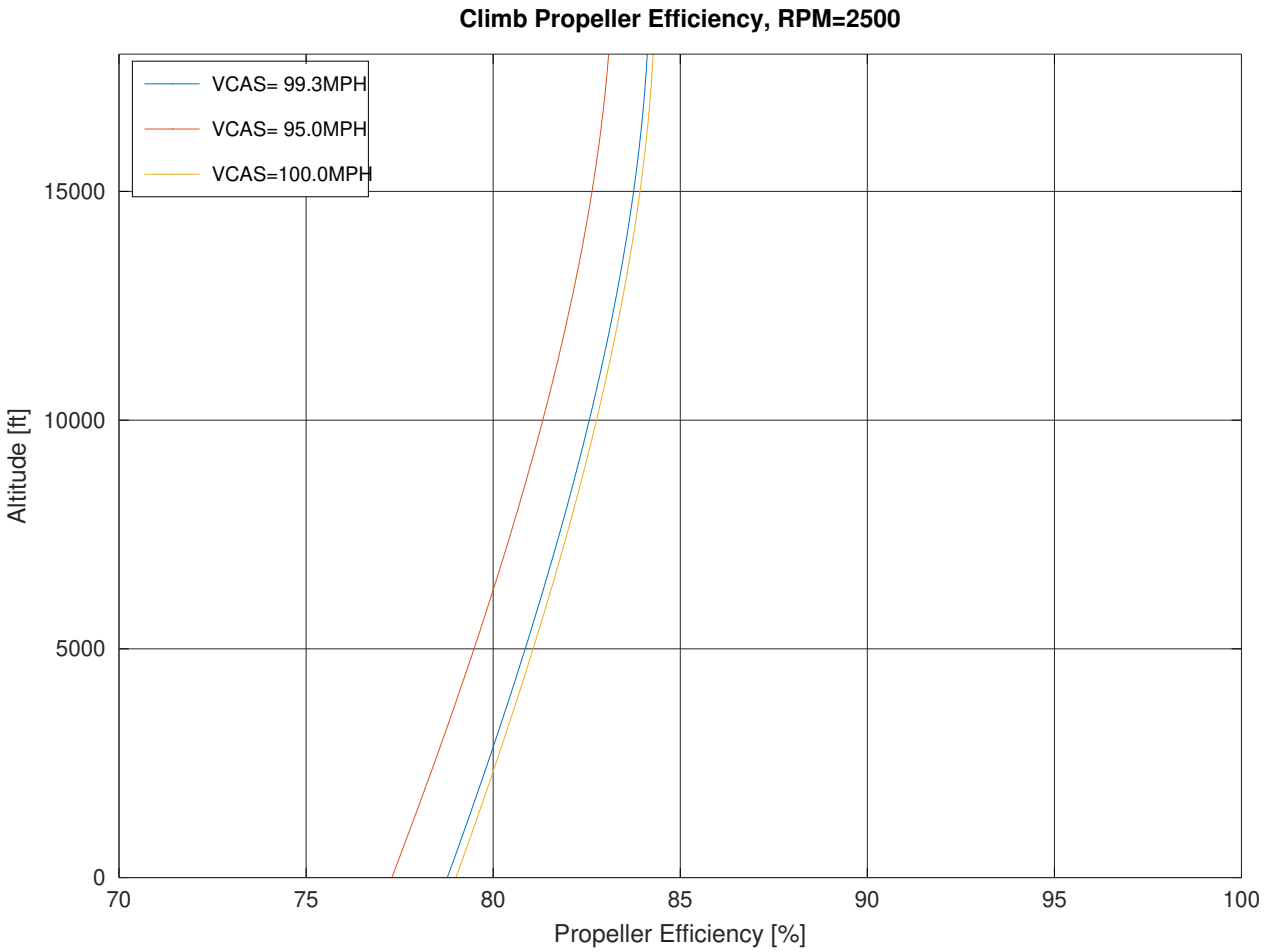

Figure 71: P28R-200B Climb Propeller Efficiency, 2500 RPM

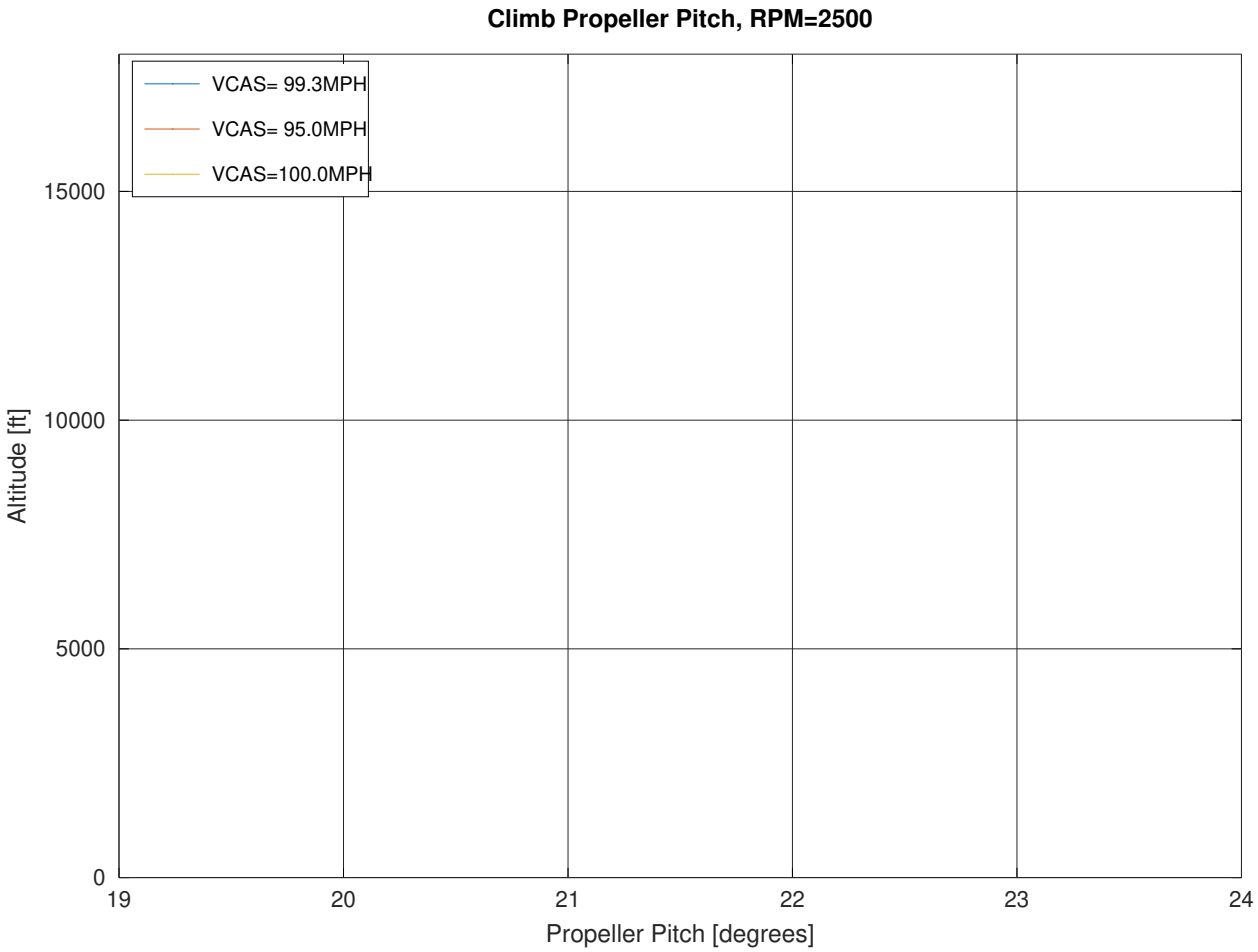

Figure 72: P28R-200B Climb Propeller Pitch, 2500 RPM

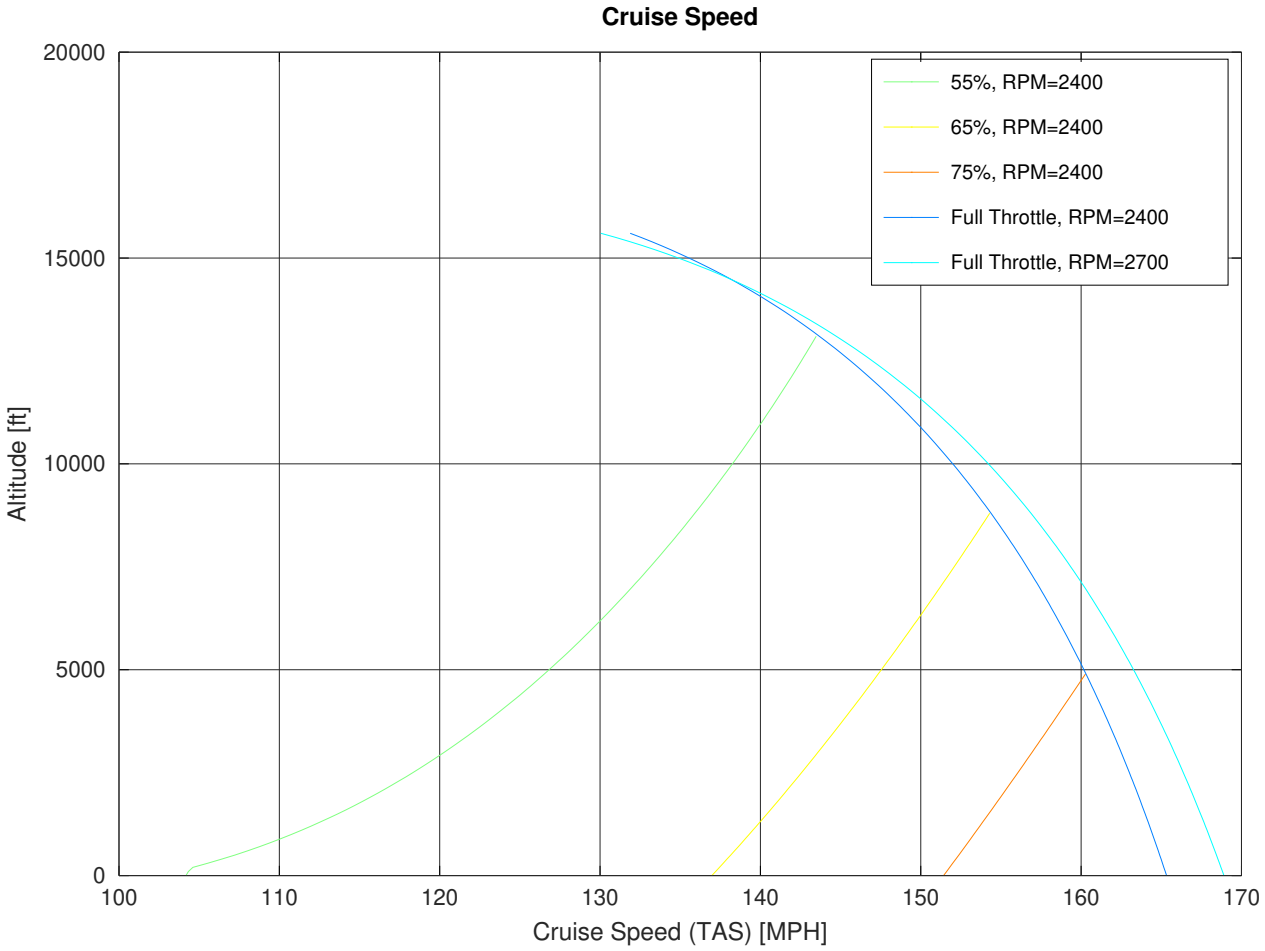

Figure 73: P28R-200B Cruise Speed

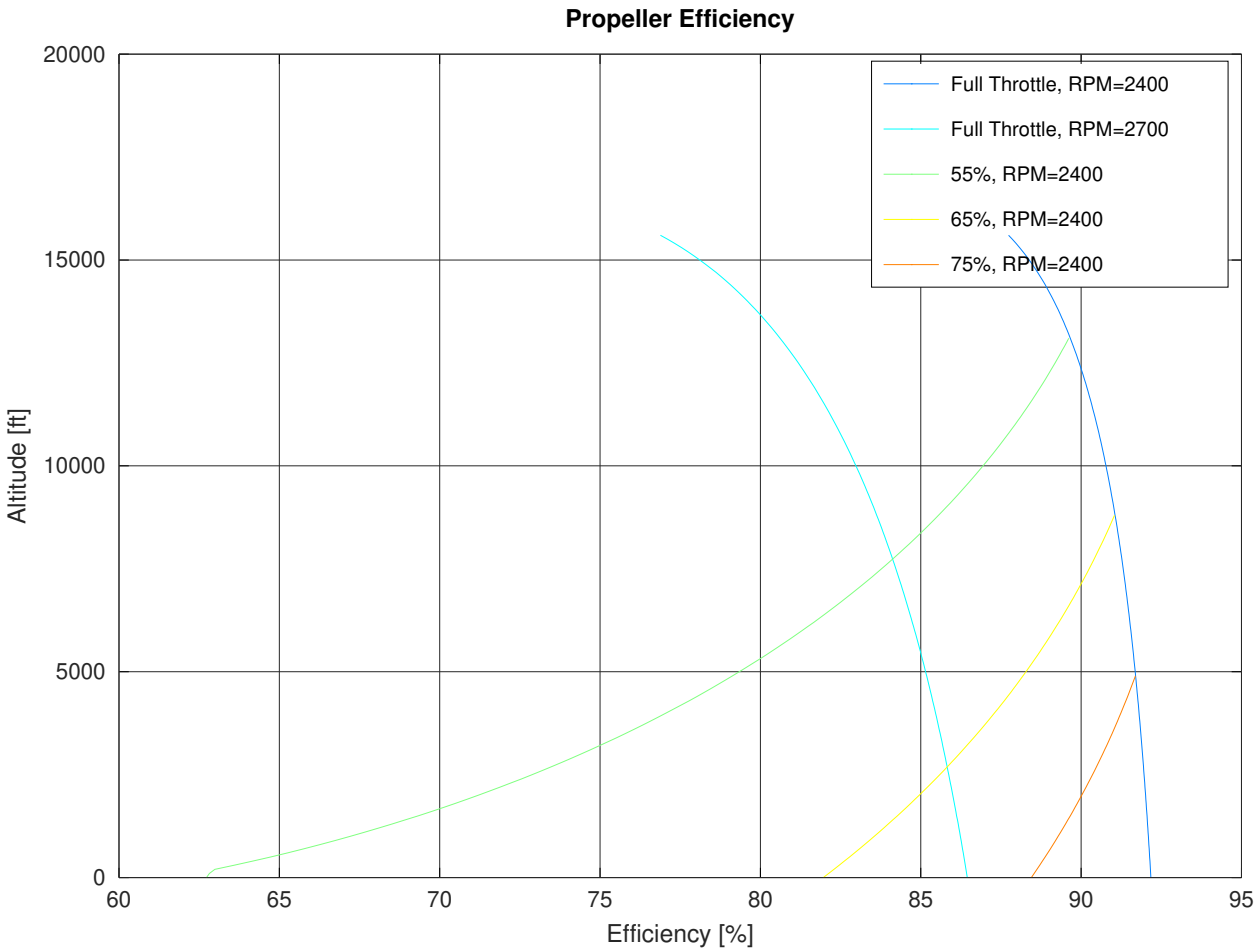

Figure 74: P28R-200B Cruise Propeller Efficiency

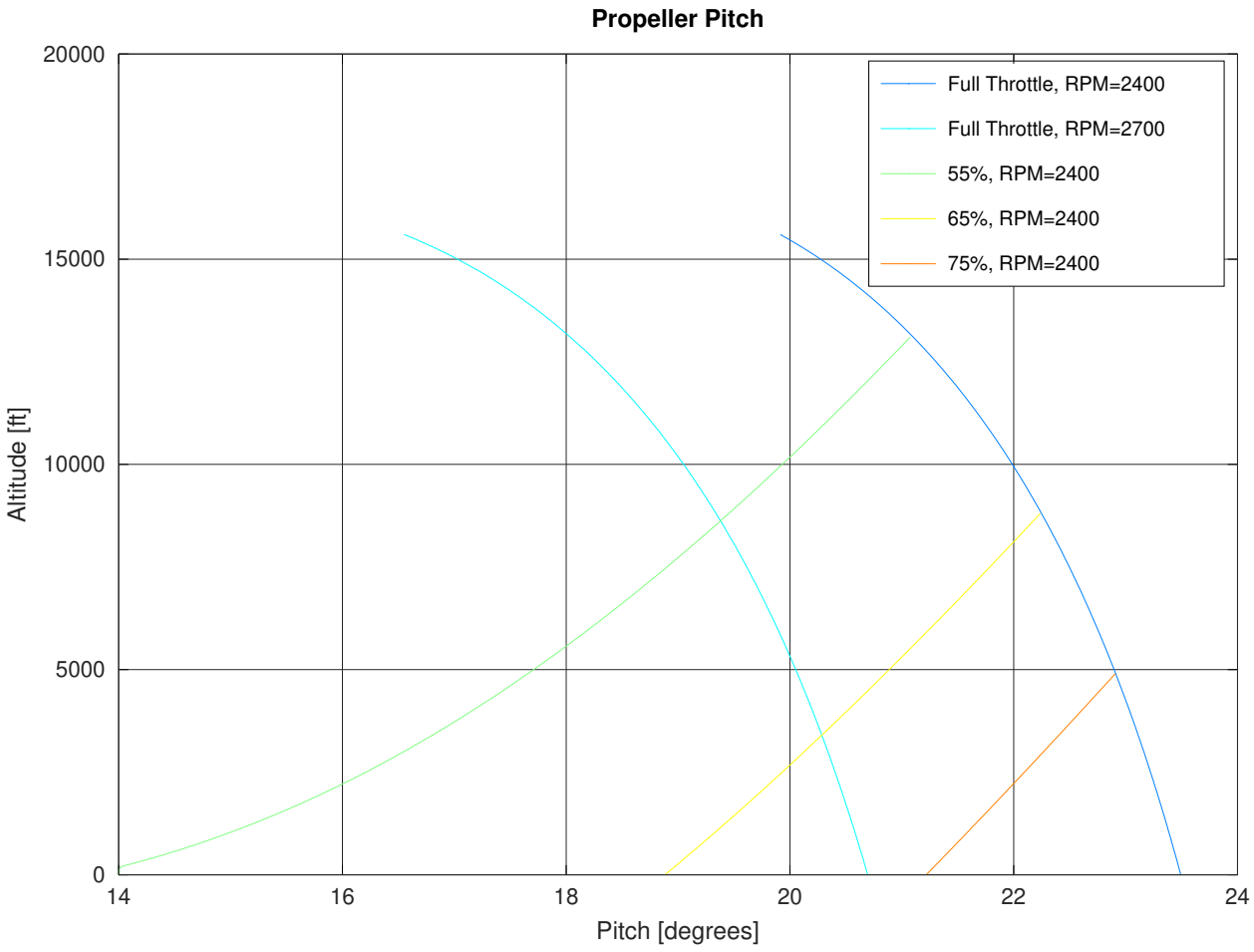

Figure 75: P28R-200B Cruise Propeller Pitch

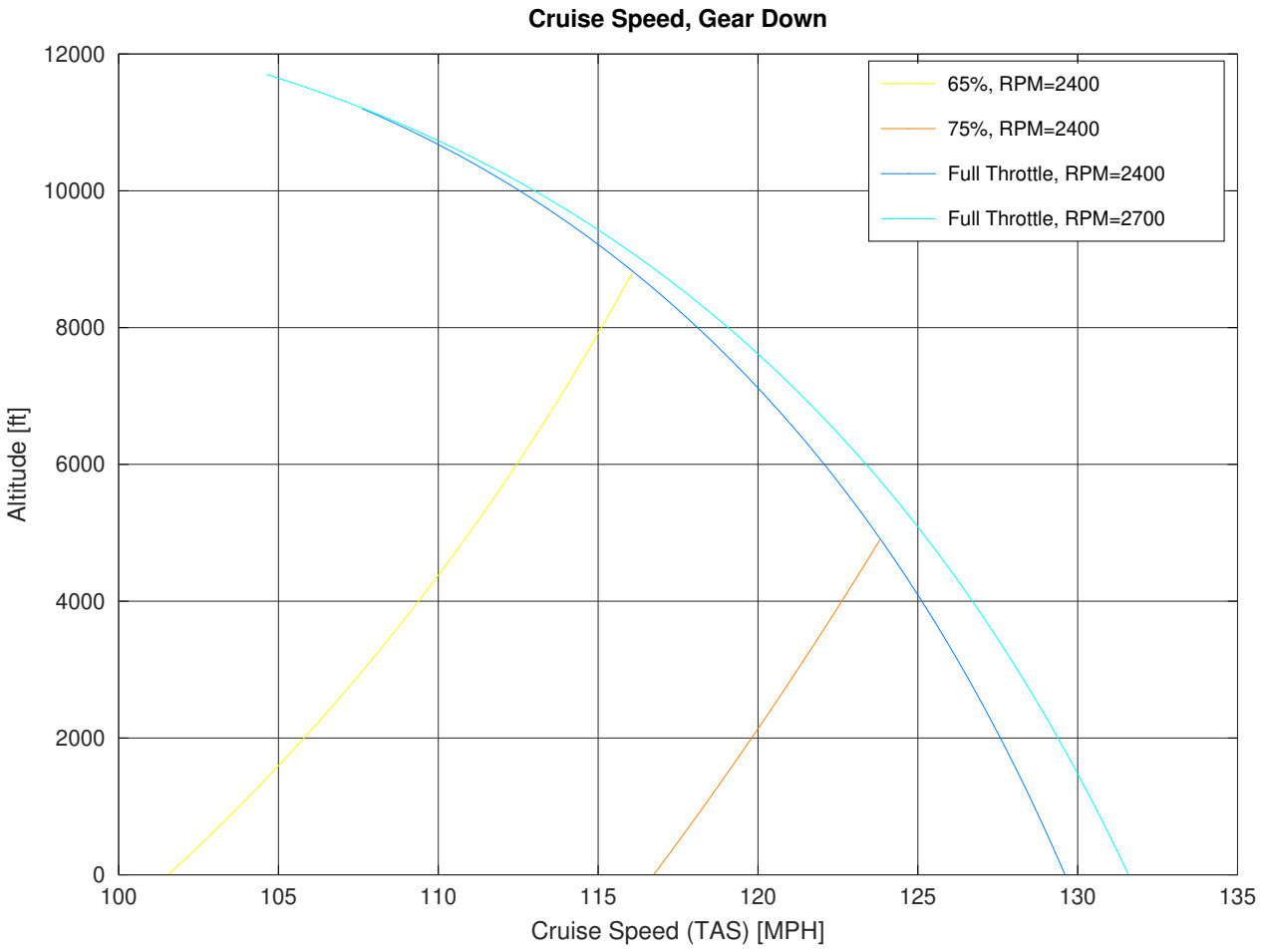

Figure 76: P28R-200B Cruise Speed, Gear Down

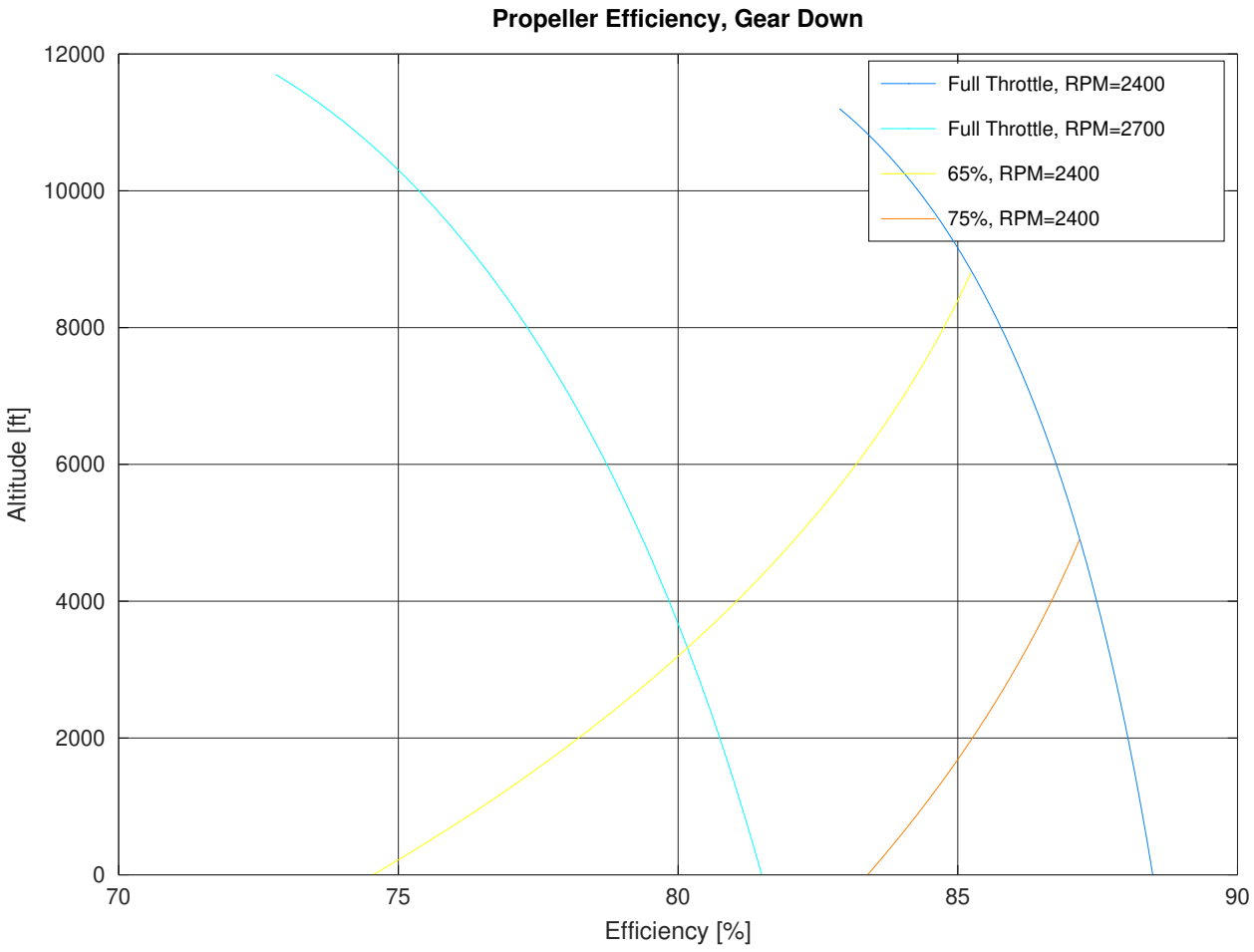

Figure 77: P28R-200B Cruise Propeller Efficiency, Gear Down

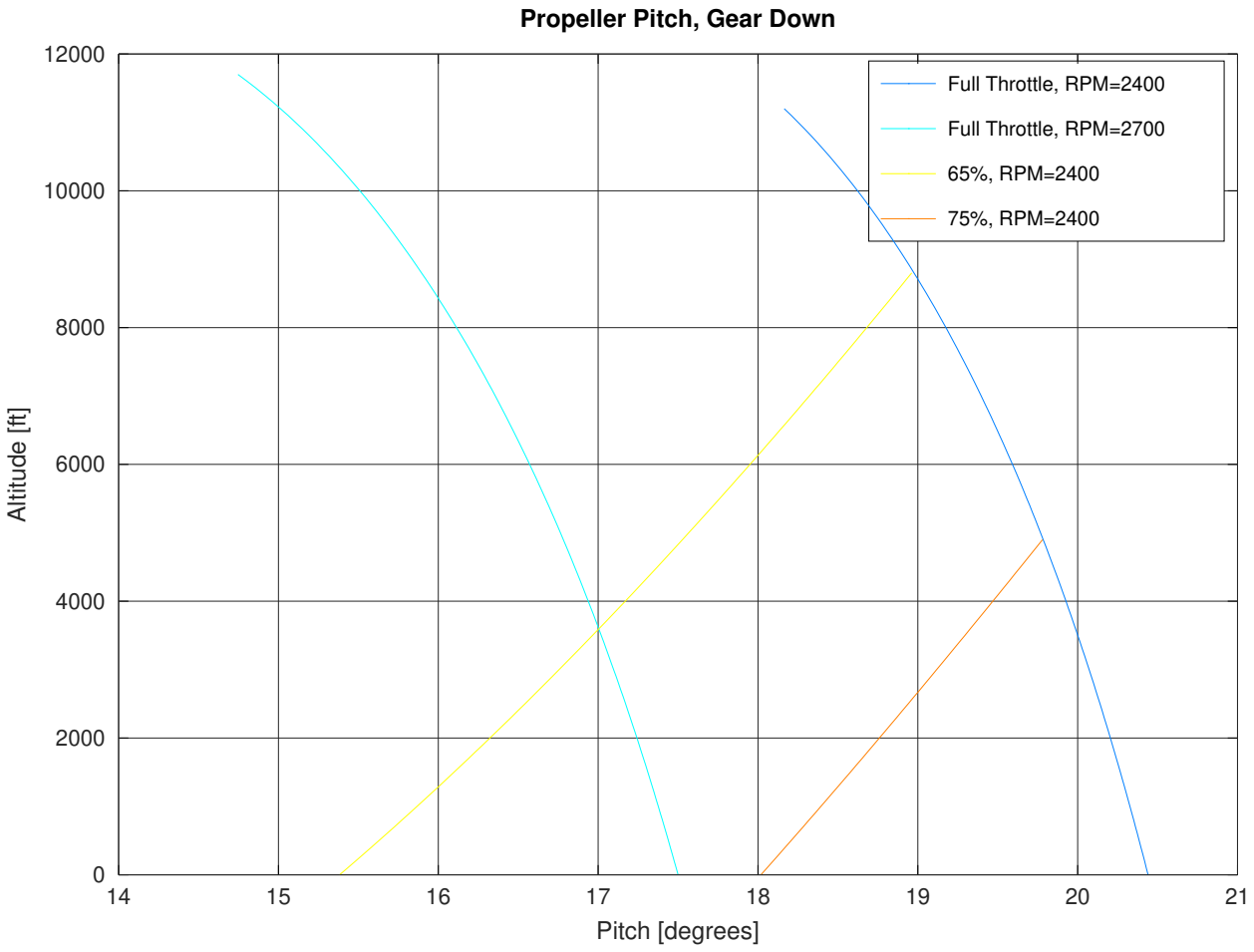

Figure 78: P28R-200B Cruise Propeller Pitch, Gear Down

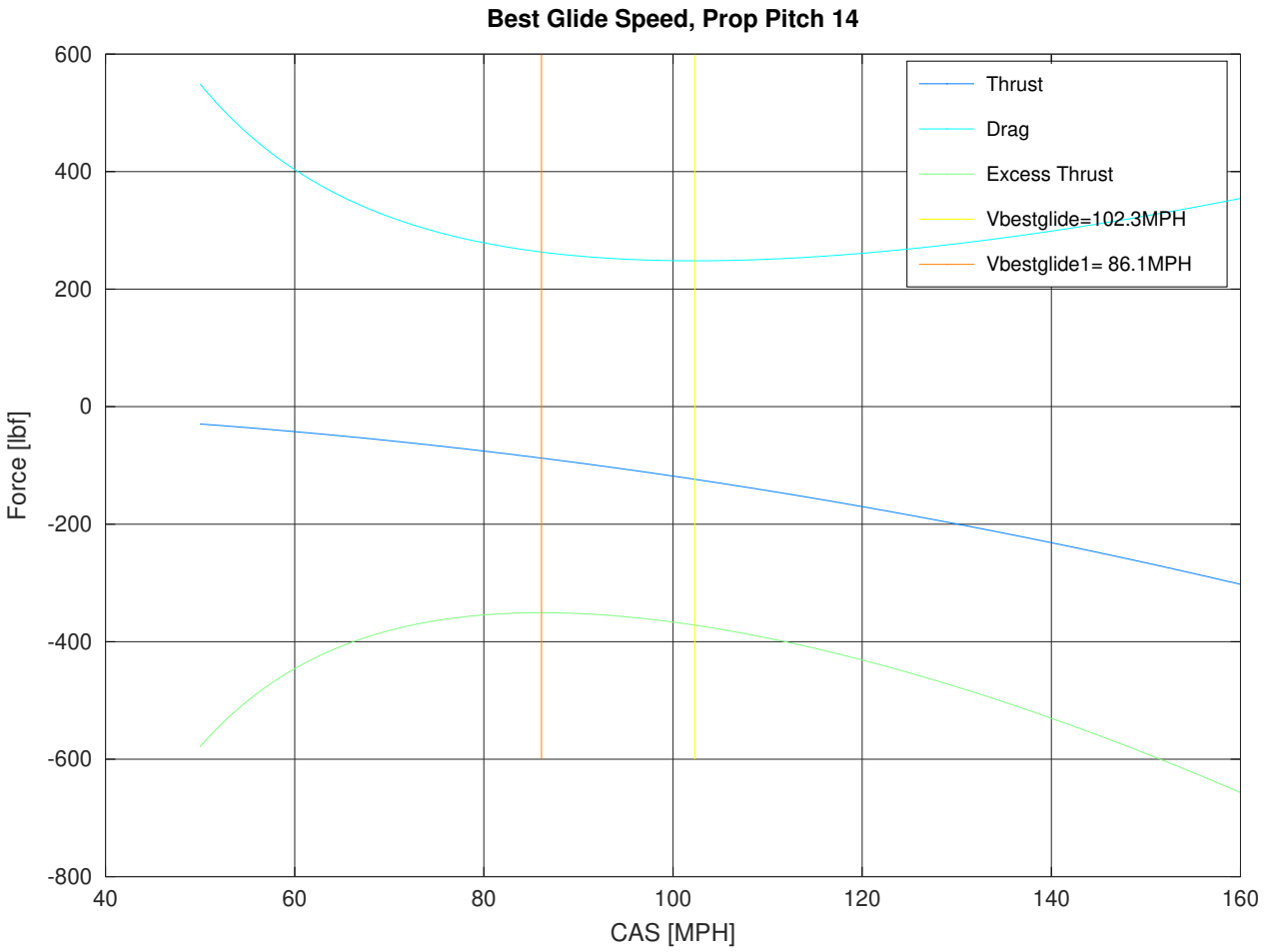

Figure 79: P28R-200B Best Glide, Minimum Propeller Pitch

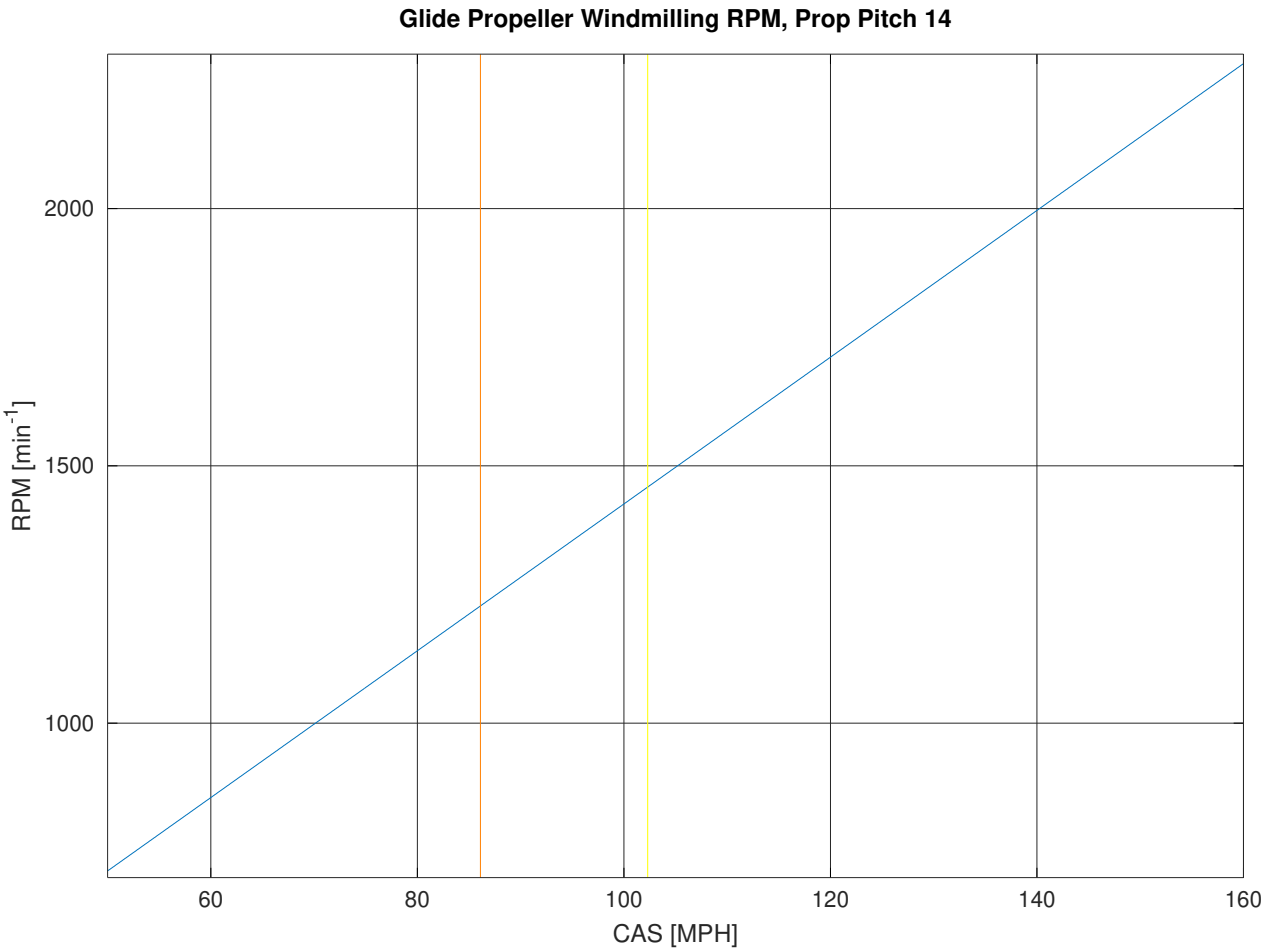

Figure 80: P28R-200B Best Glide Propeller Parameters, Minimum Propeller Pitch

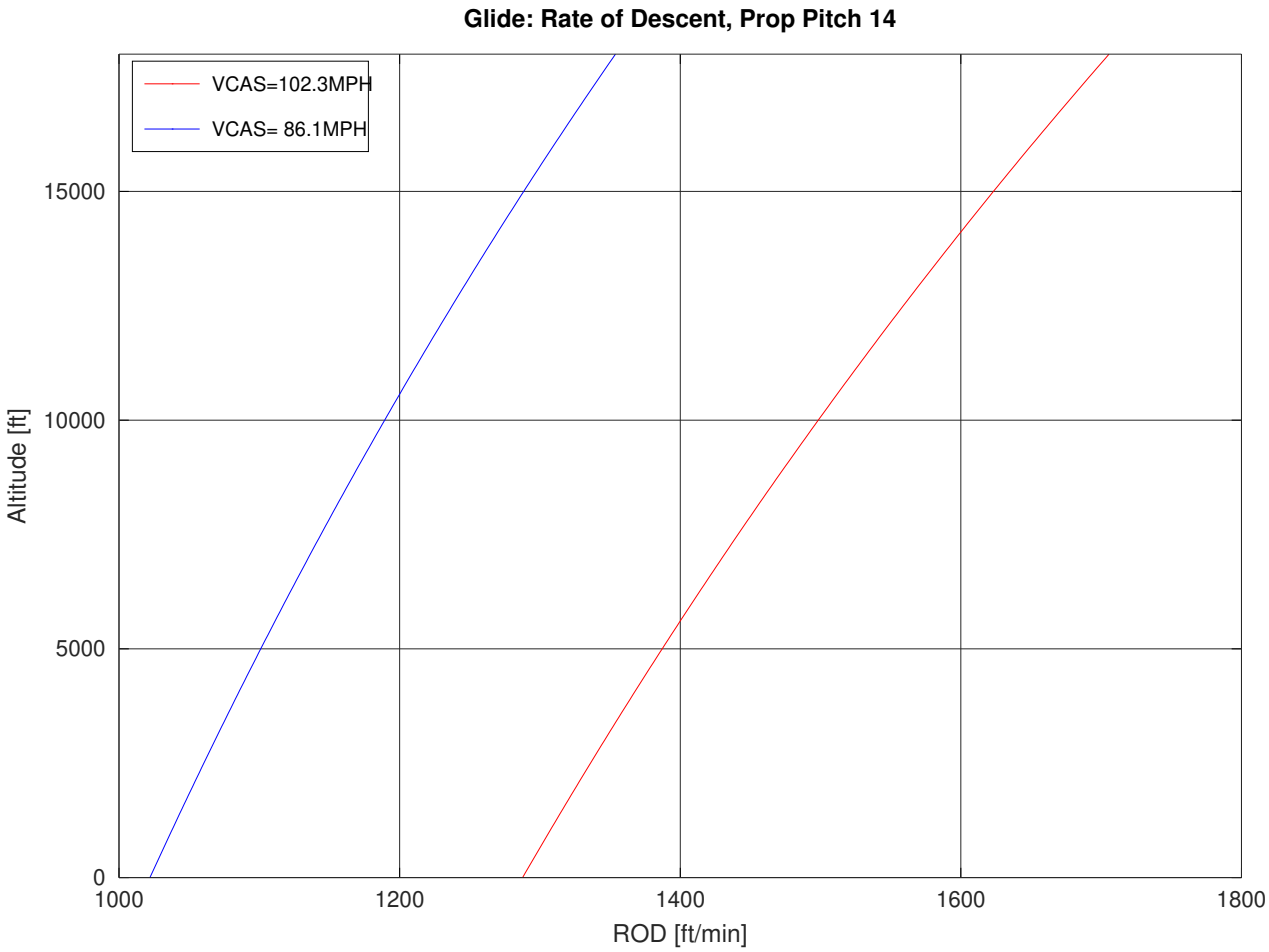

Figure 81: P28R-200B Glide Rate of Descent, Minimum Propeller Pitch

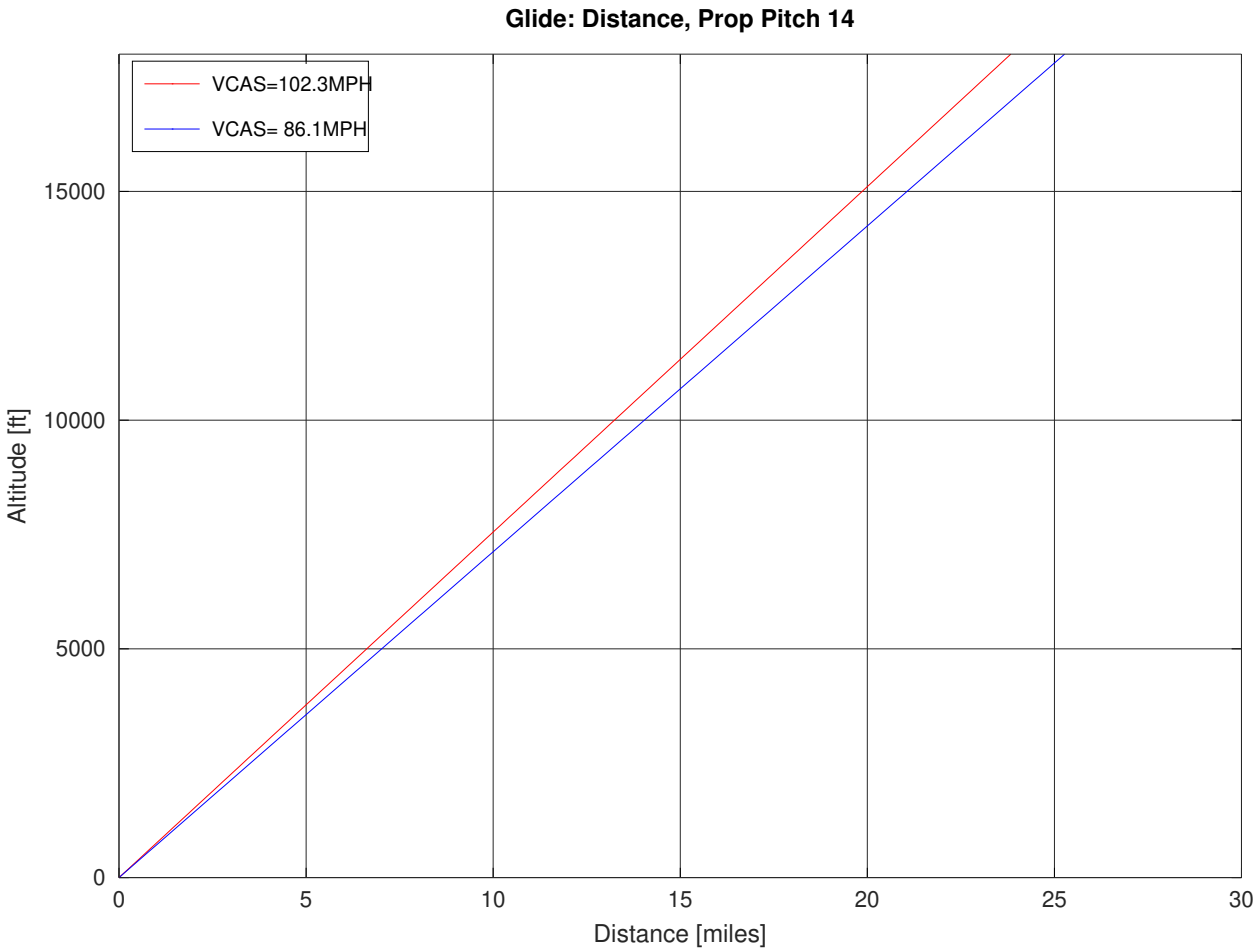

Figure 82: P28R-200B Glide Distance, Minimum Propeller Pitch

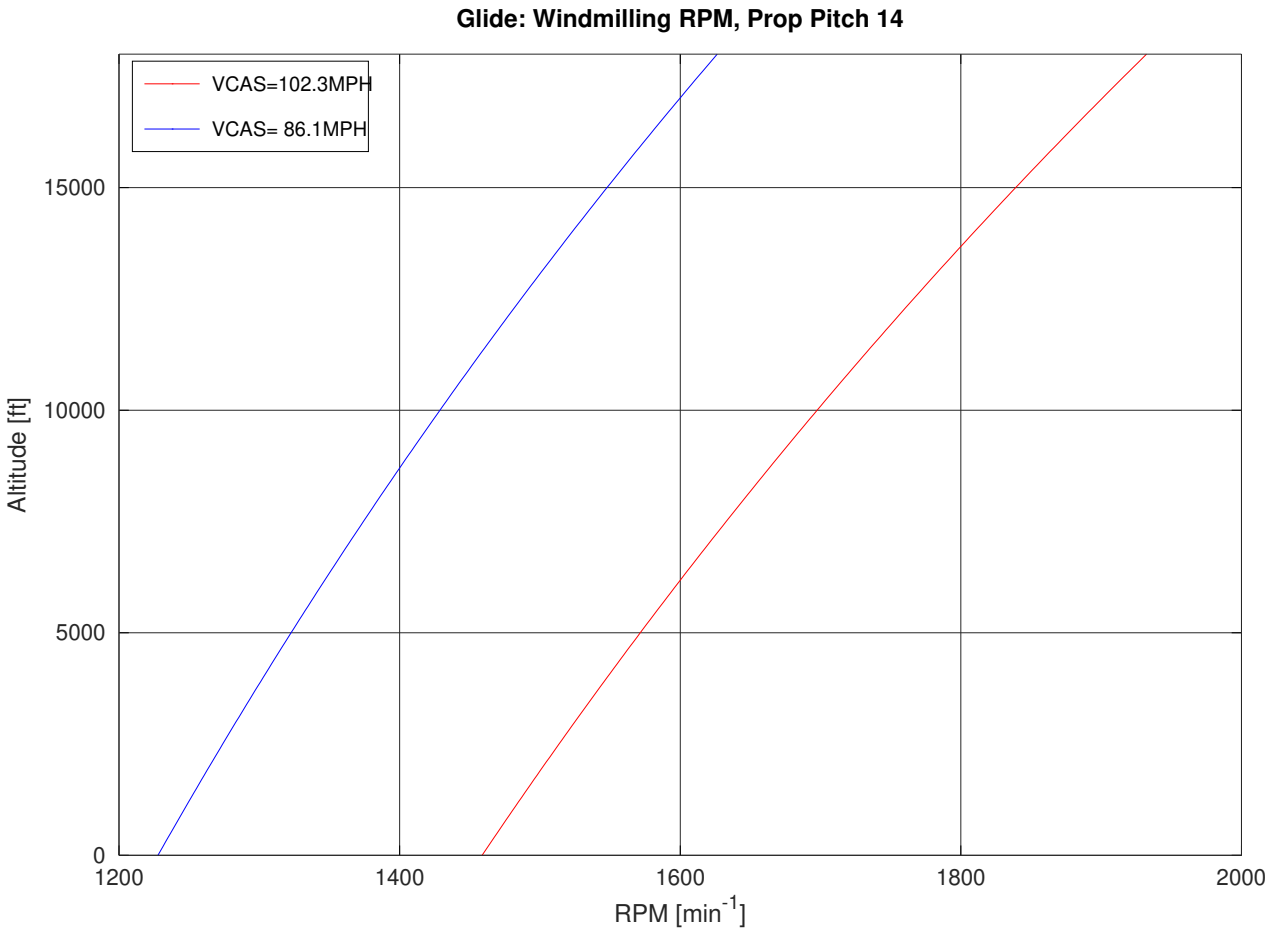

Figure 83: P28R-200B Glide Windmilling RPM, Minimum Propeller Pitch

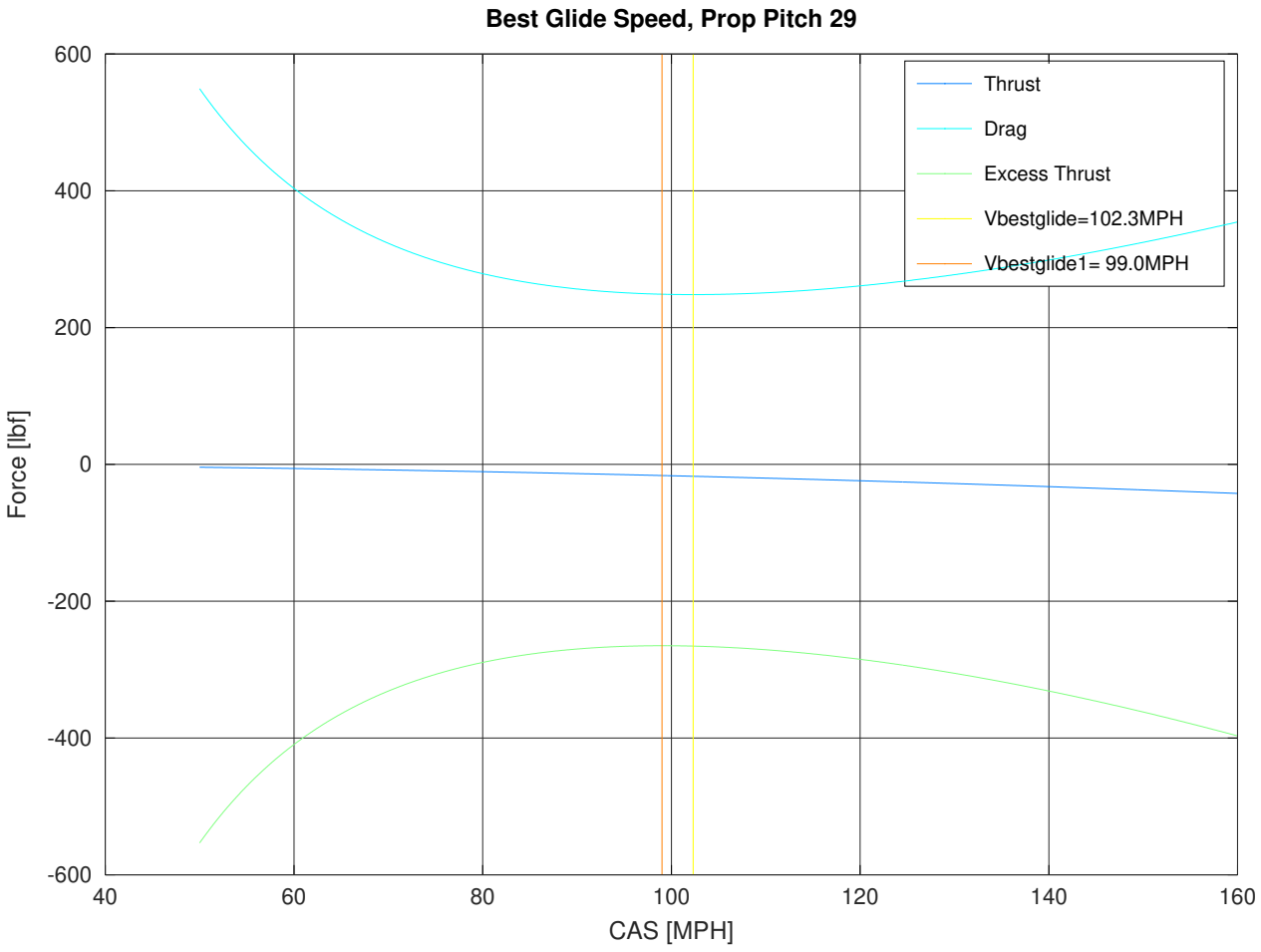

Figure 84: P28R-200B Best Glide, Maximum Propeller Pitch

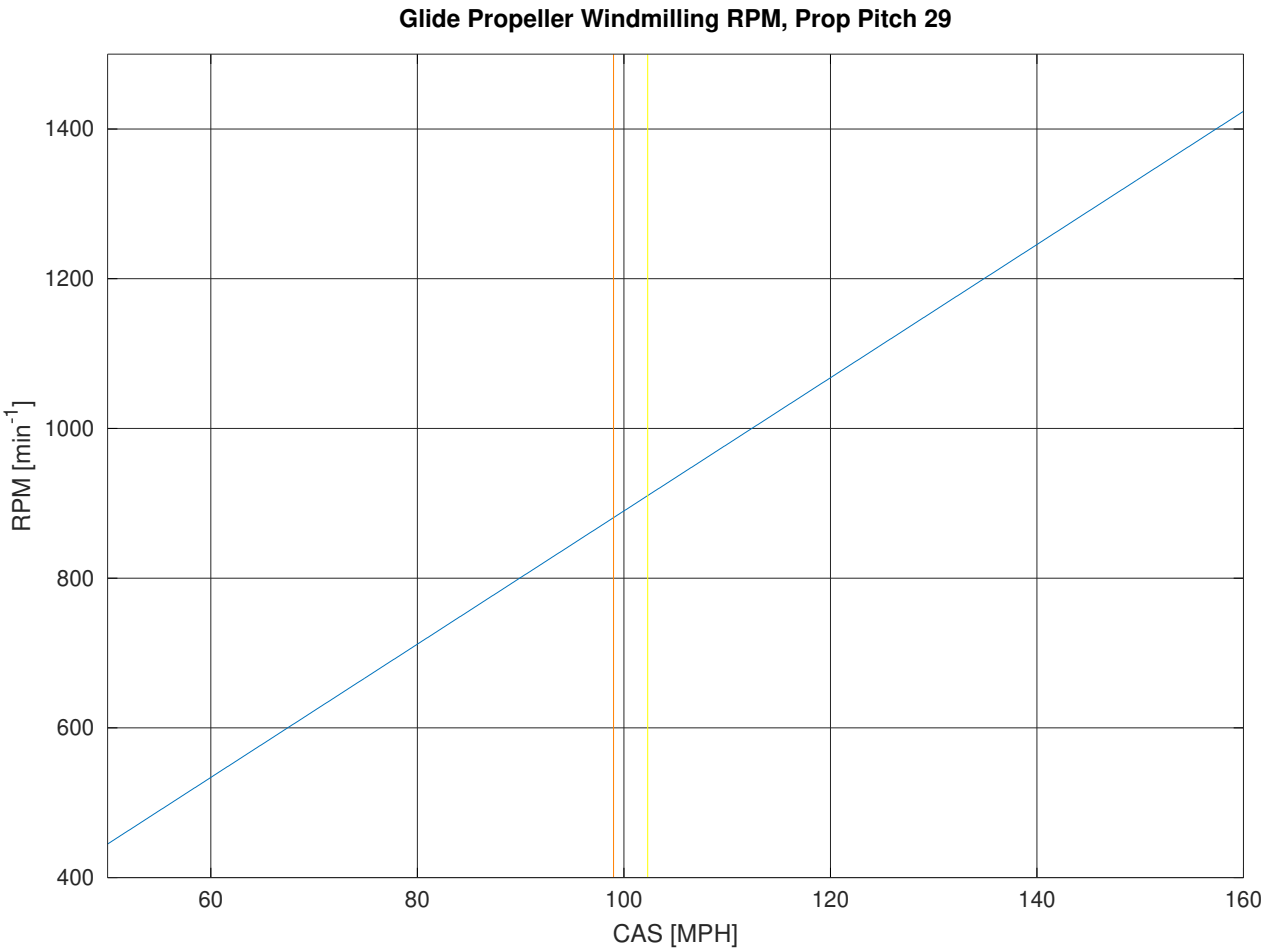

Figure 85: P28R-200B Best Glide Propeller Parameters, Maximum Propeller Pitch

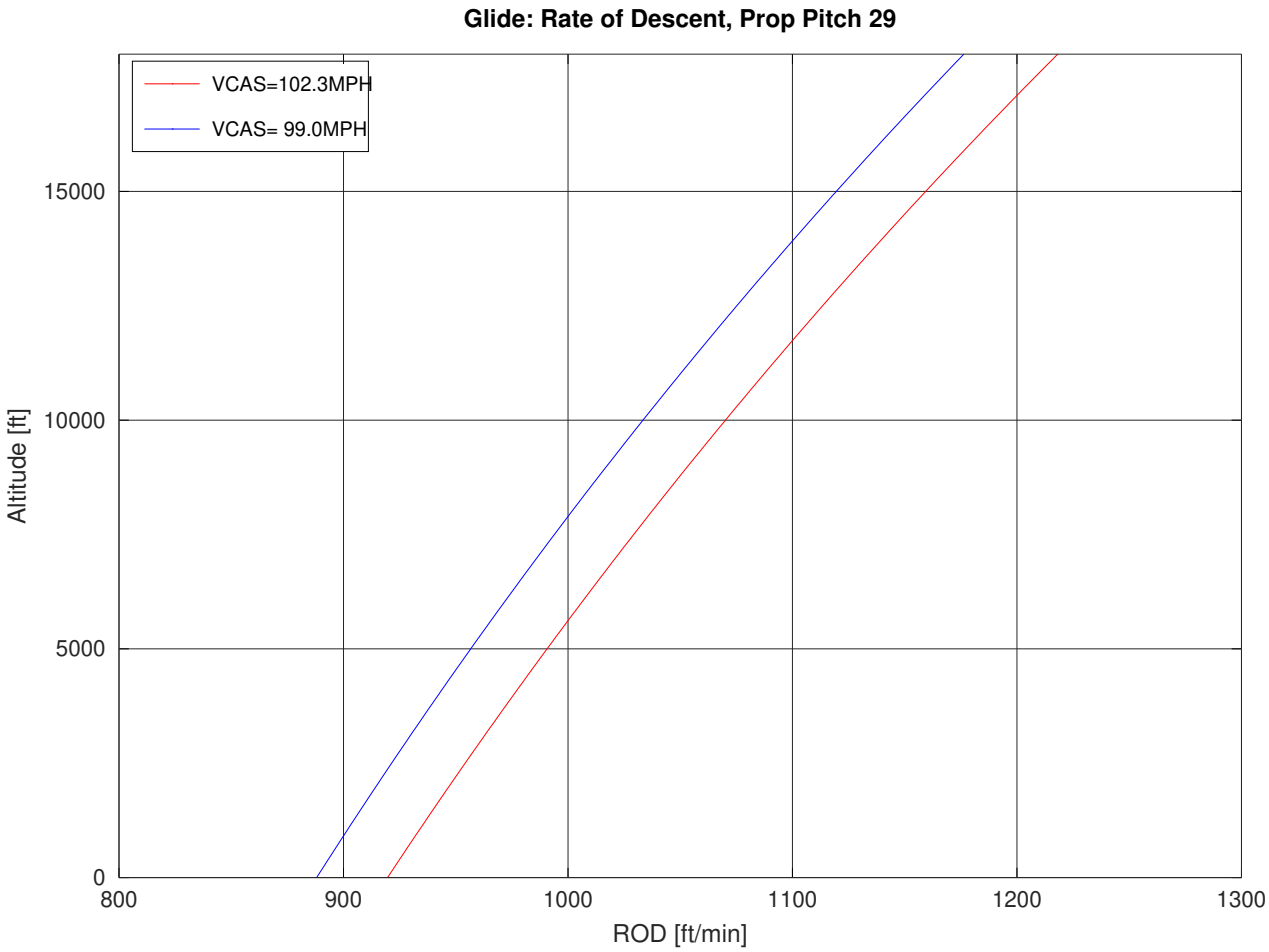

Figure 86: P28R-200B Glide Rate of Descent, Maximum Propeller Pitch

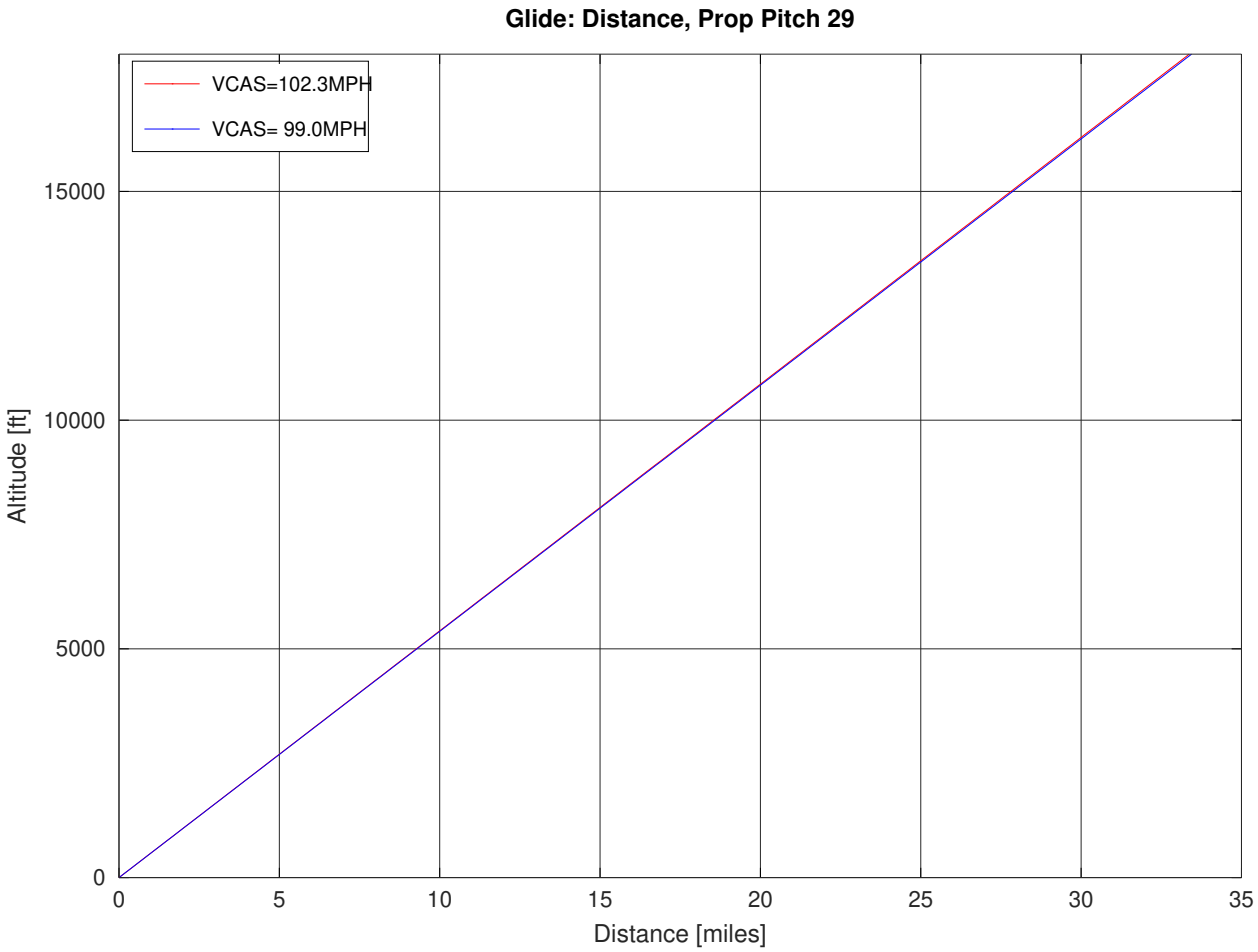

Figure 87: P28R-200B Glide Distance, Maximum Propeller Pitch

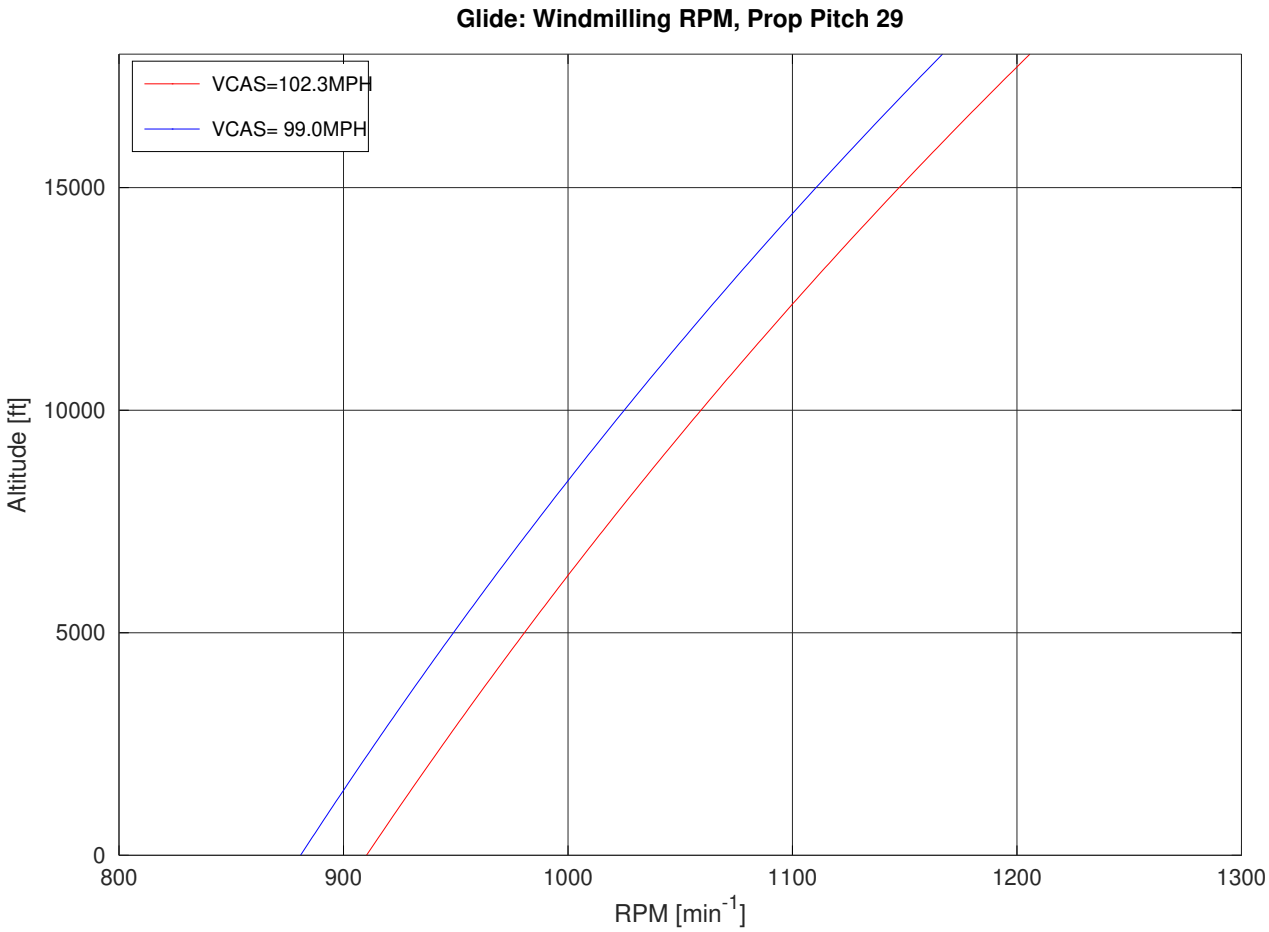

Figure 88: P28R-200B Glide Windmilling RPM, Maximum Propeller Pitch

B.7.3 Piper Cherokee Arrow Data

NACA 652–415 Profile		
Angle where Lift Coefficient is zero	α	$-3°$
Drag Coefficient at α	c_d	0.006
Drag Coefficient at $\alpha + 8°$	c_d	0.008
Lift coefficient scales with $2\pi\alpha$ (α in rad)		
Maximum Lift Coefficient	$c_{l,max}$	1.2
at angle of attack	α_{max}	12
Wing Area		160ft^2
		14.864m^2
MTOM		2600lb
		1179.3402kg
Rated Horsepower		200HP
		149.14kW
Rated RPM		2700min^{-1}

B.8 Linear Interpolation

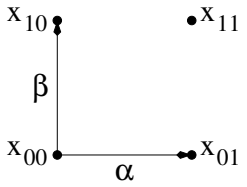

Figure 89: Linear Interpolation

Linear Interpolation is used extensively for weather data, to interpolate between two points in time and two pressure levels, or between grid points.
$0 \leq \alpha \leq 1$ and $0 \leq \beta \leq 1$.

$$x_0 = (1-\alpha)x_{00} + \alpha x_{01} \tag{29}$$
$$x_1 = (1-\alpha)x_{10} + \alpha x_{11} \tag{30}$$

$$\begin{aligned} x &= (1-\beta)x_0 + \beta x_1 = (1-\alpha)(1-\beta)x_{00} + \alpha(1-\beta)x_{01} + (1-\alpha)\beta x_{10} + \alpha\beta x_{11} \\ &= (1-\alpha-\beta+\alpha\beta)x_{00} + (\alpha-\alpha\beta)x_{01} + (\beta-\alpha\beta)x_{10} + \alpha\beta x_{11} \\ &= x_{00} + \alpha(x_{01}-x_{00}) + \beta(x_{10}-x_{00}) + \alpha\beta(x_{11}+x_{00}-x_{01}-x_{10}) \\ &= p_0 + \alpha p_1 + \beta p_2 + \alpha\beta p_3 \end{aligned} \tag{31}$$

$$\hat{\mathbf{x}} = \begin{pmatrix} \hat{x}_0 \\ \hat{x}_1 \\ \hat{x}_2 \\ \hat{x}_3 \end{pmatrix} \tag{32}$$

$$\mathbf{p} = \begin{pmatrix} p_0 \\ p_1 \\ p_2 \\ p_3 \end{pmatrix} \tag{33}$$

$$\mathbf{A} = \begin{pmatrix} 1 & \alpha_0 & \beta_0 & \alpha_0\beta_0 \\ 1 & \alpha_1 & \beta_1 & \alpha_1\beta_1 \\ 1 & \alpha_2 & \beta_2 & \alpha_2\beta_2 \\ 1 & \alpha_3 & \beta_3 & \alpha_3\beta_3 \end{pmatrix} \tag{34}$$

$$\begin{aligned}\frac{\partial}{\partial \mathbf{p}}(\hat{\mathbf{x}} - \mathbf{A}\mathbf{p})^T(\hat{\mathbf{x}} - \mathbf{A}\mathbf{p}) &= \frac{\partial}{\partial \mathbf{p}}(\hat{\mathbf{x}}^T\hat{\mathbf{x}} - \mathbf{p}^T\mathbf{A}^T\hat{\mathbf{x}} - \hat{\mathbf{x}}^T\mathbf{A}\mathbf{p} + \mathbf{p}^T\mathbf{A}^T\mathbf{A}\mathbf{p}) \\ &= -\hat{\mathbf{x}}^T\mathbf{A} + \mathbf{p}^T\mathbf{A}^T\mathbf{A} = 0\end{aligned} \tag{35}$$

$$\mathbf{p} = (\mathbf{A}^T\mathbf{A})^{-1}\mathbf{A}^T\hat{\mathbf{x}} \tag{36}$$